

**SUPERCONDUCTING SYSTEMS OF LOW
DIMENSIONALITY**

A THESIS

**SUBMITTED TO THE DEPARTMENT OF PHYSICS
AND THE INSTITUTE OF ENGINEERING AND SCIENCE
OF BILKENT UNIVERSITY
IN PARTIAL FULFILLMENT OF THE REQUIREMENTS
FOR THE DEGREE OF
DOCTOR OF PHILOSOPHY**

By

M. Zafer Gedik

September 1992

SUPERCONDUCTING SYSTEMS OF LOW
DIMENSIONALITY

A THESIS

SUBMITTED TO THE DEPARTMENT OF PHYSICS
AND THE INSTITUTE OF ENGINEERING AND SCIENCE
OF BİLKENT UNIVERSITY
IN PARTIAL FULFILLMENT OF THE REQUIREMENTS
FOR THE DEGREE OF
DOCTOR OF PHILOSOPHY

By

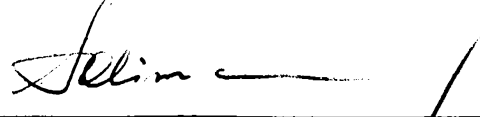
M. Zafer Gedik

September 1992

QC
612
.S8
G43
1992

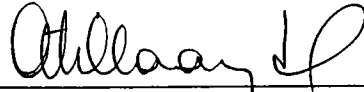
B.15133

I certify that I have read this thesis and that in my opinion it is fully adequate, in scope and in quality, as a dissertation for the degree of Doctor of Philosophy.



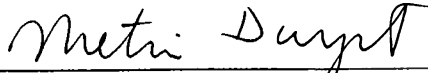
Prof. Salim ıracı (Supervisor)

I certify that I have read this thesis and that in my opinion it is fully adequate, in scope and in quality, as a dissertation for the degree of Doctor of Philosophy.



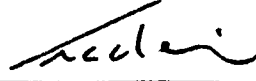
Prof. Atilla Aydınlı

I certify that I have read this thesis and that in my opinion it is fully adequate, in scope and in quality, as a dissertation for the degree of Doctor of Philosophy.



Prof. Metin Durgut

I certify that I have read this thesis and that in my opinion it is fully adequate, in scope and in quality, as a dissertation for the degree of Doctor of Philosophy.



Assoc. Prof. Atilla Erçelebi

I certify that I have read this thesis and that in my opinion it is fully adequate, in scope and in quality, as a dissertation for the degree of Doctor of Philosophy.



Prof. Mehmet Tomak

Approved for the Institute of Engineering and Science:



Prof. Mehmet Baray,
Director of Institute of Engineering and Science

Abstract

SUPERCONDUCTING SYSTEMS OF LOW DIMENSIONALITY

M. Zafer Gedik

Ph. D. in Physics

Supervisor: Prof. Salim Çıracı

September 1992

It is possible to call the last five years as the golden age of superconductivity. The two most important developments in the field are the discovery of copper oxide and fullerene superconductors. In this work, some possible pairing mechanisms for these materials are examined by giving emphasis on the reduced dimensionality. First, an older problem, spatially separated electron-hole system, is investigated to identify the possible phases in coupled double quantum well structures in electric field. Secondly, the superconducting transition temperature and response to external magnetic fields of layered systems with varying number of layers are studied by means of a microscopic model and its Ginzburg-Landau version. It is also shown that an interlayer pairing mechanism, phonon assisted tunneling, can induce superconductivity. Finally, effects of the spherical structure of fullerenes are examined by solving a two fermion problem on an isolated molecule where the particles interact via a short range attractive potential. As a possible mechanism of superconductivity in alkali metal doped fullerenes, coupling between electrons and the radial vibrations of the molecule is investigated.

Keywords: Superconductivity, coupled double quantum wells, spatially separated electron-hole system, Kosterlitz-Thouless transition, Wigner crystal, exciton condensation, layered superconductors, superconductor-insulator superlattices, superconducting thin films, high temperature superconductors, phonon assisted tunneling, electron-phonon interaction, fullerenes, bound-state formation, polaron, negative U Hubbard model.

Özet

DÜŞÜK BOYUTLU ÜSTÜNİLETKEN SİSTEMLER

M. Zafer Gedik

Fizik Doktora

Tez Yöneticisi: Prof. Salim Çıracı

Eylül 1992

Son beş yılı üstüniletkenliğin altın devri olarak adlandırmak mümkündür. Bu alandaki en önemli iki gelişme bakır oksit ve *fullerene* üstüniletkenlerin bulunuşudur. Bu çalışmada, düşük boyutluluk vurgulanarak, bu malzemelerdeki bazı olası çift oluşturma mekanizmaları incelendi. İlk olarak, etkileşen kuvantum kuyu çiftlerinin elektrik alanındaki mümkün fazlarını belirleyebilmek için, eski bir problem, uzayda ayrılmış elektron-delik sistemi çalışıldı. İkinci olarak, mikroskopik bir model ve bu modelin Ginzbur-Landau şekliyle, değişken sayıda tabakalardan oluşan yapıların üstüniletkenlik geçiş sıcaklıkları ve dış manyetik alanlara tepkileri araştırıldı. Ayrıca bir tabakalar arası çiftleşme mekanizmasının, fonon aracılı tünelleme, üstüniletkenliğe yol açabileceği gösterildi. Son olarak, *fullerene* moleküllerinin küresel şekillerinin etkileri bir molekül üzerinde kısa menzilli çekici bir potansiyelle etkileşen iki fermiyon problemi çözülerek incelendi. Alkali metal katkılı *fullerene*'lerde gözlenen üstüniletkenliğin mümkün bir mekanizması olarak, elektronlarla moleküllerin ışınsal yöndeki titreşimlerinin etkileşimleri araştırıldı.

Anahtar

sözcükler: Üstüniletkenlik, etkileşen kuvantum kuyu çiftleri, uzayda ayrılmış elektron-delik sistemleri, Kosterlitz-Thouless geçişi, Wigner kristali, uyarı yoğunlaşması, tabakalı üstüniletkenler, üstüniletken-yalıtkan üstünörgüleri, üstüniletken ince filmleri, yüksek sıcaklık üstüniletkenleri, fonon aracılı tünelleme, elektron-fonon etkileşimi, *fullerene*'ler, bağlı-durum oluşumu, polaron, negatif U Hubbard modeli.

Acknowledgement

It is my pleasure to express my deepest gratitude to my supervisor Prof. Salim Çıracı for his guidance and encouragement. I acknowledge his invaluable efforts throughout my graduate study. I have not only benefited from his wide spectrum of interest in condensed matter physics but also learned a lot from his academic personality.

I appreciate partial support by the Joint Project Agreement between IBM Zurich Research Laboratory and Department of Physics, Bilkent University. I wish to express my special thanks to Prof. Alexis Baratoff for his hospitality and discussions during my visits to the laboratory. I would like to thank to Prof. Toni Schneider for his collaboration in the studies of layered superconductors.

I am grateful to the members of the Department of Physics, Bilkent University for valuable discussions and comments.

My sincere thanks are due to my parents for their understanding and moral support. Last but not the least, I thank Nüni for her patience.

Contents

Abstract	i
Özet	iii
Acknowledgement	v
Contents	vi
List of Figures	viii
List of Tables	x
1 Introduction	1
2 Coupled Quantum Wells	8
3 Layered Systems	19
3.1 Microscopic Theory	20
3.2 Ginzburg-Landau Formalism	34
3.3 Tunneling Induced Superconductivity in Layered Systems	47
4 Fullerenes	54
4.1 Review	54
4.2 Two-Fermion Problem on a Truncated-Icosahedron	64
4.2.1 Bound-State Formation in 1D, 2D and 3D	65
4.2.2 Hubbard Model on Truncated-Icosahedron	68

4.2.3	Bound-State Formation on a Sphere	74
4.3	Local Oscillator Model for Superconducting Fullerenes	79
5	Conclusions	85
	Bibliography	88

List of Figures

2.1	GaAs coupled quantum wells	9
2.2	Photoluminescence spectra for coupled GaAs/AlGaAs quantum wells	10
2.3	Photoluminescence intensity	16
2.4	Linewidth as a function of temperature	17
3.1	Superconductor-Insulator superlattice	20
3.2	Scattering processes of two carriers due to $V_{n_1 n_2 n_3 n_4}$	22
3.3	T_c for isolated YBCO stacks with M unit cells	29
3.4	$T_c(M, N)$ for YBCO/PrBCO superlattice	30
3.5	Electrostatic model of the interaction V_3	32
3.6	Momentum dependence of the interlayer interaction V_3	32
3.7	Fermi surface and irreducible part of the Brillouin zone	34
3.8	T_c of NbSe ₂ versus M and $\cos \frac{\pi}{M+1}$	39
3.9	Transition temperature of Sn-SiO and Al-AlO ₂ structures	40
3.10	T_c for isolated YBCO stacks	41
3.11	$a(N)$ determined from the experimental data	43
3.12	$a(N)/a(0)$ versus N	44
4.1	Fullerenes	55
4.2	Doped fullerenes	57
4.3	Electronic energy levels of C ₆₀	59
4.4	The band structure of the fcc C ₆₀ solid	60
4.5	Contour plot of valence-electron density	61
4.6	T_c versus pressure	62
4.7	Labeling the sites on truncated-icosahedron	72

4.8	Two fermions on the truncated-icosahedron	74
4.9	Phase diagram for negative U Hubbard model	83

List of Tables

3.1	Estimates for $T_c(1)$ and a	42
3.2	Estimates for the coupling strengths	45
4.1	Properties of solid C_{60}	56
4.2	Properties of alkali-metal doped A_3C_{60} fullerenes	58
4.3	Free particle Green's functions	66

Chapter 1

Introduction

Dimensionality, namely the number of space dimensions, of a quantum mechanical system is one of the most important parameters in determining the dynamical behavior. There are several manifestations of the dimensionality in both single and many particle systems. The latter is especially important, because all the macroscopic systems fall in this category. In this introductory chapter we are going to mention some of the dimensional effects which turn out to be very important. We will mainly concentrate on many particle systems where a new parameter, temperature, enters into the picture and hence thermal fluctuations become effective along with the quantum fluctuations.

Although we live in a three dimensional (3D) space, there are several situations in which the effective dimensionality is lower than that. Let us consider for example a system for which the Schrödinger equation is separable in x , y and z directions so that the energy eigenvalues can be written as $E = E_x + E_y + E_z$. Each E_i is determined by the associated Schrödinger equation and the boundary conditions. According to quantum mechanics, E_i can change only in certain *quanta* which can not be smaller than say ΔE_i . For example, for a particle in a box ΔE_i is proportional to the inverse square of the size of the box, while for a free particle $\Delta E_i \rightarrow 0$. The criterion determining the effective dimensionality of a quantum mechanical system is the relative magnitudes of ΔE_i 's. Let us think of a situation in which $\Delta E_z \gg \Delta E_x, \Delta E_y$. For low lying excitations the presence

of z degree of freedom is immaterial. Because, excitations into higher levels in this direction are extremely unlikely. This is the case for example for a particle confined between two infinite walls perpendicular to z -axis. Thus, we end up with a two dimensional (2D) system as long as we deal with low energy excitations. Decreasing ΔE_z , we observe a transition from 2D to 3D. For the particle between walls, this corresponds to the increasing interwall distance. Confining the particle in more number of directions, we can create one and zero dimensional (1D and 0D) structures.

As we have mentioned above, when ΔE_z is reduced we go from 2D behavior to 3D. However, what dimension to assign to the system in between is not clear. In several cases, it is possible to assign a nontrivial dimension, which can be fractional also. For example, it is possible to show that the free energy of a system composed of weakly interacting 2D Bose gas layers is equivalent to the free energy of a $(2 + \epsilon)$ D Bose gas where the small parameter ϵ increases with the increasing interlayer separation.¹ The concept of fractional dimensionality has been successfully used in several branches of physics. This method is especially useful in solving problems in a different dimensionality, which is presumably easier to do, and finding the solution of the original problem by analytic continuation. Dimensionality is a nonperturbative parameter, and therefore the dimensional expansion provide accurate nonperturbative analytic results. For example, in D -dimensional Euclidean space, we can start from a 0D quantum field theory as the unperturbed problem, which is the simplest interacting quantum field theory that can be solved in closed form.

A familiar example for the effects of dimensionality in a single particle problem is bound state formation. A particle moving in a short range attractive potential forms a bound state if the attraction is very strong. However, what is not obvious is the behavior of the particle for a weak potential. It turns out that in 1D and 2D, a bound state is always formed, no matter how weak the attractive interaction is.^{2,3} On the other hand, in the 3D case, it is necessary for the potential to be stronger than a threshold in order to observe the same phenomenon. Furthermore, that kind of behavior is independent of the detailed structure of the system. It is

possible to verify the same theorem on a lattice instead of a continuum problem.⁴

Due to their large number of degrees of freedom, many particle systems exhibit a rich variety of phenomena originating from reduced dimensionality. Some of these effects are observable even at a classical level. The relations between the critical points of a periodic function and the dimensionality of the domain on which it is defined have found many applications both in classical problems like the vibration spectra of crystals^{5,6} and in quantum mechanical phenomena such as the electronic energy levels in a solid. According to a general theorem of Morse,⁷ any periodic function of more than one independent variable has at least a certain number of saddle points which depends only on the number of independent variables, namely dimensionality. The idea in this topological work is that the existence of some critical points necessitates the existence of others. Therefore, independent of the detailed structure of the crystal, it is possible to obtain important information on the nature of the singularities in the density of states for vibrational or electronic spectra.

Another important phenomenon, which is specific to 2D systems, is the existence of topological long range order.⁸ It has been known for a long time that in 2D solids due to the thermal motion of low energy phonons, there can not be long range order.⁹ Reduced dimensionality causes the mean square deviation of atoms from their equilibrium positions to increase logarithmically with the size of the system.¹⁰ Similarly, it can be shown that there is no spontaneous magnetization in a 2D Heisenberg magnet¹¹ and the expectation value of the superfluid order parameter for 2D Bose liquid vanishes.¹² In spite of the fact that in 2D systems thermal fluctuations destroy all of the above mentioned long range orders, Kosterlitz and Thouless showed that for short range interactions a new kind of order, so called topological order, can exist and there is a phase transition associated with this ordering.⁸

The idea of Kosterlitz and Thouless was that above a certain temperature the entropy term in the free energy expression dominates and therefore it allows the creation of excitations whose formation energy changes with the logarithm of the size of the system. In 2D crystal these excitations are dislocations, in magnets

they are vortices characterized by the phase of the spins going through an integer times 2π when a closed path around a vortex is followed and in superfluids they are simply the vortices due to the circular motion of superfluid. The common property of these excitations is that formation energy U of one excitation is proportional to the logarithm of the size of the 2D system. As can be seen from the free energy expression $F = U - TS$, the second contribution to F comes from entropy S , where T is the temperature. However, entropy is nothing but the logarithm of the number of available states for the excitations. Thus, the entropy term also changes with the logarithm of the size of the system. From the free energy expression we see that at high temperatures the entropy term takes over and isolated vortices occur. If the interactions between the dislocations or vortices are weak, the above expression can be used to predict the critical temperature at which isolated excitations are formed.

In crystal, presence of free dislocations imply that the system is not rigid because dislocations can move to the edges under the influence of an arbitrarily small shear stress and this motion produces a viscous flow. Below the critical temperature, the dislocations can occur only in pairs. The energy of a pair is finite in contrast to that of an isolated dislocation and therefore pairs can exist at any nonzero temperature. The critical temperature at which dislocation pairs are broken has been identified as the melting temperature of the 2D crystal. Later, Halperin and Nelson have pointed out that the transition to isotropic fluid phase occurs after a second step at which not only the translational but also rotational order disappears.¹³ However, melting in 2D is still one of the fields with several open problems.

Similar arguments can be used to understand the physics of the vortex unbinding transition or so called Kosterlitz-Thouless transition in neutral and charged superfluids, i.e. superconductors.¹⁴ In this case, the problem has direct relation to the practical use of superconductors. Because, the finite resistance in superconductors is associated with the motion of vortices. In thin films, the vortices can occur even in the absence of an external magnetic field because the free energy for creation of a vortex can become very small. In superconductors,

vortex unbinding is observable in spite of the fact that flux lines have finite energy which depends on the penetration depth.¹⁵ The cause of the transition is that at small distances the interaction of two vortices in a superconductor has the same distance dependence as the interaction of vortices in neutral superfluid.

In addition to the thermal fluctuations which can exist even in classical 2D systems, e.g. a 2D crystal, there are quantum fluctuations that play an important role in quantum systems even at zero temperature. Quantum fluctuations exist at any dimension but their importance increases with decreasing dimensionality. A very useful example to understand the role of quantum fluctuations is spin system. Spin is a quantum mechanical degree of freedom and its proper treatment forces us to introduce vector wave functions. We expect that if the spin S increases, so does the effective dimensionality of the system, because with increasing S we gain a new degree of freedom changing from $-S$ to S which is very similar to the spatial coordinates. In fact, this is very well demonstrated by the spin wave theory developed by Anderson¹⁶ and Kubo¹⁷ to study the ground state of antiferromagnets with large S . In spin wave theory, it is assumed that there is an antiferromagnetic long range order in the ground state and that the amplitude of quantum fluctuations about the classical Néel state is small. Then, an expansion is done in powers of $1/zS$, where z is the coordination number which we can view of as dimensionality D also. It is seen that spin S and dimensionality D enters on equal footing. For low S or low D systems, quantum fluctuations are expected to be very important. For example, the ground state of the spin-1/2 antiferromagnetic Heisenberg chain, as has been shown by Bethe,¹⁸ is not the classical Néel state but a superposition of spin singlets formed by two by two combinations of spins. In the 3D case, the antiferromagnetic Heisenberg model for $S=1/2$, admits a ground state with a long range order.¹⁹ So far, no rigorous proof is available for the same model on a 2D square lattice, which is a model of great interest due to its possible relation to copper oxide superconductors.²⁰

Finally, before presenting the relation of the above phenomena to the superconducting systems of low dimensionality, we will mention another property of 2D systems: fractional statistics. 2D systems, or in field theory language

2+1 (2 space and 1 time) dimensional systems, display some peculiar quantum mechanical phenomena. All of these phenomena, like massive gauge fields and soluble quantum gravity, are results of the special structure of rotation, Lorentz and Poincaré groups and also the existence of local, Lorentz invariant interactions, so called Chern-Simons and Hopf topological interactions, exhibiting very unusual behaviors under CP and general coordinate transformations. We will consider the implications of the peculiar structure of the spatial rotation group $SO(2)$. The group is Abelian and has a continuum of representations and hence there is no reason for angular momentum to be quantized. The absence of quantization can be seen in a very simple way. In the $SO(2)$ case, we walk on a ring where we reach the same final point independent of the order of the steps once their lengths and directions are fixed while for $SO(3)$ the motion is on the surface of a sphere and the final point to be reached depends very strongly on the order of the steps. In the latter case, the components of the the generator of the rotations, namely angular momentum operator, do not commute but instead satisfy the well known commutation relations leading to the quantization of angular momentum. In summary, in 2D systems angular momentum can take any value. This property has very far reaching results due to possible extension of the spin-statistics theorem. Since the quantum states can have angular momentum which is neither integer nor half-integer, they will be neither bosons nor fermions. Thus, we end up with *anyons* obeying a new statistics, so that when two of these particles are exchanged the many body wave function gains a phase $\exp(i\phi)$ where ϕ need not be 0 or π in contrast to bosons and fermions.

In the last five years, two new classes of superconductors have been discovered: copper oxides and fullerenes. Both classes of materials are low dimensional structures and they have very high superconducting critical temperatures. The copper oxide compounds are layered systems. The layers are composed of copper and oxygen atoms, and current carriers are confined into these planes. Therefore, depending upon the strength of the interlayer coupling, the system has an effective dimensionality between 2D and 3D as we are going to study in detail in Chapter 3. As a result we expect to observe some dimensional effects. In fact,

the Kosterlitz-Thouless type of resistivity versus temperature curves of copper oxide superconductors supports this expectation. Melting of the flux lattice in the mixed state is still one of the problems of great interest. 2D Hubbard and as a limiting case of it Heisenberg models have been studied in detail with the expectation that they describe the physics of copper oxide layers correctly. There are various implications of possible anyon superconductivity. The fullerenes, on the other hand, are 3D structures composed of spherical units. Since the spheres are finite systems, they are 0D. However, in Chapter 4 we will show that the surface of a sphere can behave like a 2D plane. Finally, it is very interesting to note that both copper oxide compounds and alkali metal doped fullerenes, although they are very good superconductors, are bad conductors in the normal state. In fact, they are very near to metal-insulator transition.

In the next chapter we will study possible states of a new 2D structure, namely spatially separated electron-hole systems in coupled double quantum wells. We will present possible explanations of the observed reduction in the photoluminescence linewidth below a certain temperature. In Chapter 3, we will consider metal-insulator superlattices and in particular artificially grown copper oxide superlattices. We will propose a microscopic mechanism, an interlayer interaction, which can explain the dependence of superconducting critical temperature on the thicknesses of superconducting and insulating layers. We then investigate the behavior of upper critical field of these structures by means of the Ginzburg-Landau formulation of the model. We also study the results of the coupling between electrons and interlayer vibration modes controlling the tunneling rate of electrons. Chapter 4 is devoted to superconductivity of alkali metal doped fullerenes. We solve a model for two fermions confined to the surface of a C_{60} molecule. We also consider the coupling of radial oscillation of molecule with electrons. Finally, in Chapter 5 we summarize the conclusions.

Chapter 2

Coupled Quantum Wells

Semiconducting heterostructures have been widely used to study the physics of low dimensional electron or hole gases. For low energy excitations, i.e. the processes in which electrons (holes) remain essentially at the bottom (top) of the conduction (valence) band, the motion of charge carriers can be described by a parabolic band. Thus, in this approximation, so called the effective mass theory, electrons and holes are treated as free particles as long as the interactions between them are not important. When two semiconductors with different energy gaps are brought together by means of an interface, interesting electronic structures may arise. For example, if GaAs and GaAlAs are grown on each other, it turns out that the charge carriers in GaAs, which has the smaller energy gap, govern decaying wave functions in GaAlAs region (figure 2.1). As a result, it is possible to obtain various quantum well structures by playing the thicknesses of the semiconducting layers. Furthermore, by changing the composition of $\text{Ga}_x\text{Al}_{1-x}\text{As}$, one can control the bandwidth and hence the height of the barrier regions.

Recently, Fukuzawa, Mendez and Hong²¹ reported that below a certain critical temperature ($T < 10$ K), the photoluminescence linewidth measured in coupled quantum wells made from GaAs/Ga_{0.7}Al_{0.3}As/GaAs compounds suddenly reduced. They found that a single, broad photoluminescence peak split into two peaks under an electric field E ($\perp xy$ -epitaxial plane); the low-energy peak became sharper and more intense with the increasing electric field at low

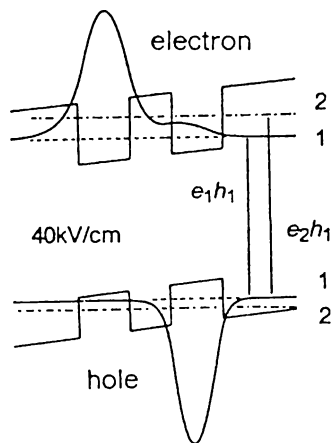


Figure 2.1: GaAs coupled quantum wells

Electron and heavy-hole wave functions for the ground state are shown on the potential profile. Each well (GaAs slabs) is 50 Å wide and the barrier (GaAlAs region) is 40 Å thick. The electric field tilts the potential profile. From reference 21.

temperature (figure 2.2). The reduction of linewidth was observed only under an electric field for certain excitation power densities in the region of 0.6 Wcm^{-2} , and for certain barrier thickness ($\simeq 40 \text{ Å}$) allowing only weak coupling between adjacent quantum wells. These observed changes were attributed to the transition of excitons in the quantum wells to an ordered phase with a long coherence length, so their energy is prevented from broadening due to the structural imperfections.

For more than two decades the possibility of such a phase transition leading to a liquid state or droplets has been of continuing interest in condensed matter physics.²²⁻²⁴ It has been proposed that two fermions, electron and hole, can form a composite particle, so called exciton, which exhibits bosonic properties, particularly a tendency to Bose-Einstein condensation. The effective mass of excitons is relatively small, and as a result quantum effects are enhanced. This is apparent from the expression for the critical temperature T_c of the ideal Bose gas at which the phase transition occurs,

$$k_B T_c = 3.31 \hbar^2 N^{2/3} M^{-1} . \quad (2.1)$$

Here, N is the concentration and M is the mass of the particles. For $M \sim 10^{-24}$ –

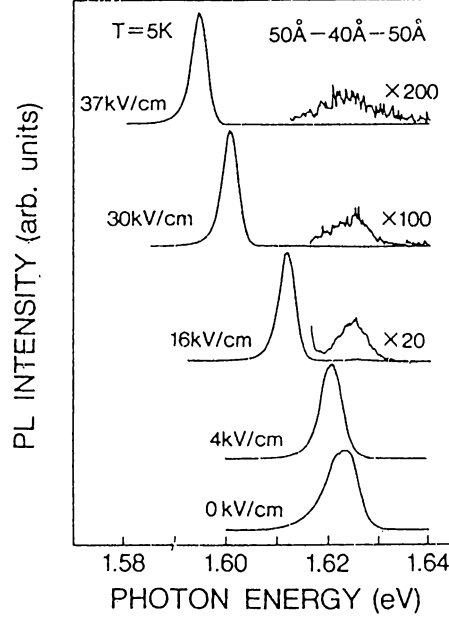


Figure 2.2: Photoluminescence spectra for coupled GaAs/AlGaAs quantum wells

The peak for 0 kV/cm corresponds to the e_1h_1 transition of figure 2.1. With increasing electric field, a new peak from the e_2h_1 and e_1h_2 transitions appears. From reference 21.

10^{-25} kg, concentrations about 10^{24} m^{-3} are enough to reach critical temperatures as high as 100 K. However, ideal Bose gas model is a good approximation only at low densities. If the separation between the excitons becomes comparable to their sizes, the internal structure of the excitons begin to play an important role. Even in the absence of Coulomb interaction, the ideal boson picture breaks down due to bare quantum statistical effects (Pauli principle). A more quantitative criterion for the validity of the structureless boson model can be obtained by introducing the exciton operators

$$Q_{\vec{K}} = \sum_{\vec{k}} \phi(\vec{k}) e_{\frac{\vec{K}}{2} + \vec{k}} h_{\frac{\vec{K}}{2} - \vec{k}} , \quad (2.2)$$

where Q , e and h are exciton, electron and hole annihilation operators, respectively. \vec{k} is the relative momentum of the electron and hole while \vec{K} is the exciton momentum. $\phi(\vec{k})$ is simply the normalized ground state wave function

of the exciton. Now, the bosonic nature of the Q operators is justified if they satisfy the usual commutation relations. It can be easily shown that

$$[Q_{\vec{K}}, Q_{\vec{K}'}] = \delta_{\vec{K}\vec{K}'} - \sum_{\vec{k}} \phi(\vec{k} + \frac{\vec{K}}{2})\phi(\vec{k} + \frac{\vec{K}'}{2})(e_{\vec{k}+\vec{K}}^\dagger, e_{\vec{k}+\vec{K}} + h_{\vec{k}+\vec{K}}^\dagger, h_{\vec{k}+\vec{K}}) . \quad (2.3)$$

Therefore, as long as the second term is small enough the boson commutation relation is satisfied. However, the matrix elements of the second term are of the order of the concentration N of the electrons and holes times exciton volume a_0^3 . As a result, the structureless boson picture is only accurate to terms of the order Na_0^3 .

Earlier, Lozovik and Yudson²⁵ and Shevchenko²⁶ pointed out a fundamentally different pairing mechanism and, hence, formation of a superconducting phase. This was the Coulomb attraction between quasi-2D electrons and holes, separated by dielectric media, which may lead to a finite gap of single particle excitations. Inspired by the work of those authors, Fukuzawa *et al.*²⁷ predicted earlier a phase transition that was similar to one observed experimentally.²¹ In an electric field the electrons and holes can, in fact, be confined in spatially adjacent wells to form excitons. A simple argument based on the minimization of electrostatic energy due to oppositely charged sheets suggests that the density of excitons of this kind is proportional to the electric field. This is because there are two terms competing with each other in lowering the electrostatic energy. One is the interaction of electrons and holes with the applied electric field E and the other is simply the electrostatic energy of the plate capacitor. The first term is linearly proportional to the exciton density n , while the second one increases with n^2 . Thus, minimization with respect to the density gives $n \propto E$. Accordingly, the intensity of the e_1h_1 transition²¹ increases linearly with E , while that of e_2h_1 decreases. This is qualitatively the situation observed in experiment.²¹ Because of this effect of E , the time for recombination increases with the decrease of overlap between the electron and hole wave functions, and a situation identical to that described by the above-mentioned theories^{25,26} will be created.

If what was observed by Fukuzawa *et al.* is a phase transition, it might be of one of the following three types: Wigner crystal, Bose-Einstein condensation,

and BCS-like.²⁸ By examining the limits of these types, we argue that the model described by Fukuzawa *et al.*²⁷ may lead to a BCS-type phase transition, but neither to a Bose-Einstein condensation²⁴ nor to a Wigner crystal. In these phase transitions two parameters are of prime importance: the spatial extend of the exciton in the xy -plane (λ), and the exciton-exciton separation (l). if $\lambda \ll l$, one can consider the Wigner crystal or Bose-Einstein condensation. In this low density limit, electrons and holes can be viewed as individual quasiparticles, which can form excitons, but not other condensed forms (droplets or molecules), because the parallel dipoles repel in the xy -plane. The other limit, $\lambda \gg l$, is appropriate for the BCS transition. By consideration of the expected exciton density²¹ $\rho_e (\sim 10^{10} \text{cm}^{-2})$ one can obtain the very crude estimates $l \simeq 1000 \text{ \AA}$ and $\lambda \simeq 200 \text{ \AA}$ for the given separation of quantum wells of 40 \AA .

The possible lattice structure of the Wigner crystal was studied earlier²⁹ for a similar system under a dipole-dipole interaction. This 2D Wigner crystal is assumed to melt via a Kosterlitz-Thouless transition, with the melting temperature given by

$$T_c = \frac{mb^2v_t^2v_l^2}{8\pi k_B a(v_t^2 + v_l^2)} . \quad (2.4)$$

Here, v_t , v_l , b , and a are respectively, longitudinal and transverse sound velocities, the Burgers vector and the area of the unit cell. With appropriate parameters and $m = m_h + m_e$, we found that T_c is negligibly small. Very low T_c as well as a significant value of λ/l rules out the Wigner crystal. As for the second possibility within the low-density limit, we assume that the system is an ideal Bose gas, since excitons can be treated as bosons at this limit. Then the total number of bosons, N , can be calculated from the following expression

$$N = z \frac{\partial}{\partial z} \ln Z(z, V, T) , \quad (2.5)$$

with Z the grand partition function, z the fugacity and T the temperature. For free bosons confined in a 2D box of area S with infinite walls, we find that

$$\frac{N}{S} = \frac{2\pi m_b k_B T}{h^2} \ln(N_0 + 1) + \frac{N_0}{S} \quad (2.6)$$

where N_0 is the number of bosons in the zeroth energy level, $m_b (= m_e + m_h)$ is the mass of the boson. We note that $N_0 = N$ for $T=0$ K. Since the first term on the right-hand side changes slowly in comparison to the second one, near $T=0$ K, N_0 decreases from N (i.e. from the maximum value it attains at $T=0$ K) linearly with temperature. The slope of this linear dependence is approximately $2\pi m_b k_B \ln N/h^2$, which is in the region of $10^{14} \ln N \text{ m}^{-2}\text{K}^{-1}$. With the values reported from the experiment for N/S , this slope is $\sim 10^{15} \text{ m}^{-2}\text{K}^{-1}$. This means that even for $T \simeq 0.05$ K, N_0/S drops half of its initial value. Furthermore, full solution of equation 2.6 shows that there is no critical temperature T_c at which N_0/S suddenly becomes non-zero. Instead, it changes from zero gradually as the temperature is decreased. In view of the fact that the ordered phase in 2D can occur through the Kosterlitz-Thouless transition, the relation

$$k_B T_c = \frac{\pi \hbar^2 \rho_e}{2m} \quad (2.7)$$

yields $T_c \simeq 0.3$ K. This simple analysis also shows that if the observed reduction of the linewidth is due to a phase transition of the electron-hole system in the weakly coupled quantum wells, this phase transition cannot be a Bose-Einstein condensation.

If the density of excitons is not very low, the interactions between electron gas in one well and hole gas in the other well are enhanced with the diminishing of the excitons. In this case an electron-hole pair is treated like a Cooper pair, but neither as boson nor as a free exciton. The Hamiltonian of this system can be written²⁵ by analogy with the standard BCS theory. To this end, one assigns creation and annihilation operators for electron states of energy $\epsilon_e(\vec{k})$, as well as hole states $\epsilon_h(\vec{k})$. The coupling constant is a screened, attractive Coulomb potential $V(\vec{q})$, through which an electron-hole pair of wave vectors \vec{k} and $-\vec{k}$, respectively, is annihilated while another pair of wave vectors $\vec{k} + \vec{q}$ and $-\vec{k} - \vec{q}$ is created. Therefore, we start with the following Hamiltonian

$$H = \sum_{\vec{k}} [\epsilon_e(\vec{k}) e_{\vec{k}}^\dagger e_{\vec{k}} + \epsilon_h(\vec{k}) h_{\vec{k}}^\dagger h_{\vec{k}}] + \sum_{\vec{q}, \vec{k}, \vec{k}'} V(\vec{q}) e_{\vec{k}+\vec{q}}^\dagger e_{\vec{k}} h_{\vec{k}'-\vec{q}}^\dagger h_{\vec{k}'} \quad (2.8)$$

As we have mentioned above, for simplicity, we look for the zero pair momentum

solutions, i.e. $\vec{k} = -\vec{k}'$. For this purpose we introduce the order parameter $\Delta(\vec{k})$ defined by

$$\Delta(\vec{k}) = \langle \sum_{\vec{q}} V(\vec{q}) e_{-\vec{k}-\vec{q}} h_{\vec{k}+\vec{q}} \rangle , \quad (2.9)$$

and write down the resulting effective Hamiltonian as

$$H_{eff} = \sum_{\vec{k}} \{ \epsilon_e(\vec{k}) e_{\vec{k}}^\dagger e_{\vec{k}} + \epsilon_h(\vec{k}) h_{\vec{k}}^\dagger h_{\vec{k}} + [\Delta(\vec{k}) h_{\vec{k}}^\dagger e_{-\vec{k}}^\dagger + h.c.] \} . \quad (2.10)$$

H_{eff} can be diagonalized by generalizing the familiar Bogoliubov transformation to take into account the presence of two different kinds of fermions

$$\begin{aligned} e_{\vec{k}} &= u_{\vec{k}} \alpha_{-\vec{k}}^\dagger + v_{\vec{k}} \beta_{-\vec{k}}^\dagger \\ h_{\vec{k}} &= u_{\vec{k}} \beta_{\vec{k}} - v_{\vec{k}} \alpha_{\vec{k}} , \end{aligned} \quad (2.11)$$

where

$$\begin{aligned} u_{\vec{k}}^2 &= \frac{1}{2} \left(1 + \frac{\xi_{\vec{k}}}{E_{\vec{k}}} \right) \\ v_{\vec{k}}^2 &= \frac{1}{2} \left(1 - \frac{\xi_{\vec{k}}}{E_{\vec{k}}} \right) \\ u_{\vec{k}} v_{\vec{k}} &= \frac{1}{2} \frac{\Delta(\vec{k})}{E_{\vec{k}}} \\ \xi_{\vec{k}} &= \frac{1}{2} [\epsilon_e(\vec{k}) + \epsilon_h(\vec{k})] \\ E_{\vec{k}} &= \sqrt{\xi_{\vec{k}}^2 + \Delta(\vec{k})^2} . \end{aligned} \quad (2.12)$$

Substituting the above expressions into the definition of the order parameter gives the gap equation. Another way to obtain the same result is to treat the ground state energy as a functional of $\Delta(\vec{k})$, and to do a variational calculation. Equivalence of the two approaches is due to the fact that they both stem from the mean field approximation in which $\Delta(\vec{k})$ is assumed to be very small and the total energy is expanded in terms of it to the second order. The energy spectrum of the quasi-particles that describe the excited states of the ordered phase is therefore given by $[(\epsilon_e(\vec{k}) + \epsilon_h(\vec{k}))^2/4 + \Delta(\vec{k})^2]^{1/2}$. In the weak coupling limit, for $T_c \simeq 8.5$ K at which the sharp reduction of the photoluminescence linewidth has been observed, we estimate the energy gap at zero temperature to be 1.3 meV.

Validity of the theory depends upon whether the mean field approximation is justified. As is well known strong thermal fluctuations prevents the formation of long range order in infinite 1D and 2D systems.¹² For a finite 2D system, since the phase of Δ changes logarithmically with the size of the system, it may be possible to apply the mean field theory. However, if the size goes to infinity existence of long range order is ruled out. In this case, the phase transition to the superfluid phase still exists but it should be treated in the context of Kosterlitz-Thouless theory.

The peak observed in the photoluminescence experiment for the double well structure is simply due to the annihilation of an electron-hole pair to create a photon (i.e. recombination) as a result of the single-particle excitation across the energy gap. The spectrum $I(\omega)$ is calculated by assuming that E is strong enough that electrons and holes have already formed the BCS phase before they are recombined; furthermore, the effects of imperfections are neglected. $I(\omega)$ is expressed in atomic units as

$$I(\omega) = 2\pi \sum_{\vec{q}} | \langle \Psi_{\vec{q}} | V | \Psi_0 \rangle |^2 \delta(E(\vec{q}) - E_0 + \omega) . \quad (2.13)$$

Here Ψ_0 is the BCS wave function with the eigenvalue E_0 , and $\Psi_{\vec{q}}$ is the wave function obtained from the former by eliminating one electron-hole pair of $(\vec{q}, -\vec{q})$. Therefore,

$$\begin{aligned} |\Psi_0 \rangle &= \prod_{\vec{k}} (u_{\vec{k}} + v_{\vec{k}} e_{\vec{k}}^\dagger h_{-\vec{k}}^\dagger) |0 \rangle \\ |\Psi_{\vec{q}} \rangle &= e_{\vec{q}} h_{-\vec{q}} |\Psi_0 \rangle , \end{aligned} \quad (2.14)$$

where $|0 \rangle$ is the vacuum. Note that for parabolic energy bands $E(\vec{q}) - E_0 = E_{\vec{q}} - (E_g + q^2/2m)$ in terms of the band gap E_g and the reduced mass m of the electron-hole pair. Choosing the vector potential $\vec{A}(\vec{r}, z)$, \vec{r} being the 2D radius vector in the xy -plane, in the Coulomb gauge $\nabla \cdot \vec{A} = 0$, the operator V for the interaction of electrons and holes with the electromagnetic field has the following approximate form when linearized with respect to \vec{A} :

$$V = -\frac{e_e}{2m_e c} \sum_{\vec{k}, \vec{q}} (2\vec{k} + \vec{q}) \cdot \vec{A}_{\vec{q}}^e e_{\vec{k}+\vec{q}}^\dagger e_{\vec{k}} - \frac{e_h}{2m_h c} \sum_{\vec{k}, \vec{q}} (2\vec{k} + \vec{q}) \cdot \vec{A}_{\vec{q}}^h h_{\vec{k}+\vec{q}}^\dagger h_{\vec{k}} . \quad (2.15)$$

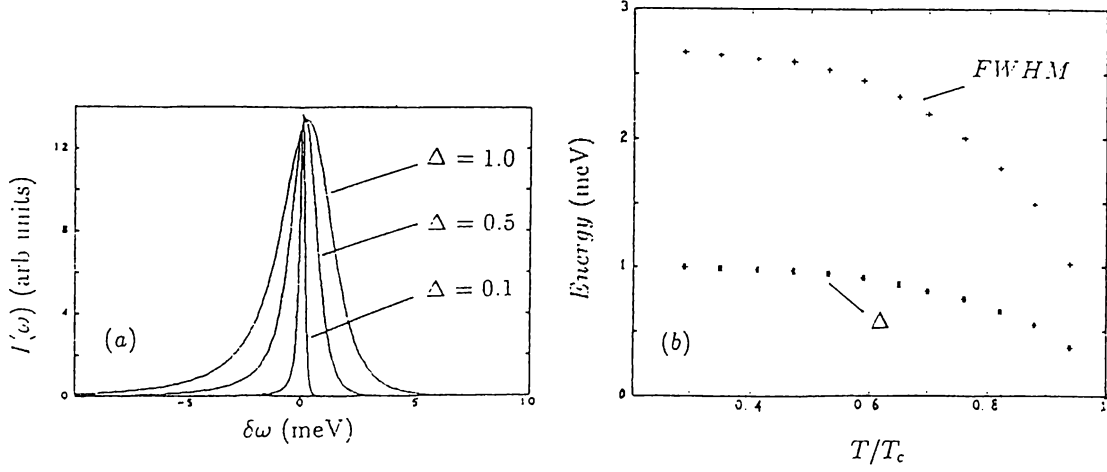


Figure 2.3: Photoluminescence intensity

(a) $I(\omega)$ calculated for various values of Δ . (b) The variation of the FWHM and Δ with T/T_c . The calculations are carried out with $q_F^2/4m=20$ meV.

Here m_e and m_h are effective masses of electrons and holes, respectively. For a coordinate system whose origin falls at the middle of the electron and hole planes of separation d , the vector potentials are given by

$$\begin{aligned}\vec{A}^e(\vec{r}) &= \vec{A}(\vec{r}, +d/2) = \sum_{\vec{q}} \exp(i\vec{q} \cdot \vec{r}) \vec{A}_{\vec{q}}^e \\ \vec{A}^h(\vec{r}) &= \vec{A}(\vec{r}, -d/2) = \sum_{\vec{q}} \exp(i\vec{q} \cdot \vec{r}) \vec{A}_{\vec{q}}^h.\end{aligned}\quad (2.16)$$

In order to produce equation 2.13 the following assumptions are made: (i) all the electrons and holes are separated in different wells, there is no exciton confined in a single well; (ii) the system at the hand is in the ground state (i.e. all the electrons and holes are paired). Since the excited states are separated by a gap from the ground state, the second approximation is valid as long as the temperature is not too close to T_c . Substituting V into equation 2.13, we obtain

$$I(\omega) = CA^2(4m\xi + q_F^2)u^2v^6/(1 + v^2)|_{\xi=\xi_0}, \quad (2.17)$$

where $\xi_0 = (2\delta\omega - \sqrt{\delta\omega^2 + 3\Delta^2})/3$ with $\delta\omega = \omega - (E_g + q_F^2/2m)$; q_F is the Fermi momentum; $A = A_0^e = A_0^h$; u and v are the usual coherence factors expressed in terms of the energy spectrum of normal and superconductive states; C is a constant. In figure 2.3 (a), we show $I(\omega)$ for various values of the superconducting gap, $\Delta(T)$. Note that the larger the value of Δ , the larger the

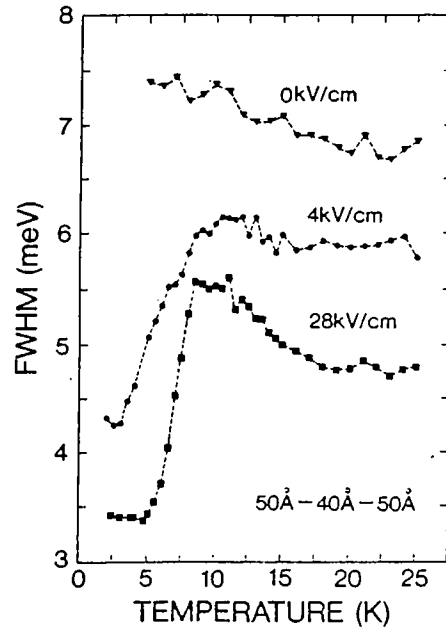


Figure 2.4: Linewidth as a function of temperature

Linewidth of the e_1h_1 transition is plotted for $E=0, 4$ and 28 kV/cm. The sharp reduction of FWHM is apparent from the 28 kV/cm curve. From reference 21.

full width at half maximum (FWHM). Since Δ is a function of temperature, so is $I(\omega)$. In figure 2.3 (b), we plot FWHM as a function of T/T_c . On the same plot we show the temperature dependence of the BCS gap. The FWHM is proportional to Δ . This is an expected result, since an electron and a hole can be recombined only if they are first excited from the ground state by $\sim \Delta$. Accordingly, the FWHM is expected to show the behavior depicted in figure 2.3 (b) in the interval $0 < T/T_c \leq 1$, if the observed transition is the BCS-like transition. The experimental variation of FWHM also indicates the contribution of a different type of broadening mechanism, which is insensitive to the variation of temperature, but increases with decreasing E (figure 2.4). Therefore, the FWHM can never become zero as $T/T_c \rightarrow 1$.

In conclusion, the behavior of the photoluminescence linewidth below T_c can be considered as a *fingerprint* for deciding whether or not the observed event originates from a BCS-like phase transition of electrons and holes. Recently, Kash

et al. proposed that the temperature dependence of FWHM can be explained by Fermi-Dirac distribution of excitons.³⁰ They claim that due to the repulsion between them, excitons can not occupy the same spatial position and hence they behave like fermions. Further experimental investigation in the range below T_c is expected to shed light on the nature of the observed transition.

Chapter 3

Layered Systems

Superconductivity of layered crystals has been of great interest with the hope of obtaining high transition temperatures.³¹ The motivation underlying the synthesis of two-dimensional (2D) systems of the sandwich type is to locate an easily polarizable medium adjacent to a conducting layer, and hence to realize the exciton mechanism of superconductivity. The transition-metal dichalcogenides and intercalation compounds have been candidates for the observation of this kind of electronic pairing mechanisms. Strong anisotropy of crystals of this class pointed to the fact that the superconductivity can be dealt with almost 2D motion of conduction electrons. The discovery of copper oxide superconductors³² opened new horizons in the field of low-dimensional systems. Several experiments have led to the conclusion that charge carriers in these high- T_c materials are mainly localized in 2D copper oxide planes separated by insulating media. Not only their unusually high critical temperatures but also peculiar normal state properties of high- T_c compounds have been subject to several studies.

In this chapter we are going to concentrate on layered systems, where 2D Fermi liquids are coupled weakly in the third direction. In the next section we study the transition temperature of a superconductor-insulator superlattice with a particular type of interlayer interaction. Then, we explore the Ginzburg-Landau version of the model to understand the dimensional crossover observed in these systems. In the last section, starting from a microscopic mechanism, we show that

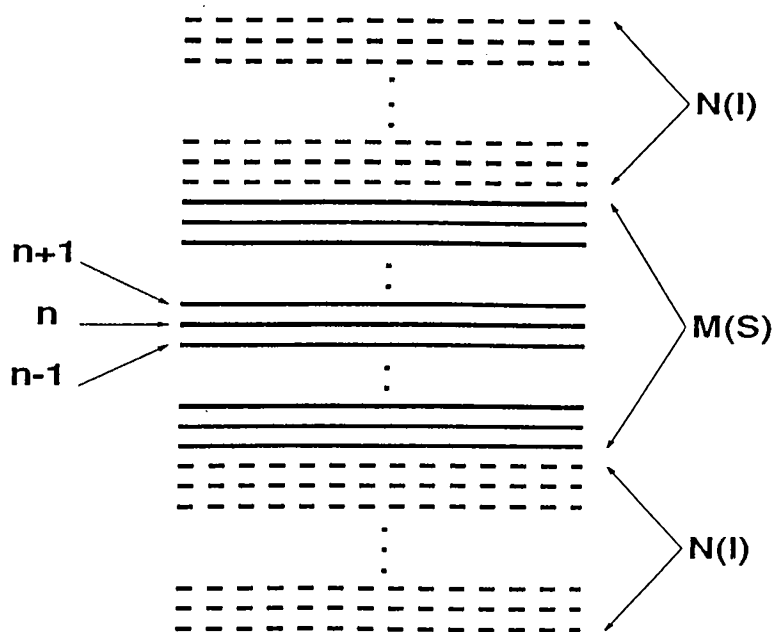


Figure 3.1: Superconductor-Insulator superlattice

Schematic sketch of the superlattice consisting of M cells of superconducting material (S) separated by N unit cells thick insulating (I) layers. The letter n labels the unit cells within S.

interlayer tunneling process coupled to phonons can induce superconductivity in metallic layers.

3.1 Microscopic Theory

Recently, considerable progress has been made in fabricating and studying $(M \times N)$ superlattices, in which YBCO layers consisting of M ($=1, 2, 3, 4, \dots$) unit cells are separated by insulating PrBCO layers N unit cells thick.³³⁻³⁷ By varying N and M independently, the dependence of the critical temperature T_c on the YBCO thickness (M) and the intercell separation (N) has been determined. According to these measurements, T_c initially decreases rapidly with increasing PrBCO thickness (N), but saturates at $T_c=20, 53$ and 72 K for $M=1, 2$ and 3 , respectively. The fact that T_c of nearly isolated YBCO slabs strongly depends on the number M of adjacent YBCO unit cells can be interpreted as

an evidence for an intercell pairing interaction between YBCO cells, raising T_c from 20 K (corresponding to $M=1$, $N=20$) to the bulk value 92 K. A related phenomenon is the rise of T_c with the number of CuO_2 layers (l) in the bismuth and thallium compounds ($\text{Bi}_2\text{Ca}_{l-1}\text{Sr}_2\text{Cu}_l\text{O}_x$, $\text{Tl}_2\text{Ca}_{l-1}\text{Sr}_2\text{Cu}_l\text{O}_x$).^{38,39} Moreover, a significant increase in T_c was also observed in ultrathin NbSe_2 films, as the number of unit cells was increased.⁴⁰ These experimental findings suggest that superconductivity occur in a layer as thick as one unit cell, but that coupling between superconducting layers is needed to reach the higher bulk value. The rise of T_c with the number of layers is not restricted to high- T_c materials, but appears to be a common feature of all layered superconductors when finite-size effects become important. Furthermore, as we will see, a similar phenomenon has also been observed in magnetic systems composed of weakly coupled layers.

In this section, we present a microscopic model for the explanation of these phenomena.⁴¹ For this purpose, we extend the theory of layered superconductors⁴²⁻⁴⁴ by adopting a mixed representation for the single-particle wave functions. In this representation, for the intra-plane degrees of freedom, momentum space wave function is used while the interplane motion is studied directly in the real space. Taking the scattering of two carriers within and between adjacent layers into account, there are four possible processes as sketched in figure 3.2. The intracell process (i) and the intercell processes ((ii) and (iii)) have been widely studied.⁴²⁻⁴⁴ Here, we also consider the interaction (iv), which turns out to be indispensable for obtaining the observed dependence of T_c on M and N . We solve the problem using the mean field approximation. To this end, we derive the Gorkov's equations for the Green's functions in the mixed representation and solve them with free end boundary conditions.

We start with a brief description of the extension of the Gorkov's equations.⁴⁵ In the mixed representation, the electron field operators are expressed in terms of the states $\{n, \vec{p}\}$. Here n labels the unit cells in the superconducting slabs and \vec{p} is the wave vector parallel to the (a, b) -plane. This is the most natural representation, since the electrons exhibit wave functions extended in the planes and localized in the perpendicular direction. Therefore, the electron field operator

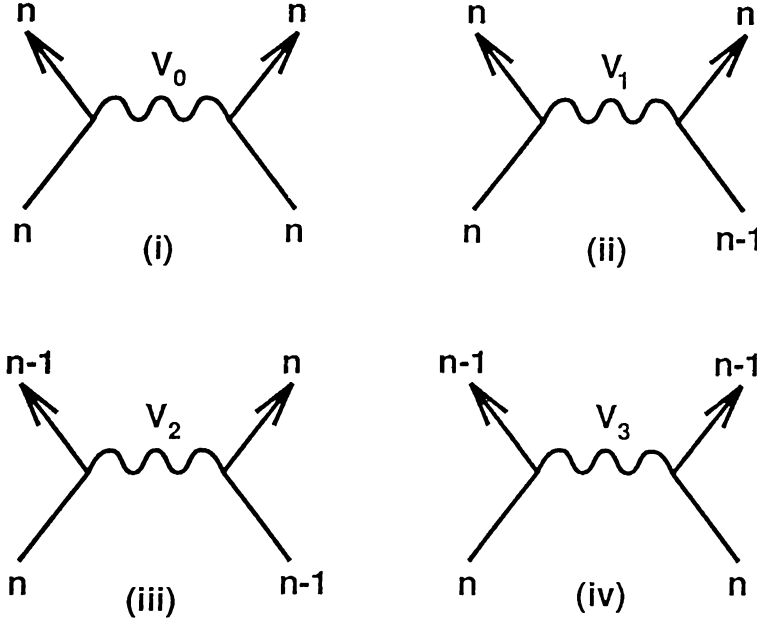


Figure 3.2: Scattering processes of two carriers due to $V_{n_1 n_2 n_3 n_4}$. Here, n labels the cells and $n \pm 1$ the adjacent ones. V_m denotes the coupling constant of the corresponding potential $V_{n_1 n_2 n_3 n_4}$.

$\Psi_\sigma(\vec{r})$ can be written as

$$\Psi_\sigma(\vec{r}) = \sum_{n\vec{p}} \phi_{n\vec{p}}(\vec{r}) c_{n\vec{p}\sigma} \quad , \quad (3.1)$$

where we made an expansion for $\Psi_\sigma(\vec{r})$ in $n\vec{p}$ -basis. Here, $c_{n\vec{p}\sigma}$ is the creation operator for an electron in layer n with momentum (in the layer) \vec{p} and $\phi_{n\vec{p}}(\vec{r})$ is the corresponding expansion coefficient which is nothing but a wave function localized at layer n . We will consider a very general problem. Electrons, localized into the planes with 2D energy bands $\epsilon(\vec{p})$, can jump from one layer (n) to another (n'). These two motions, in-plane and interplane hopping processes, give a 3D energy band structure with relatively flat bands in the perpendicular direction. Introducing a general pairing potential $V(\vec{r}, \vec{r}')$, the Hamiltonian reads

$$H = \sum_{n\vec{p}\sigma} \epsilon(\vec{p}) c_{n\vec{p}\sigma}^\dagger c_{n\vec{p}\sigma} + \sum_{nn'\sigma} t_{nn'} c_{n\vec{p}\sigma}^\dagger c_{n'\vec{p}\sigma} \quad (3.2)$$

$$+ \frac{1}{2} \sum_{n_1 n_2 n_3 n_4 \vec{p}\vec{p}' \vec{q}\vec{q}\sigma\sigma'} V_{n_1 n_2 n_3 n_4} c_{n_1 \vec{p} + \vec{q}\sigma}^\dagger c_{n_2 \vec{p}' - \vec{q}\sigma'}^\dagger c_{n_3 \vec{p}'\sigma'} c_{n_4 \vec{p}\sigma}$$

where

$$V_{n_1 n_2 n_3 n_4} = \frac{1}{2} \int d\vec{r} d\vec{r}' \phi_{n_1 \vec{p} + \vec{q}}^\dagger(\vec{r}) \phi_{n_2 \vec{p}' - \vec{q}}^\dagger(\vec{r}') V(\vec{r}, \vec{r}') \phi_{n_3 \vec{p}'}(\vec{r}') \phi_{n_4 \vec{p}}(\vec{r}) . \quad (3.3)$$

$t_{nn'}$ is the single-particle hopping integral between the layers n and n' . Here we assume that during the hopping process, spin σ and the momentum \vec{p} (which is parallel to the planes) are conserved. Apparently, the pairing potential involves four layer indices. This exhausts all possible interactions between two electrons. We have dropped the momentum indices because in our calculations we are going to assume that the interactions are independent of them (or we use the interaction matrix elements averaged over the Fermi surface). The pairing of electrons causes correlations in their relative motion which can be described by the Green's functions⁴⁶

$$\begin{aligned} G_{nn'}(\vec{p}, \tau - \tau') &= - \langle T_\tau c_{n\vec{p}\sigma}(\tau) c_{n'\vec{p}\sigma}^\dagger(\tau') \rangle \\ F_{nn'}(\vec{p}, \tau - \tau') &= \langle T_\tau c_{n-\vec{p}1}(\tau) c_{n'\vec{p}1}(\tau') \rangle \\ F_{nn'}^\dagger(\vec{p}, \tau - \tau') &= \langle T_\tau c_{n\vec{p}1}^\dagger(\tau) c_{n'-\vec{p}1}(\tau') \rangle \end{aligned} \quad (3.4)$$

Using the equations of motion, we will derive the self consistency equations for the correlation functions G , F and F^\dagger . It is enough to consider one of F and F^\dagger because both give the same equation. Since the Green's functions are defined in terms of the expectation values of the electron field operators, we will need (imaginary) time derivatives of these operators. We first consider

$$\frac{\partial}{\partial \tau} c_{n\vec{p}\sigma}(\tau) = [H, c_{n\vec{p}\sigma}(\tau)] = -\epsilon(\vec{p}) c_{n\vec{p}\sigma} - \sum_{n_2 n_3 n_4 \vec{p}' \vec{q} \sigma'} V_{nn_2 n_3 n_4} c_{n_2 \vec{p}' - \vec{q} - \sigma}^\dagger c_{n_3 \vec{p}' - \sigma} c_{n_4 \vec{p} - \vec{q} \sigma} . \quad (3.5)$$

In the interaction term n_2 , n_3 and n_4 are dummy indices while n labels the operator $c_{n\vec{p}\sigma}$. From the definition of the time ordering operator T_τ , the time development of G can easily be found by the help of the rule for taking the derivative of a product. Since

$$\frac{\partial}{\partial \tau} G_{nn'}(\vec{p}, \tau - \tau') = -\delta(\tau - \tau') \delta_{nn'} - \langle T_\tau \left[\frac{\partial}{\partial \tau} c_{n\vec{p}\sigma}(\tau) \right] c_{n'\vec{p}\sigma}^\dagger(\tau') \rangle , \quad (3.6)$$

we can substitute the above expression for the time derivative of the operator $c_{n\vec{p}\sigma}(\tau)$ and end up with

$$\begin{aligned} & \left(-\frac{\partial}{\partial\tau} - \epsilon(\vec{p})\right)G_{nm'}(\vec{p}, \tau - \tau') \\ + \sum_{n_2 n_3 n_4 \vec{p}' \vec{q} \sigma'} V_{n_2 n_3 n_4} & \langle T_\tau c_{n_2 \vec{p}' - \vec{q} - \sigma'}^\dagger(\tau) c_{n_3 \vec{p}' - \sigma'}(\tau) c_{n_4 \vec{p} - \vec{q} \sigma}(\tau) c_{n' \vec{p} \sigma}^\dagger(\tau') \rangle = \delta(\tau - \tau') \delta_{nn'} . \end{aligned} \quad (3.7)$$

To derive an equation for G and F^\dagger , everything should be expressed in terms of these two functions. However, the above equation contains a four operator term which cannot be reduced to two. For this purpose, we apply a mean field approximation which is equivalent to replacing the four operator terms by two operator terms multiplied by the expectation value of the other two.⁴⁵ As a result, equation 3.7 takes the form

$$\begin{aligned} & \left(-\frac{\partial}{\partial\tau} - \epsilon(\vec{p})\right)G_{nm'}(\vec{p}, \tau - \tau') \\ + \sum_{n_2 n_3 n_4 \vec{p}' \vec{q} \sigma'} V_{n_2 n_3 n_4} & [\delta_{n_2 n_4} \delta_{\vec{p}' \vec{q}} \delta_{\sigma \sigma'} n_{n_2 \vec{p} - \vec{q}} G_{n_3 n'}(\vec{p}, \tau - \tau') \\ & - \delta_{\sigma_1 - \sigma'} \delta_{\vec{p}' \vec{q} - \vec{p}} F_{n_3 n_4}(\vec{p} - \vec{q}) F_{n' n_2}^\dagger(\vec{p}, \tau' - \tau)] = \delta(\tau - \tau') \delta_{nn'} . \end{aligned} \quad (3.8)$$

A similar equation can be derived for F^\dagger . This time we start with the equation of motion for $c_{n\vec{p}\sigma}^\dagger(\tau)$, which is given by

$$\frac{\partial}{\partial\tau} c_{n\vec{p}\sigma}^\dagger(\tau) = [H, c_{n\vec{p}\sigma}^\dagger(\tau)] = -\epsilon(\vec{p}) c_{n\vec{p}\sigma}^\dagger - \sum_{n_1 n_2 n_3 \vec{p}' \vec{q} \sigma'} V_{n_1 n_2 n_3 n} c_{n_1 \vec{p}' - \vec{q} - \sigma}^\dagger c_{n_2 \vec{p}' + \vec{q} \sigma'} c_{n_3 \vec{p}' \sigma'} . \quad (3.9)$$

Then from

$$\frac{\partial}{\partial\tau} F_{nm'}^\dagger(\vec{p}, \tau - \tau') = \langle T_\tau \left[\frac{\partial}{\partial\tau} c_{n\vec{p}\sigma}^\dagger(\tau) \right] c_{n' - \vec{p} \sigma}^\dagger(\tau') \rangle , \quad (3.10)$$

we obtain

$$\begin{aligned} & \left(-\frac{\partial}{\partial\tau} + \epsilon(\vec{p})\right)F_{nm'}^\dagger(\vec{p}, \tau - \tau') \\ + \sum_{n_1 n_2 n_3 \vec{p}' \vec{q} \sigma'} V_{n_1 n_2 n_3 n} & \langle T_\tau c_{n_1 \vec{p} - \vec{q} \sigma}^\dagger(\tau) c_{n_2 \vec{p}' + \vec{q} \sigma'}^\dagger(\tau) c_{n_3 \vec{p}' \sigma'}(\tau) c_{n' - \vec{p} \sigma}^\dagger(\tau') \rangle = 0 . \end{aligned} \quad (3.11)$$

Note that there is no Dirac delta term in contrast to the equation for G . This is because F^\dagger involves two creation operators. For small fluctuations, the four

operator term can again be approximated by means of the mean field theory. The analogue of equation 3.8 is

$$\begin{aligned}
& \left(-\frac{\partial}{\partial \tau} + \epsilon(\vec{p})\right) F_{nn'}^\dagger(\vec{p}, \tau - \tau') \quad (3.12) \\
& - \sum_{n_1 n_2 n_3 \vec{p}' \vec{q} \sigma'} V_{n_1 n_2 n_3 n} \delta_{\sigma' 1} \delta_{\vec{p}' - \vec{p}} F_{n_1 n_2}^\dagger(\vec{p} - \vec{q}, 0) G_{n_3 n'}(-\vec{p}, \tau - \tau') \\
& \quad + \sum_{n_1 n_2 n_3 \vec{p}' \vec{q} \sigma'} V_{n_1 n_2 n_3 n} \delta_{\vec{q} 0} \delta_{n_2 n_3} n_{n_2 \vec{p}'} F_{n_1 n'}^\dagger(\vec{p}, \tau - \tau') \\
& \quad + \sum_{n_1 n_2 n_3 \vec{p}' \vec{q} \sigma'} V_{n_1 n_2 n_3 n} \delta_{\vec{p}' \vec{p} - \vec{q}} \delta_{\sigma' 1} \delta_{n_1 n_2} n_{n_1 \vec{p} - \vec{q}} F_{n_2 n'}^\dagger(\vec{p}, \tau - \tau') = 0 \quad .
\end{aligned}$$

Equations 3.8 and 3.12 can be written as two coupled set of algebraic equations by introducing the Fourier transforms of the Green's functions

$$\begin{aligned}
G_{nn'}(\vec{p}, \tau) &= \frac{1}{\beta} \sum_{\omega_l} e^{-i\omega_l \tau} G_{nn'}(\vec{p}, i\omega_l) \quad (3.13) \\
F_{nn'}(\vec{p}, \tau) &= \frac{1}{\beta} \sum_{\omega_l} e^{-i\omega_l \tau} F_{nn'}(\vec{p}, i\omega_l) \\
F_{nn'}^\dagger(\vec{p}, \tau) &= \frac{1}{\beta} \sum_{\omega_l} e^{-i\omega_l \tau} F_{nn'}^\dagger(\vec{p}, i\omega_l)
\end{aligned}$$

where β is the inverse temperature and ω_l 's are the Matsubara frequencies. Substituting the transforms into equations 3.8 and 3.12, we obtain the Gorkov's equations.

$$\begin{aligned}
& [i\omega_l - \epsilon(\vec{p})] G_{nn'}(\vec{p}, i\omega_l) - \sum_{n' \neq n} t_{nn'} G_{nn'}(\vec{p}, i\omega_l) \quad (3.14) \\
& - \sum_{n_2 n_3 n_4 \vec{q}} V_{nn_2 n_3 n_4}(\vec{q}) F_{n_3 n_4}(\vec{p} - \vec{q}, 0) F_{n' n_2}^\dagger(\vec{p}, i\omega_l) = \delta_{nn'} \\
& [i\omega_l + \epsilon(\vec{p})] F_{nn'}^\dagger(\vec{p}, i\omega_l) + \sum_{n' \neq n} t_{nn'} F_{nn'}^\dagger(\vec{p}, i\omega_l) \\
& - \sum_{n_1 n_2 n_3 \vec{q}} V_{n_1 n_2 n_3 n}(\vec{q}) F_{n_1 n_2}^\dagger(\vec{p} - \vec{q}, 0) G_{n_3 n'}(\vec{p}, i\omega_l) = 0
\end{aligned}$$

This system is still complicated to find a complete solution. According to the observation that the in-plane coherence length ξ_{ab} is large compared to ξ_c , we can neglect several processes. Confinement of the pairs into the layers can be interpreted as an evidence for the weakness of the interlayer correlations which

implies that $F_{nn'}^\dagger$ is diagonal, i.e. vanishing for $n \neq n'$. Thus, the dominating pairing interactions must be those in which both carriers belong to the same layer. Among the processes shown in figure 3.2, (ii) and (iii) involve interlayer correlations and hence we neglect them. (i) is already a completely in-plane process. In spite of the fact that (iv) is an interlayer interaction, it can be described by diagonal $F_{nn'}^\dagger$ elements and hence we keep it. We will also discard the single particle hopping $t_{nn'}$ not only because it is small but mainly due to the fact its only effect is to introduce anisotropy to the system. Our interest is not the conventional anisotropic superconductivity. As we have mentioned above, we assume that $V_{n_1 n_2 n_3 n_4}(\vec{q})$ is independent of \vec{q} , since \vec{q} -dependence gives rise only to gap anisotropy within the (a,b)-planes. Therefore, we are left with the pairing interactions $V_0 = -V_{nnnn}$ and $V_3 = -V_{n\pm 1n\pm 1nn}$. After all these simplifications let us rewrite the Gorkov's equations as

$$\begin{aligned}
 & [i\omega_l - \epsilon(\vec{p})]G_n(\vec{p}, i\omega_l) & (3.15) \\
 -F_n^\dagger(\vec{p}, i\omega_l) \sum_{\vec{q}} V_0 F_n(\vec{p} - \vec{q}, 0) + V_3 [F_{n+1}(\vec{p} - \vec{q}, 0) + F_{n+1}(\vec{p} - \vec{q}, 0)] & = 1 \\
 & [i\omega_l + \epsilon(\vec{p})]F_n^\dagger(\vec{p}, i\omega_l) \\
 -G_n(\vec{p}, i\omega_l) \sum_{\vec{q}} V_0 F_n^\dagger(\vec{p} - \vec{q}, 0) + V_3 [F_{n+1}^\dagger(\vec{p} - \vec{q}, 0) + F_{n-1}^\dagger(\vec{p} - \vec{q}, 0)] & = 0
 \end{aligned}$$

where $G_n = G_{nn}$ and $F_n^\dagger = F_{nn}^\dagger$. We are going to solve this equation for a periodic system in which M unit cells of a superconducting material are separated by insulating layers that are N unit cells thick. The values of the correlation functions G and F^\dagger for $\tau = 0$ can be found by doing the summations over the Matsubara frequencies using the contour integration.⁴⁵ Since, we are interested in the critical temperature T_c , we investigate the solution for $T \simeq T_c$ at which the energy gap vanishes and hence we end up with the condition that the determinant

of the matrix

$$\begin{bmatrix} X & Y & 0 & 0 & & & & & & . \\ Y & X & Y & 0 & & & & & & . \\ 0 & Y & X & Y & . & & & & & . \\ 0 & 0 & Y & X & Z & . & . & . & & . \\ . & & & Z & X & Y & 0 & . & & . \\ & & & & Y & X & & . & & . \\ & & & & 0 & & & . & & . \\ . & & & & & & & . & & . \end{bmatrix} \quad (3.16)$$

must be zero. Here all the blocks on the diagonal are $M \times M$ square matrices and the entries are given by

$$X = 1 - V_0 f \quad (3.17)$$

$$Y = -V_3 f$$

$$Z = Z(N) := -V_3 \exp(-\kappa N d)$$

where

$$f = \sum_{\vec{p}} \frac{1}{\epsilon(\vec{p})} \tanh \frac{\beta_c \epsilon(\vec{p})}{2} \quad (3.18)$$

and $\beta_c = 1/k_B T_c$. Y describes the pairing interaction V_3 acting between the unit cells in the superconducting material and $Z(N)$ that between the stacks separated by N insulating units. $Z(N)$ is expected to decay exponentially according to $Z(N) = -V_3 \exp(-\kappa N d)$, where d denotes the c-axis lattice constant of the insulator. For large N , we have widely separated superconducting stacks consisting of M units ($Z(N)=0$). In this limiting case the determinant equation reduces to

$$1 - [V_0 + 2|V_3| \cos(\frac{\pi}{M+1})] f = 0 \quad (3.19)$$

For $M=1$, corresponding to an isolated unit cell, T_c is the lowest and fixed by V_0 . In the bulk, where $M \rightarrow \infty$, the effective coupling and, in turn, T_c reach their maximum values. As a consequence, the M -dependence of T_c is traced back to the interaction V_3 and its interesting property to form pairs within the unit cells by an intercell interaction. Owing to this intercell coupling, the effective interaction

becomes M -dependent, namely $2|V_3| \cos[\pi/(M+1)]$ and varies for $M=1$ to ∞ between 0 and $2|V_3|$. Considering the bulk as the infinite system, we see that the M -dependence of T_c is a finite size effect, corresponding to the crossover from the nearly two to three dimensional behavior. This phenomenon has been observed in YBCO/PrBCO superlattices³³⁻³⁷ and in ultrathin NbSe₂ films.⁴⁰ To illustrate this behavior, we use the weak coupling solution of equation 3.19. For an unretarded pairing interaction, the sum in the definition of f extends from the bottom to the top of the band, i.e. \vec{p} must run over all the occupied states. In the end, we obtain

$$T_c = \Theta \exp\left[-\frac{1}{\lambda_0 + 2\lambda_3 \cos[\pi/(M+1)]}\right] \quad (3.20)$$

with $\lambda_0 = D(0)V_0$, $\lambda_3 = D(0)V_3$. Here $D(0)$ is the density of states at the Fermi level. Due to the assumed nature of the pairing interaction, Θ is given in terms of the Fermi energy E_F (measured from the bottom of the band) and the bandwidth W , by⁴³

$$k_B \Theta = \sqrt{E_F(W - E_F)} \quad (3.21)$$

Determining Θ , λ_0 and λ_3 from the experimental values of $T_c(M)$ for $M=1, 2$, and 3 , equation 3.21 leads to the M -dependence of T_c shown in figure 3.3. Here we have also included the experimental data for comparison. The resulting parameters are $\Theta=4000$ K, $\lambda_0=0.19$ and $\lambda_3=0.04$, consistent with our assumption that $\Theta \gg T_c$. Apparently, even the weak coupling expression describes the essential features of the M -dependence of T_c very well. Initially T_c increases rapidly with M and saturate for large values. To provide further evidence for the importance of the pairing interaction V_3 , we turn to the variation of T_c with N for fixed M -values. For $M=1$ to 4 , the $M \times N$ matrix vanishes if

$$[V_0 + 2F(M, N)] = 1 \quad (3.22)$$

where

$$\begin{aligned} F(1, N) &= |V_3| \exp(-\kappa N d) \quad (3.23) \\ F(2, N) &= \frac{1}{2} [F^2(1, N) + 2F(1, N)|V_3| + V_3^2]^{1/2} \end{aligned}$$

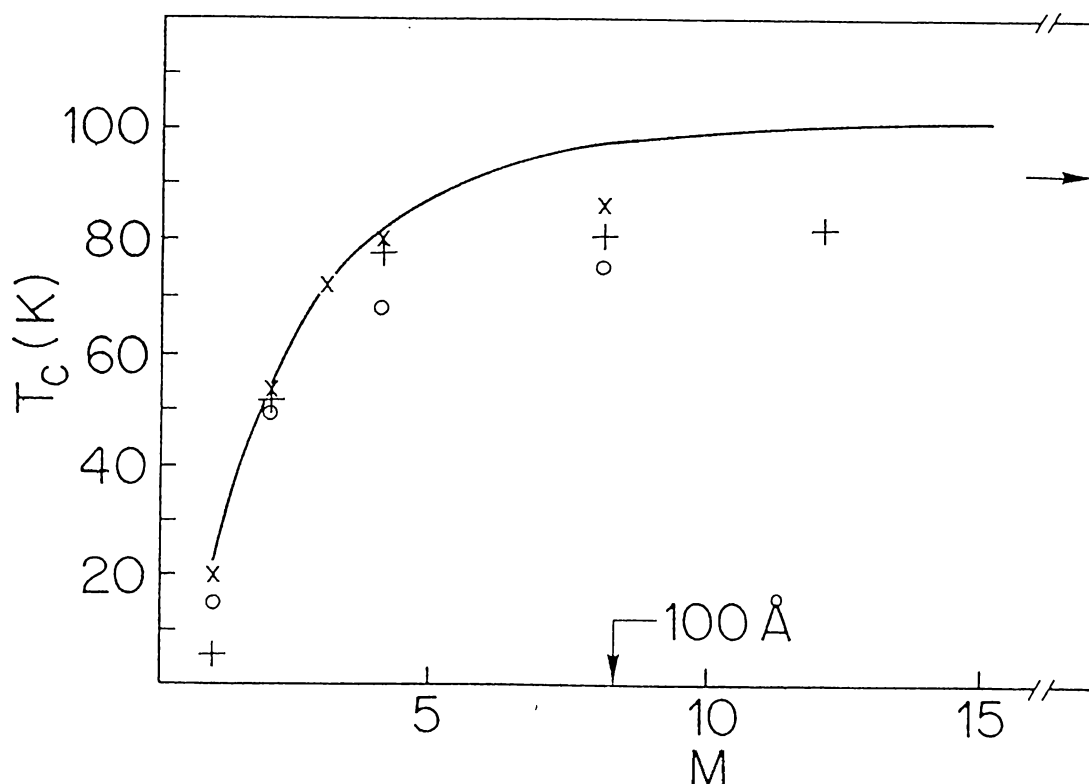


Figure 3.3: T_c for isolated YBCO stacks with M unit cells

The solid line is obtained from equation 3.21. The experimental data was taken from references \times :37, o :35, $+$:36. In determining θ , λ_0 and λ_3 we used $T_c(M = 1, 2, 3)$ of reference 37. The arrow at the right hand side marks the experimental bulk value of T_c .

$$\begin{aligned}
 F(3, N) &= \frac{1}{4}[F(1, N) + \sqrt{8V_3^2 + F^2(1, N)}] \\
 F(4, N) &= \frac{1}{2\sqrt{2}}[3V_3^2 + F^2(1, N) \\
 &+ \sqrt{(3V_3^2 + F^2(1, N))^2 - 4(V_3^4 - 2V_3^3 F(1, N) + V_3^2 F^2(1, N))}]^{1/2} .
 \end{aligned}$$

For $N=0$, these expressions reduce to the equation for the bulk superconductor, while for $N \rightarrow \infty$ one recovers equation 3.19. To illustrate the N -dependence of T_c for fixed M , we again use the weak coupling solutions corresponding to equation 3.20. The only additional parameter, κ , was determined from the experimental data for $M=1$, yielding $\kappa=0.03 \text{ \AA}^{-1}$. The resulting $T_c(M, N)$ is depicted in figure 3.4, including the experimental values for comparison. In

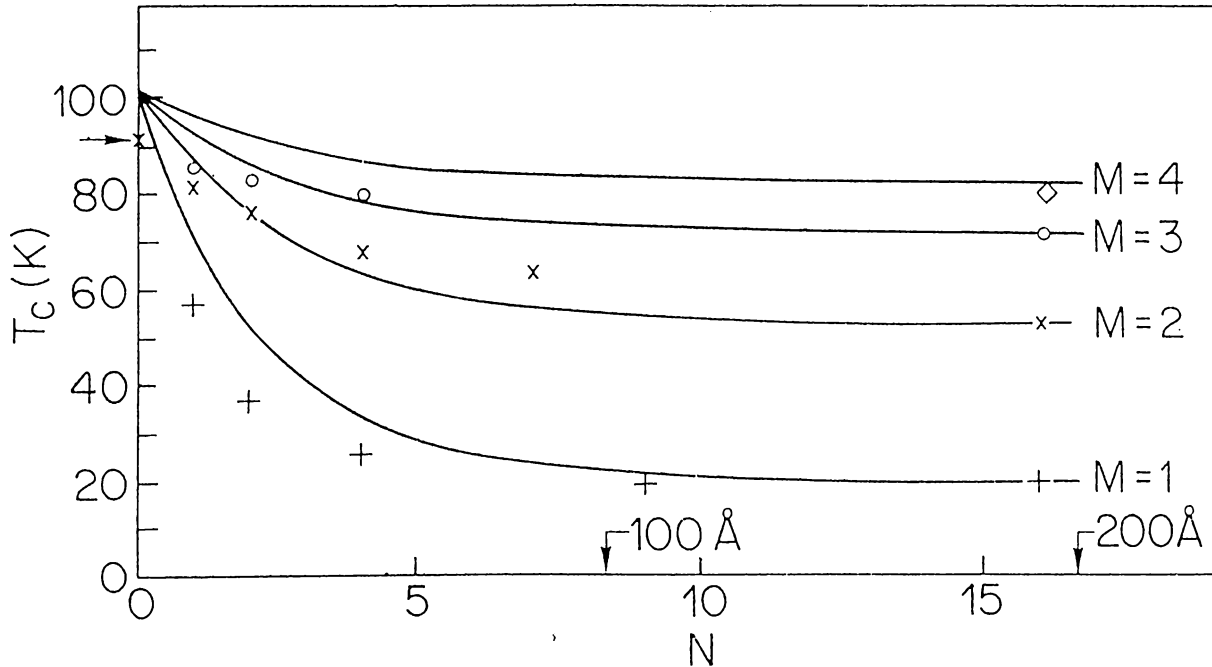


Figure 3.4: $T_c(M, N)$ for YBCO/PrBCO superlattice

The solid lines are obtained from the weak coupling solution. κ was determined from the experimental data for $M=1$. The experimental values were taken from reference 37: $+$ $M=1$; \times $M=2$; \circ $M=3$, and \diamond $M=4$. The arrow marks the experimental bulk value of T_c .

view of the fact that we only fixed κ , the inverse decay length of the coupling V_3 between YBCO layers separated by PrBCO, it is quite remarkable that the theoretical curves reproduce the essential trends. Moreover, $1/\kappa=30 \text{ \AA}$ points to an interlayer interaction of rather long range.

To summarize, we have extended the theory of layered superconductors by including the intercell interaction V_3 , which pairs carriers within a unit cell. It renormalizes the intracell interaction, but its effective strength varies between 0 ($M=1$) and $2|V_3|$ ($M \rightarrow \infty$), depending on the number M of unit cells in the superconducting slabs. Because T_c saturates at the bulk value, the M -dependence of T_c is a finite size effect, corresponding to the crossover from nearly two to three dimensional behavior. Considering then the CuO_2 layers (l) in the bismuth

and thallium compounds ($\text{Bi}_2\text{Ca}_{l-1}\text{Sr}_2\text{Cu}_l\text{O}_x$, $\text{Tl}_2\text{Ca}_{l-1}\text{Ba}_2\text{Cu}_l\text{O}_x$)^{38,39} as units, the rise of T_c with l can be understood along these lines also. It should be kept in mind, however, that the present treatment corresponds to a mean field solution, leaving room for improvement. Nevertheless, we have identified the pairing interaction that raises T_c from low (20 K) to high (92 K) temperature. Finally, we note that the Ginzburg-Landau functional for the model treated here differs markedly from the widely used Lawrence-Doniach free energy as we are going to show in the next section.

Before closing this section, we will present a possible microscopic mechanism, an electrostatic model leading to V_3 . The interlayer coupling constant V_3 is given by

$$V_3 = \frac{1}{2} \int d\vec{r} d\vec{r}' \phi_{n\vec{p}+\vec{q}}^\dagger(\vec{r}) \phi_{n\vec{p}-\vec{q}}^\dagger(\vec{r}') V(\vec{r}, \vec{r}') \phi_{n+1\vec{p}'}(\vec{r}') \phi_{n+1\vec{p}}(\vec{r}) . \quad (3.24)$$

V_3 corresponds to the process in which two electrons moving in the S sheet of a unit cell n are scattered together to the cell $n \pm 1$. The term V_3 vanishes if there is no overlap between the wave functions of the consecutive layers $t = \int \phi_n(\vec{r}) \phi_{n+1}(\vec{r}) d\vec{r}$. Since the overlap, which increases with the integrand $\phi_n(\vec{r}) \phi_{n+1}(\vec{r})$, will be largest between the superconducting S sheets, V_3 is essentially the Coulomb repulsion e^2/ρ of electrons between two S units, where ρ denotes the separation of the electrons parallel to the planes. For metallic S sheets, the bare Coulomb repulsion will be reduced by the interaction of one electron with the images of the other and by the effect of polarization. In the electrostatic limit, V_3 can be estimated from^{47,48}

$$V_3 \simeq t^2 V(\rho, d) \quad (3.25)$$

where

$$V(\rho, d) = \frac{e^2}{d} V(r), \quad r = \frac{\rho}{d} \quad (3.26)$$

and

$$V(r) = \frac{1}{r} + 2 \sum_{n=1}^{\infty} \frac{(-1)^n}{(r^2 + n^2)^{1/2}} - 16\pi\alpha \frac{1}{(1 + r^2)^{3/2}} . \quad (3.27)$$

The first term is the bare Coulomb repulsion, reduced by the second contribution, which describes the interaction of one electron with the images of

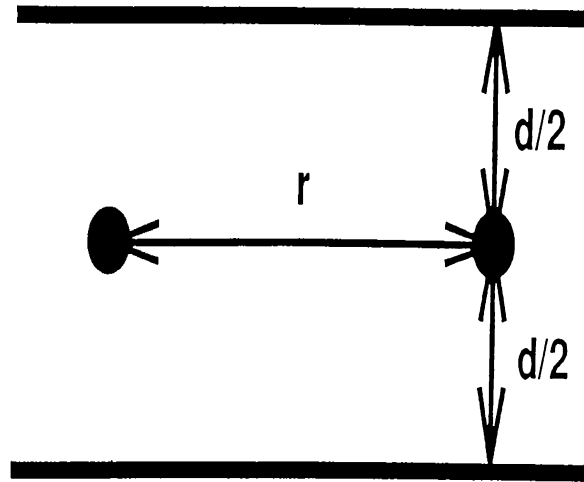


Figure 3.5: Electrostatic model of the interaction V_3 . V_3 corresponds to the electrostatic interaction of two electrons separated by a distance r between two conducting plates of separation d .

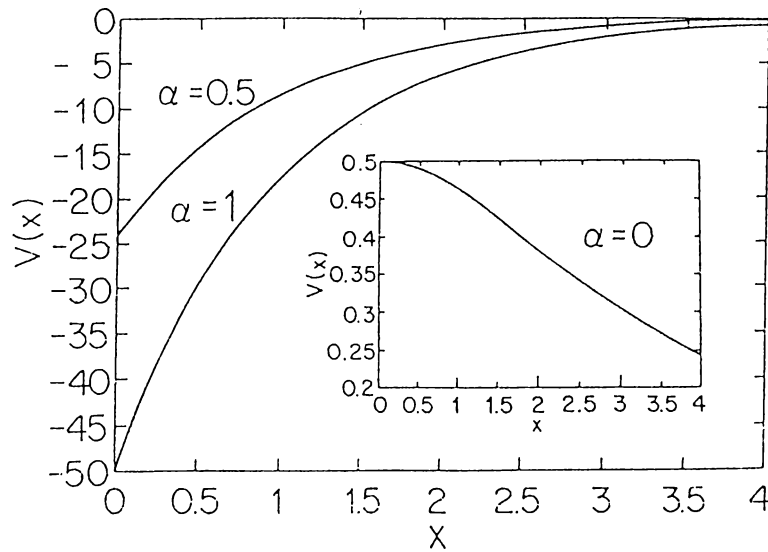


Figure 3.6: Momentum dependence of the interlayer interaction V_3 . Vertical axis is $V(pd = x)$ for $\alpha=0, 0.5$ and 1 .

the other. The third term arises from the polarization effects. An electron interact with the dipoles induced by the other, with the moments oriented perpendicular to the sheets. These in turn lower the energy of the second electron in proportion

to the polarizability α of the layer. We neglected here the effect of screening. This is justified in the copper oxides with pronounced ionic nature. More generally, the polarizability is frequency dependent

$$\alpha(\omega) = \sum_m \frac{\alpha_m}{1 - (\omega/\omega_m)^2} + \sum_l \frac{\alpha_{el}}{1 - (\omega/\omega_l)^2} . \quad (3.28)$$

The first term comes from the optical phonons with frequency ω_m , while the second one is the electronic contribution with $\hbar\omega_l$ of the order of an atomic excitation energy. Here we assume that the dominant contribution to superconductivity comes from the energy shell $\pm k_B\Theta$ around the Fermi level with $\hbar\omega_m < k_B\Theta < \hbar\omega_l$. In this case V_3 is unretarded and given by equation 3.1 with $\alpha = \alpha_e$. Of greater relevance is the Fourier transform of $V(\rho)$,

$$V_3 = t^2 \frac{2\pi e^2 d}{a^2} \int_0^\infty dr r J_0(pdr) V(r) = t^2 \frac{2\pi e^2 d}{a^2} V(pd) \quad (3.29)$$

where for $pd = x$,

$$V(x) = \frac{1}{x} + 2 \sum_{n=1}^{\infty} \frac{(-1)^n}{x} \exp(-nx) - 16\pi\alpha \exp(-x) . \quad (3.30)$$

The momentum dependence of V is depicted in figure 3.6 for $\alpha=0, 0.5$ and 1 . As expected, sufficiently large polarizability leads to attraction, namely to a range of p values where $V_3(\vec{p})$ is negative. As far as superconductivity is concerned, the coupling mediated by $V_3(\vec{p})$ comes from the scattering of electrons with Fermi momenta \vec{p}_F and \vec{p}'_F , with momentum transfer $|\vec{p}_F - \vec{p}'_F| = p$. According to the photoemission results⁴⁹ and the band structure calculations,⁵⁰ we approximate the Fermi surface by a circle around the X point of the Brillouin zone, as shown in figure 3.7. To estimate the coupling strength, we average V_3 over the hole Fermi surface with radius $k_F \simeq \pi/2a$. We call this average g_3 and use for V_3 in our model where we assumed that the interaction is momentum independent.

Thus

$$g_3 = t^2 \frac{2\pi e^2 d}{a^2} \langle V(x) \rangle \quad (3.31)$$

where

$$\langle V \rangle = \frac{1}{\pi} \int_0^\pi d\phi V(d\sqrt{2}k_F\sqrt{1 - \cos\phi}) . \quad (3.32)$$

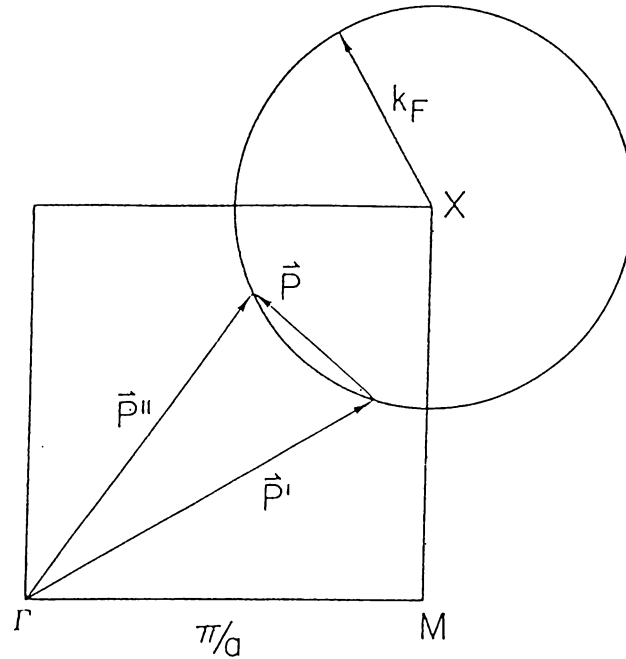


Figure 3.7: Fermi surface and irreducible part of the Brillouin zone k_F is the radius of the hole Fermi surface. A typical scattering process on the Fermi surface due to $V_3(p)$ is also shown.

Replacing d by $d(N) = d \times (N + 1)$, with $d=12 \text{ \AA}$, the thickness of YBCO or PrBCO unit cells, we obtain

$$\lambda_3(N) = 2\pi e^2 t^2 d(N) \langle V(pd(N)) \rangle > D(0) . \quad (3.33)$$

We will use this result to explain the change of T_c with the number of S layers in the next section.

3.2 Ginzburg-Landau Formalism

Having proposed a microscopic mechanism, we will explore its Ginzburg-Landau version.⁵¹ It turns out that the order parameter coupling of the model is of Heisenberg type, analogous to layered magnets. The mean-field result for $T_c(M, N)$ is found to be in excellent agreement with experiment for ultrathin NbSe₂ crystals and Sn-SiO, Al-AlO₂, YBCO/PrBCO superlattices.

The fact that $T_c(M, N)$ increases with increasing M is traced back to a finite size effect, corresponding to a crossover from nearly two to three dimensional superconductivity. This change from low to high-temperature superconductivity is found to be independent of the sign of the interlayer interaction. We will show that the orbital upper critical field H_{c2}^{\parallel} is unlimited while H_{c2}^{\perp} is proportional to $T_c(M, N)$.

The mechanisms responsible for the behavior of the cuprate high-temperature superconductors have remained elusive. Nevertheless these materials also share a generic property of layered superconductors, including superlattices, namely that the transition temperature exhibits a pronounced size dependence. This property appears to be very similar to the rise of T_c in layered magnetic systems, where T_c increases with the number M of magnetic layers and saturates at large M values, provided there is a finite interlayer spin interaction of ferro- or antiferromagnetic nature. Here the phenomenon has been traced back to a size effect, corresponding to a crossover from 2D to 3D behavior.⁵²⁻⁵⁶

In the previous section we identified an interlayer electron-electron interaction, which leads to a dimensional crossover in terms of a Heisenberg-like coupling between the order parameters of adjacent layers. Now, we will derive the Ginzburg-Landau functional F of the model (F has nothing to do with the correlation function that we mentioned above). If the interlayer interaction V_3 is absent, then the problem is equivalent to a well known model: Superconducting layers coupled by Josephson tunneling which is known as Lawrence-Doniach model.^{57,42} In this case F is given by

$$F = \sum_n \int d\vec{r} \left(\frac{g_0^2 D(0)}{T_1} (T - T_1) |\phi_n(\vec{r})|^2 + \eta |\phi_n(\vec{r}) - \phi_{n+1}(\vec{r})|^2 \right) . \quad (3.34)$$

where $\eta \propto t^2$. The term T_1 is the transition temperature of one unit cell, $D(0)$ is the density of states at the Fermi level, g_0 is the coupling constant for intracell pairing, which is given by the average of V_0 on the Fermi surface. It is readily verified that the interlayer coupling of this model, resulting from the single particle hopping t , does not alter T_c .

At this point, it is useful to consider a related problem, namely the transition

temperature of layered magnetic systems. For the Ising model consisting of M layers, a mean field treatment yields

$$\begin{aligned} k_B T_c(M) &= 2J(1 + \frac{|J'|}{J} \cos \frac{\pi}{M+1}) \\ &= T_1(1 + \frac{|J'|}{J} \cos \frac{\pi}{M+1}) \end{aligned} \quad (3.35)$$

where J is the ferromagnetic interaction within the sheets and J' is the interlayer coupling. Apparently, T_c is independent of the sign of J' , which merely determines the magnetic order perpendicular to the layers. The resulting increase of T_c is neither an artifact of the mean field approximation nor a peculiar feature of the Ising model.⁵²⁻⁵⁴ It also occurs in Heisenberg systems for any n , the number of components of the order parameter.⁵⁴⁻⁵⁶ The physical reason for the increase of T_c is the dimensional crossover, corresponding to a size effect driven by the increasing number of effective nearest neighbors in the bilinear interaction of the spins $S_i S_j$.

We will show that the transition temperature of layered superconductors for both conventional and high- T_c compounds is well described by equation 3.35, as far as the $\cos[\pi/(M+1)]$ dependence is concerned. This points to the existence of an interlayer interaction of Heisenberg form, namely $\phi_n \phi_{n+1} + c.c.$. In our discussion for the microscopic model, we have shown that this interaction follows from the process V_3 . A mean field treatment⁵⁸ of the model yields

$$F = \sum_n \int d\vec{r} \left(\frac{g_0^2 D(0)}{T_1} (T - T_1) |\phi_n(\vec{r})|^2 - \frac{g_3}{2} [\phi_n^\dagger(\vec{r})(\phi_{n-1}(\vec{r}) + \phi_{n+1}(\vec{r})) + c.c.] \right) . \quad (3.36)$$

where g_3 is the average of V_3 over the Fermi surface. Considering a stack of M unit cells and free end boundary conditions, minimizing the Ginzburg-Landau

functional, T_c then follows from

$$\begin{vmatrix} \tilde{X} & 1 & 0 & 0 & \dots \\ 1 & \tilde{X} & 1 & 0 & \\ 0 & 1 & \tilde{X} & 1 & \\ \cdot & & & & \\ \cdot & & & & \end{vmatrix} = 0 \quad (3.37)$$

where

$$\tilde{X} = \frac{g_0^2 D(0)}{T_1 g_3} [T_c(M) - T_1] \quad (3.38)$$

The highest T_c (which corresponds to the minimum free energy) is then given by

$$T_c(M) = T_1 \left[1 + a \cos\left(\frac{\pi}{M+1}\right) \right] \quad (3.39)$$

with

$$a = \frac{2|g_3|}{g_0^2 D(0)} = \frac{2|\lambda_3|}{\lambda_0^2} \quad (3.40)$$

In contrast to the magnetic analog (equation 3.35), a is not proportional to the ratio between the inter- and the intralayer coupling constants, but to $|\lambda_3|/\lambda_0^2$. As in the magnetic case, however, the rise of T_c with increasing M is independent of the sign of the interlayer interaction. In both layered magnets and superconductors, the substitution $\phi_n \rightarrow (-1)^n \phi_n$ leads to the same functional F , provided we change the sign of g_3 . Thus the sign of λ_3 affects only the phase of the order parameter and even a repulsive λ_3 will enhance T_c .

Turning back to the general case, where M S -unit cells are separated by

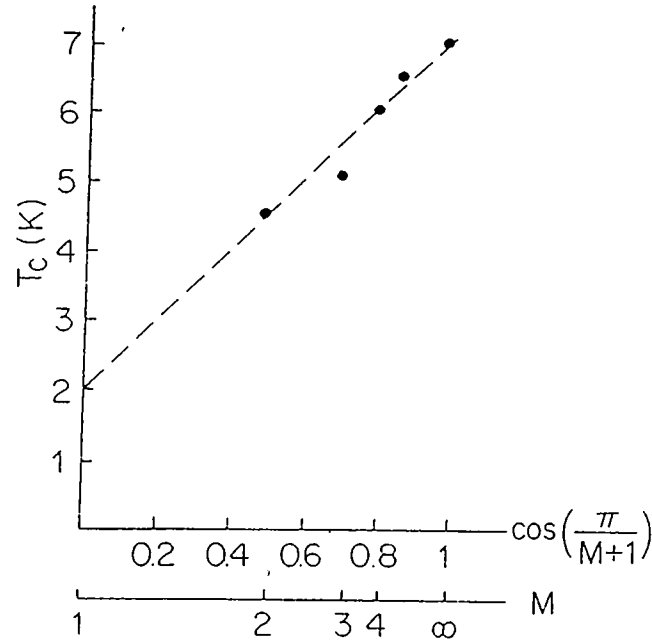


Figure 3.8: T_c of NbSe₂ versus M and $\cos \frac{\pi}{M+1}$

M is the number of Nb layers in the ultrathin crystals. •: experimental values are taken from reference 40. The straight line corresponds to $T_c(1)=2$ K and $a=2.5$ in equation 3.39.

For $N \rightarrow 0$, $a(N)$ approaches $a(0) = 2|\lambda_3|/\lambda_0$ and $T_c(M, N)$ tends to the result of the bulk superconductor, while for $N \rightarrow \infty$, $a(N) = 0$ and one recovers equation 3.39. As in the finite slab, $T_c(M, N)$ is independent of the sign of $\lambda_3(N)$, which determines the phase of the order parameter. Analogous to equation 3.39, even a repulsive coupling λ_3 enhances T_c . We will compare these results for $T_c(M, N)$ with experiments on superlattices and ultrathin films.

$T_c(M, N)$ was investigated in NbSe₂ crystals made up of stacks of NbSe₂ layers, each layer consisting of a sheet of Nb atoms between two sheets of Se atoms.⁴⁰ The separation of the Nb sheets is 6.3 Å. According to equation 3.39, $T_c(M)$ is expected to depend linearly on $\cos[\pi/(M + 1)]$. As shown in figure 3.8, the experimental data is remarkably consistent with this behavior. The straight line yields $T_c(1) = 2$ K and $a = 2|\lambda_3|/\lambda_0^2=2.5$. Increases in the transition temperature of a structure consisting of alternate 60 Å layers of superconductor S and insulator

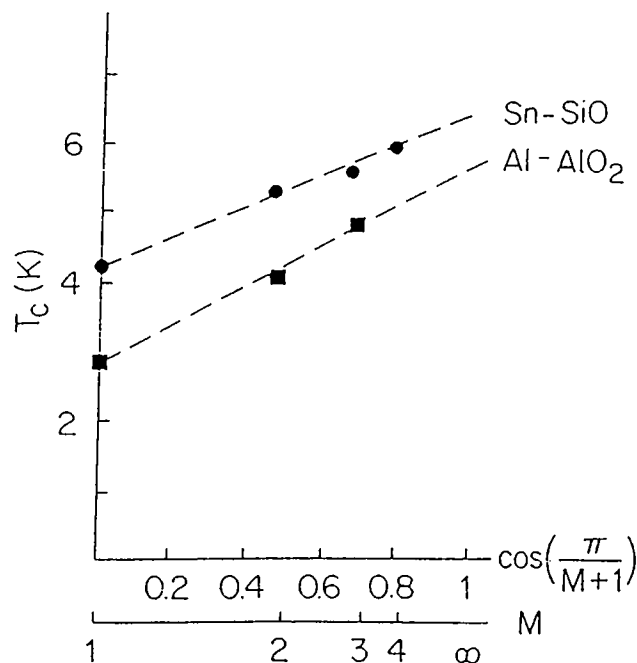


Figure 3.9: Transition temperature of Sn-SiO and Al-AlO₂ structures. The *SI* structure consists of M alternate 60 Å thick layers. The experimental data is from reference 59. ●: Sn-SiO, □: Al-AlO₂. The straight line is given by equation 3.39 with: $T_c(1)=4.25$ K, $a=0.48$ for Sn-SiO; $T_c=2.6$ K, $a=0.61$ for Al-AlO₂.

I have been observed in Sn-SiO and Al-AlO₂ when the number M of S layers were increased.⁵⁹ The experimental data, plotted versus $\cos[\pi/(M+1)]$ is shown in figure 3.9. Finally, we turn to high T_c materials and consider $(M \times N)$ superlattices, in which YBCO layers consisting of $M(=1, 2, 3, \dots)$ unit cells are separated by insulating PrBCO layers N unit cells thick.

According to equations 3.45 and 3.47, the superlattice corresponds for large n values to stacks of independent and ultrathin YBCO crystals each M unit cells thick, where $T_c(M, N \rightarrow \infty)$ is given by equation 3.39. As can be seen from figure 3.10, this behavior is nicely confirmed by the experimental $T_c(M)$ values yielding $T_c(1)=20$ K, and $a=3.6$.

The fact that the experimental data of rather different systems closely follow equation 3.39, strongly suggests that the rise of T_c with increasing M is indeed a size effect, corresponding to the crossover from nearly two to three dimensional

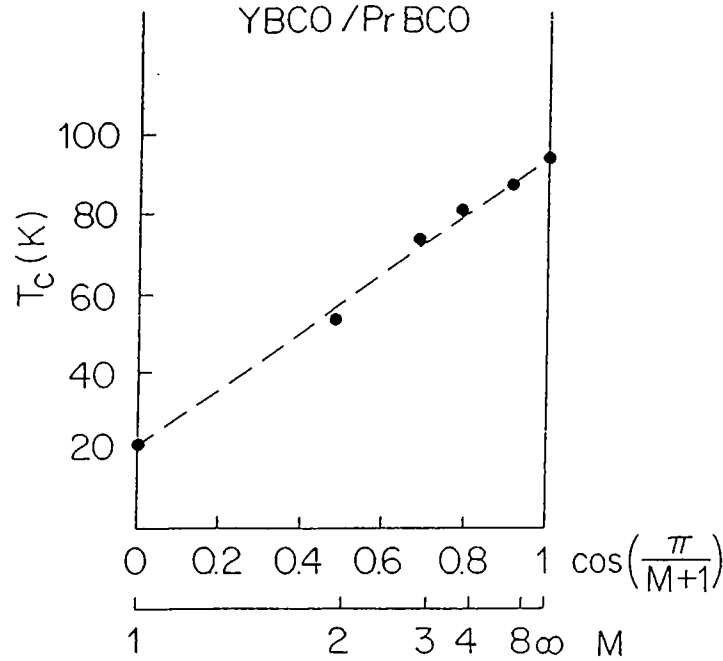


Figure 3.10: T_c for isolated YBCO stacks

Each stack is M unit cell thick. The experimental data was taken from references 35–37. The straight line corresponds to equation 3.39 with $T_c(1)=20$ K and $a=3.6$.

superconductivity. This phenomenon is intimately related to the existence of the interlayer coupling V_3 , corresponding to the Heisenberg interaction in magnetic systems. The value of $T_c(M)$ is then determined by $T_c(1)$ and $2|\lambda_3|/\lambda_0^2$. Estimates for these parameters, as derived from the straight lines in figures 3.8, 3.9, 3.10 are summarized in table 3.1. It is important to keep in mind that the rise of T_c up to the bulk value

$$T_c(M \rightarrow \infty) = T_c(1) \left(1 + \frac{2|\lambda_3|}{\lambda_0^2}\right), \quad (3.47)$$

does not depend upon the sign of λ_3 . Both attractive and repulsive interlayer coupling will enhance T_c . The sign of $\lambda_3 = g_3 D(0)$, however, determines the phase of the order parameter ϕ_n .

As far as the N -dependence of $T_c(M, N)$ for fixed M is concerned, equations 3.45 and 3.47 imply that this behavior is fully controlled by $a(N)$ for all M . To test this prediction we evaluated $a(N)$ from the available experimental data^{36,37}

	$T_c(1)$ (K)	$a = \frac{2 \lambda_3 }{\lambda_0^2}$	$T_c(M \rightarrow \infty)$ (K)
NbSe ₂	2.5	1.7	7
Sn-SiO	4.25	0.48	6.3
Al-AlO ₂	2.6	0.61	4.2
YBCO/PrBCO	20	3.6	92

Table 3.1: Estimates for $T_c(1)$ and a

The parameters have been derived from the straight lines in figures 3.8, 3.9 and 3.10.

for YBCO/PrBCO superlattices with $T_c(1, \infty)=20$ K and $a(0)=3.6$. The resulting $a(N)$ is depicted in figure 3.11. As expected, $a(N)$ decreases with increasing N , which is the number of PrBCO unit cells separating the M -YBCO units. It is important to point out that an uncertainty of 10 percent in $T_c(M, N)$ affects $a(N)$ up to 20 percent. In view of this, the experimental data shown in figure 3.11 appear to be fairly consistent with an N -dependence, fully controlled by $a(N)$ for all M , with $a(0) = 2|\lambda_3|/\lambda_0^2$, as assumed in equations 3.45 and 3.47. To summarize, the essential characteristics of the dimensional crossover or equivalently of a finite size effect driven by the interaction V_3 are in good agreement with experiments for rather different, layered SI superconductors. In view of this, the Heisenberg-type interaction, mediated by V_3 , appears to be a generic feature of superconductor-insulator superlattices and controls $T_c(M, N)$.

Now, let us try to apply the electrostatic model that we have introduced in the last section to predict the coupling constants. From equation 3.33, we find that

$$a(N) = \frac{4\pi e^2}{\lambda_0^2} t^2 d(N) \langle V(pd(N)) \rangle / \langle V(pd(0)) \rangle \quad (3.48)$$

Because $(I)_N$ stacks are not uniform, but consist of several insulating layers that differ substantially on an atomic scale, the assumption of a single exponential decay, $t \propto \exp(-\kappa d(1 + N))$, appears to be an oversimplification. The identification of the dominant contribution to the N -dependence of $a(N)$ is simplified considerably by noting that $d(N) \langle V(pd(N)) \rangle / \langle V(pd(0)) \rangle$

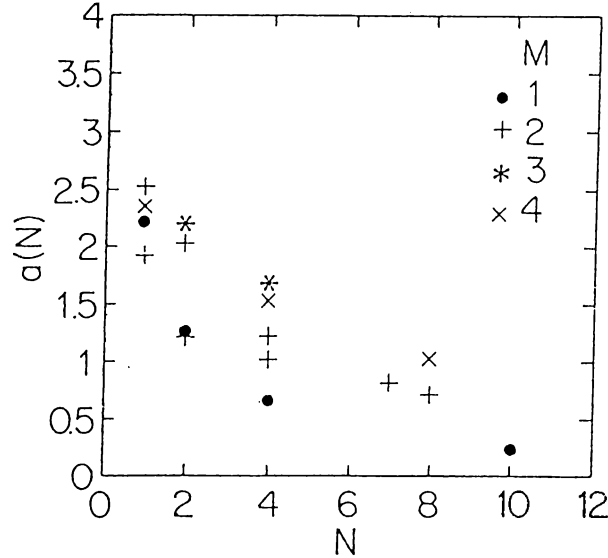


Figure 3.11: $a(N)$ determined from the experimental data $a(N)$ is calculated from the $T_c(M, N)$ values measured in YBCO/PrBCO superlattices^{36,37} with $T_c(1, \infty)=20$ K and $a(0)=3.6$.

is nearly independent of N for $\alpha > 1$. Thus, the N -dependence of $a(N)/a(0)$ depicted in figure 3.12 predominantly probes $t^2(N)$. The decay is reasonably well described by the exponential $t^2(N)/t^2(0) = \exp(-2\kappa d(N))$, as depicted in figure 3.12 with $1/\kappa = 6.7d$, pointing to a rather long range interlayer interaction.

The remaining problem is the assessment of $a(0) = 2|\lambda_3|/\lambda_0^2$ and in particular of λ_3 where α enters. To estimate $\lambda_3(N=0) = g_3(N=0)D(0)$ in $\text{YBa}_2\text{Cu}_3\text{O}_7$, we take $a=3.8$ Å and $d=12$ Å. The density of states $D(0)$ is of the order of $2/3$ eV⁻¹, while $t(N=0)$ can be estimated from the interlayer hopping matrix element $C \simeq 20$ meV,⁶⁰ yielding $t \simeq Cd^2/e^2 \simeq 1.65 \times 10^{-2}$. The resulting values for $\langle V(pd) \rangle$, λ_3/t^2 and λ_3 are listed in table 3.2 for various values of the polarizability α . Apparently, λ_3 increases rapidly with α and becomes negative above a threshold value. The corresponding strength of the interlayer pairing interaction λ_0 is readily obtained from $a(0) = |\lambda_3|/\lambda_0^2$ and equation 3.47, and yields with the BCS-type formula $T_c(1) = 1.14\Theta \exp(-1/\lambda_0)$ and $T_c(1)=20$ K,

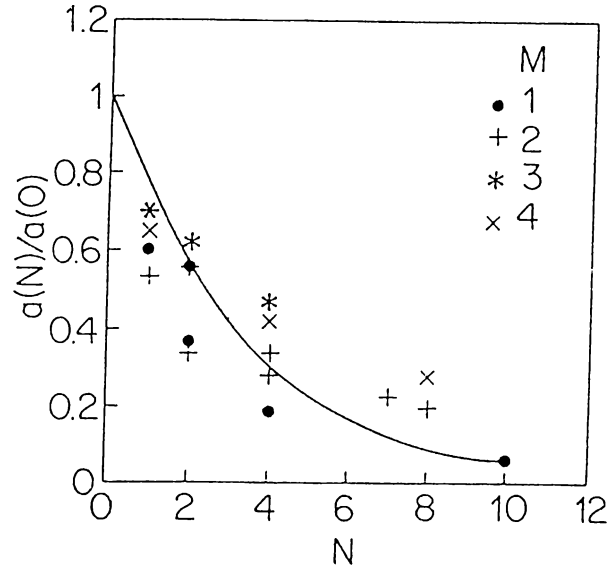


Figure 3.12: $a(N)/a(0)$ versus N

For comparison with the experimental data,^{36,37} we included the exponentially decaying curve of $t^2(N)/t^2(0) = \exp(-2\kappa d(N))$ with $\kappa d=0.15$.

an estimate for the cutoff temperature Θ . The resulting λ_0 and Θ values are also included in table 3.2. Our assumption of an unretarded interaction requires $k_B\Theta \gg \hbar\omega_{ph}$, where ω_{ph} is a characteristic phonon frequency. This is certainly the case for $\Theta > 1000$ K. Moreover, Θ values exceeding the width of the conduction band ($=0.6$ eV) are unphysical. According to table 3.2, consistency with the assumption of an unretarded V_3 then requires α values in the range $1 < \alpha < 2$, which coincides with the physical range in YBCO.⁶⁰ Additional evidence for the unretarded nature of the interactions comes from the correlation between the Hall coefficient, penetration depth and transition temperature.⁶¹

In summary, the overlap integral controls the N -dependence and determines the rather long range of the interaction, while the electronic polarizability enters as a crucial factor, raising the coupling strength to the range where retardation effects can be neglected and where V_3 is attractive. The resulting estimates for λ_0 , the coupling strength of the intralayer pairing interaction, are within the range of conventional superconductors. Thus the high- T_c property of YBCO is

a	$\langle V(pd) \rangle$	λ_3/t^2	λ_3	λ_0	$\Theta(\text{K})$
0.0	0.2	15	0.004	0.048	-
0.5	-1.4	-110	-0.029	0.130	4×10^4
1.0	-3.1	-230	-0.063	0.190	3700
1.5	-4.7	-350	-0.096	0.230	1300
2.0	-6.3	-475	-0.130	0.270	700
2.5	-8.0	-600	-0.160	0.300	490
3.0	-9.6	-720	-0.200	0.330	360

Table 3.2: Estimates for the coupling strengths $\langle V(pd) \rangle$, λ_3/t^2 , λ_3 , λ_0 , Θ are calculated for various polarizabilities α with $a=3.8 \text{ \AA}$, $d=12 \text{ \AA}$, $k_F = \pi/2a$, $D(0)=2/3 \text{ eV}^{-1}$ and $t \simeq 1.65 \times 10^{-2}$.

due to the high cutoff temperature and to the pronounced crossover from 2D to 3D superconductivity, controlled by $|\lambda_3|/\lambda_0^2$.

Finally, using the Ginzburg-Landau formulation, we will calculate the orbital upper critical field, the magnetic field strength at which the critical temperature vanishes, for our model. For this purpose, we introduce the vector potential \vec{A} into the free energy functional. The resulting Ginzburg-Landau functional, in CGS units, is given by

$$\begin{aligned}
F = & \int d\vec{r} \sum_n \left\{ \frac{\hbar^2}{2m_{\parallel}} |(i\nabla + 2e\vec{A})\phi_n(\vec{r})|^2 \right. \\
& - \frac{g_0^2 D(0)}{T_1} (T_c(H) - T_1) |\phi_n(\vec{r})|^2 \\
& - g_3 [\phi_{n+1}(\vec{r}) \exp(-i \frac{2e}{\hbar c} \int_{nd}^{(n+1)d} A_z dz) \phi_n(\vec{r}) \\
& \left. + \phi_{n-1}(\vec{r}) \exp(-i \frac{2e}{\hbar c} \int_{nd}^{(n-1)d} A_z dz) \phi_n(\vec{r}) \right\} .
\end{aligned} \tag{3.49}$$

Note that F has an unusual form in that the vector field enters not only the kinetic energy term but also the interaction g_3 terms. This is a result of the peculiarity of V_3 , which involves interlayer motion of electrons. \vec{A} enters due to gauge invariance. Order parameters, which describe the center of mass motion of the Cooper pairs, of adjacent layers are coupled as a result of the V_3 interaction. When a pair goes from one layer to another it gets a phase, which is nothing but the exponential term in the above expression for the free energy.

The Ginzburg-Landau equation is obtained by the variational calculation $\delta F/\delta\phi_n=0$ for all n which gives

$$\begin{aligned} & \frac{\hbar^2}{2m_{\parallel}}(i\nabla + 2e\vec{A})\phi_n(\vec{r}) \\ & - \frac{g_0^2 D(0)}{T_1}(T_c(H) - T_1)\phi_n(\vec{r}) \\ & - g_3[\phi_{n+1}(\vec{r}) \exp(-i\frac{2e}{\hbar c} \int_{nd}^{(n+1)d} A_z dz) \\ & + \phi_{n-1}(\vec{r}) \exp(-i\frac{2e}{\hbar c} \int_{nd}^{(n-1)d} A_z dz)] = 0 . \end{aligned} \quad (3.50)$$

Due to the assumed 2D isotropy of the layers, it is enough to give the magnitude H of the magnetic field \vec{H} and the angle θ it makes with the c (or z) direction. Thus, $\theta=0$ and $\theta = \pi/2$ corresponds to \vec{H} perpendicular and parallel to layers, respectively. We use the gauge

$$\vec{A} = H(0, x \cos \theta, -x \sin \theta) , \quad (3.51)$$

where x, y are parallel and z is perpendicular to the S units. Since we have chosen \vec{A} to be independent of y , this coordinate can be eliminated to give

$$\begin{aligned} & \frac{\hbar^2}{2m_{\parallel}}[-\frac{d^2}{dx^2} + (\frac{2e}{\hbar c} H x \cos \theta)^2]\phi_n \\ & - \frac{g_0^2 D(0)}{T_1}(T_c(H) - T_1)\phi_n \\ & - g_3[\phi_{n+1} \exp(i\frac{2e}{\hbar c} x d H \sin \theta) \\ & + \phi_{n-1} \exp(-i\frac{2e}{\hbar c} x d H \sin \theta)] = 0 . \end{aligned} \quad (3.52)$$

The upper critical field is obtained by looking for the solution of the above equation with the largest H so that $T_c(H)=0$. Solutions with $\theta=0$ and $\theta = \pi/2$ give H_{c2}^{\perp} and H_{c2}^{\parallel} , respectively. For, $\theta=0$ we end up with

$$[g_0^2 D(0) + \frac{\hbar^2}{2m_{\parallel}}(-\frac{d^2}{dx^2} + \frac{4e^2}{\hbar^2 c^2} H^2 x^2)]\phi_n - g_3(\phi_{n+1} + \phi_{n-1}) = 0 , \quad (3.53)$$

which can be readily solved for $n=1, \dots, M$, to give

$$H_{c2}^{\perp} = \frac{m_{\parallel} c}{e \hbar} g_0^2 D(0) (1 + a \cos \frac{\pi}{M+1}) , \quad (3.54)$$

where $a = 2|\lambda_3|/\lambda_0^2$. Thus, H_{c2}^\perp and T_c have the same M -dependence, such that

$$\frac{H_{c2}^\perp}{T_c(M)} = \frac{m_{\parallel}c}{e\hbar} \frac{g_0^2 D(0)}{T_c(1)} . \quad (3.55)$$

Lastly, the upper critical field for \vec{H} parallel to the layers is given by

$$\begin{aligned} & \left[-\frac{\hbar^2}{2m_{\parallel}} \frac{d^2}{dx^2} - \frac{g_0^2 D(0)}{T_1} (T_c(H) - T_1) \right] \phi_n \\ & - g_3 \left[\phi_{n+1} \exp\left(i \frac{2e}{\hbar c} x dH\right) \right. \\ & \left. + \phi_{n-1} \exp\left(-i \frac{2e}{\hbar c} x dH\right) \right] = 0 . \end{aligned} \quad (3.56)$$

Again, evaluation of H_{c2}^\parallel is tantamount to determining the largest field H for which these equations have a solution. This leads to an eigenvalue problem of a Hermitian matrix. It turns out that the relevant eigenvalue is independent of the phase and merely yields $T_c(M)$ for any finite M . Thus, according to the Ginzburg-Landau model, a parallel field does not affect T_c . In fact, this is what has been observed experimentally up to 90 kG.⁶²

3.3 Tunneling Induced Superconductivity in Layered Systems

In this section, we study the effects of phonon modes which modify the interlayer distances in systems consisting of a sequence of conducting and insulating layers.⁶³ This is an example for interlayer pairing mechanism that we discussed in the preceding sections. In fact, there are no intralayer interactions in this model. The only electron-electron interaction is an interlayer coupling mediated by phonons, which is very similar to V_3 process of section 3.1. However, since for this model it is more convenient to study in the band picture rather than the layer picture, we will use the band indices. We show that the modification of interlayer transition rate of electrons by phonons can lead to an attractive electron-electron interaction. We conclude that a bare interlayer interaction is enough for a superconducting transition in layers which are otherwise normal.

For simplicity, we consider a system composed of two conducting (metallic) layers separated by an insulating medium. This system contains the essential ingredients of the tunneling-induced superconductivity as revealed in this study. Recently thin films of high- T_c superconductor of $\text{YBa}_2\text{Cu}_3\text{O}_7$ have been grown artificially, allowing to investigate the properties of a one-unit-cell thick films⁶⁴ which contains two copper oxide layers only. For such a system we assume that the metallic layers can be treated within the 2D Fermi liquid picture and the only interaction between the layers is phonon assisted tunneling. The Hamiltonian relevant for the said system is given by

$$H = \epsilon \sum_{ni\sigma} c_{ni\sigma}^\dagger c_{ni\sigma} + t \sum_{n\sigma \langle ij \rangle} c_{ni\sigma}^\dagger c_{nj\sigma} + \sum_{\vec{q}} \hbar\omega_{\vec{q}} (b_{\vec{q}}^\dagger b_{\vec{q}} + \frac{1}{2}) + \sum_{i\sigma} (t_i c_{2i\sigma}^\dagger c_{1i\sigma} + h.c.). \quad (3.57)$$

Here, ϵ is the self-energy, σ is the spin of the electron, and t is the hopping matrix element between nearest neighbor lattice sites. These lattice sites (labeled by i or j) lie in the same metallic layer (labeled by n). The first two terms in equation 3.57, represent on-site and nearest neighbor hopping processes, respectively, and they lead to the electronic energy structure of the layers in the absence of interlayer interaction. The third term stands for the phonons. For the purpose of this study, we are going to consider only transversal phonon mode with displacements perpendicular to the layers. Phonon assisted tunneling introduced via the last term describes the interaction between the metallic layers. The factor t_i is simply the hopping matrix element for an electron to go from site i in layer 1 to the corresponding site in layer 2. This term is the first order contribution of the interlayer interaction within the tight binding approximation. The coupling to phonon degree of freedom comes from the dependence of t_i on the interlayer separation.⁶⁵ We assume that t_i is of the form $t_\perp e^{-\kappa\zeta_i}$, where ζ_i is the displacement of the site i from the equilibrium value. This assumption is justified by the fact that the atomic orbitals have radial part decaying exponentially. Note also that in the case of square barrier the transmission amplitude is exponentially dependent on the width of of the tunneling barrier. In both cases, the adiabatic approximation is valid. That is the changes in t_i are treated as very slow in

comparison to the interlayer tunneling rate of electron. This is nothing but the Born-Oppenheimer approximation applied to the current problem. For small displacements the exponential can be expanded to give $t_{\perp}(1 - \kappa\zeta_i)$. Here ζ_i is linear in phonon operators and is given by

$$\zeta_i = \sum_{\vec{q}} \left(\frac{\hbar}{2LM_{ion}\omega_{\vec{q}}} \right)^{1/2} (b_{\vec{q}} + b_{-\vec{q}}^{\dagger}) e^{i\vec{q}\cdot\vec{R}_i} \quad (3.58)$$

where L is the number of lattice sites, M_{ion} is the ion mass and \vec{R}_i is the equilibrium position of site i . Here, we do not take into account the modification of the intralayer hopping matrix element t by the phonons since these changes are only second order in ζ_i . The Hamiltonian takes a familiar form by two successive canonical transformations. The first one is the usual Fourier transformation which changes site label to wave vector \vec{k} , and also introduces the energy bands $\epsilon_{\vec{k}}$. The electron layer-operators $c_{n\mathbf{i}\sigma}$ are now changed to $c_{n\vec{k}\sigma}$. In the absence of interlayer tunneling this transformation would diagonalize the Hamiltonian completely resulting in two identical energy bands $\epsilon_{\vec{k}}$. The next transformation is obtained by taking the symmetric and the antisymmetric combinations of the layer-operators $c_{n\vec{k}\sigma}$ in order to diagonalize the interlayer tunneling term. The composed transformation can be written as

$$d_{m\vec{k}\sigma} = \frac{1}{\sqrt{2L}} \sum_i (c_{1i\sigma} + (-1)^{m+1} c_{2i\sigma}) e^{-i\vec{q}\cdot\vec{R}_i}. \quad (3.59)$$

Note that this is actually a three dimensional Fourier transformation with only two different values (0 and π) for the component in the perpendicular direction. We introduce the split energy bands $\epsilon_{m\vec{k}}$ and the electron-phonon interaction constant $g_{\vec{q}}$ by

$$\epsilon_{m\vec{k}} = \epsilon_k + (-1)^{m+1} t_{\perp} \quad (3.60)$$

and

$$g_{\vec{q}} = -t_{\perp} \kappa \left(\frac{\hbar}{2LM_{ion}\omega_{\vec{q}}} \right)^{1/2}, \quad (3.61)$$

respectively. Neglecting the Umklapp processes, we can write the transformed

Hamiltonian as

$$H = \sum_{m\vec{k}\sigma} \epsilon_{m\vec{k}} d_{m\vec{k}\sigma}^\dagger d_{m\vec{k}\sigma} + \sum_{\vec{q}} \hbar\omega_{\vec{q}} (b_{\vec{q}}^\dagger b_{\vec{q}} + \frac{1}{2}) + \sum_{\vec{q}m\vec{k}\sigma} (-1)^{m+1} g_{\vec{q}} (b_{\vec{q}} d_{m\vec{k}\sigma}^\dagger d_{m\vec{k}+\vec{q}\sigma} + h.c.). \quad (3.62)$$

Clearly, this is nothing but Fröhlich Hamiltonian⁴⁵ for two independent subsystems labeled by m since the band index m is a good quantum number. As a result, the conventional BCS theory⁶⁶ can be applied to each band separately. Earlier, BCS theory of superconductivity was generalized to take into account the materials having several energy bands.^{67,68} Our Hamiltonian after the canonical transformation is simply a two-band model with vanishing interlayer coupling. Thus, we can use the results of existing solutions of the two-band model.

It should be noted that the calculation of the electron-phonon coupling constant in terms of the variation of the hopping integrals owing to the change of interatomic distances was first proposed by Fröhlich.⁶⁵ Later, Ashkenazi *et al.*⁶⁹ showed that this method is equivalent to the Bloch approach.⁷⁰ The same method has been used by Weber⁷¹ to calculate the electron-phonon coupling leading to high T_c in $\text{La}_{2-x}(\text{Ba,Sr})_x\text{CuO}_4$. In this section, we use the Fröhlich approach to study the effect of phonon modes modifying the distance between two conducting layers in normal state. We find that modification of the interlayer transition rate of electrons and hence phonon induced tunneling can lead to an attractive electron-electron interaction. As a result the normal layers become superconducting due to an interlayer interaction alone.

According to two-band model of superconductivity, the Hamiltonian in equation 3.62 will adopt a solution with two order parameters Δ_1 and Δ_2 corresponding to the bands 1 and 2, respectively. Furthermore, as a result of vanishing interband interaction there will be two critical temperatures, one for each band.^{67,68} However, in our case the energy bands given by equation 3.60 are identical apart from a small splitting, and hence there is only one critical temperature T_c . The strength of the electron-phonon coupling is measured by the dimensionless parameter λ . In the case of vanishing Coulomb coupling constant μ^* , $T_c \sim \hbar\omega_0 e^{-1-1/\lambda}$ where ω_0 is the maximum phonon frequency.³¹

The critical temperature for the present model can be calculated by using the known parameters of some materials, but it is not always reliable since T_c is a very sensitive function of λ . Nevertheless, we are going to determine the order of magnitude only. The value of λ can be calculated in terms of the electronic matrix element g , (which is constant and is given by $g = t_{\perp}\kappa$ in our case), and phonon frequencies ω . The expression for the dimensionless electron-phonon coupling constant is

$$\lambda = \frac{D(0) \langle g^2 \rangle}{M_{ion} \langle \omega^2 \rangle}. \quad (3.63)$$

Here $\langle g^2 \rangle$ is the square of the electronic matrix element averaged over the Fermi surface and $\langle \omega^2 \rangle$ is an average of the square of the phonon frequency. $D(0)$ is the electronic density of states(DOS) at the Fermi level and M_{ion} is the atomic mass. Since the two bands of the system we are considering differ by a small splitting only, $D(0)$ and hence T_c is the same for both bands. Considering the acoustic branch of phonons we see that the average $\langle \omega^2 \rangle$ can simply be taken as ω_0^2 . Since, we are dealing with the weakly interacting two 2D layers, the interlayer hopping matrix element t_{\perp} is small as compared to its intralayer counterpart. Therefore, if we assume that the latter is ~ 1 eV then t_{\perp} can be taken to be ~ 0.1 eV. An estimation for κ can be obtained by using a square barrier modeling of the interlayer tunneling process. As a result, for typical values of the parameters given by $M_{ion} \sim 10^{-26}$ kg, $\omega_0 \sim 10^{13}$ s $^{-1}$, $D(0) \sim 10$ eV $^{-1}$, $\kappa \sim 1$ Å $^{-1}$ and $t_{\perp} \sim 10^{-1}$ eV, the electron-phonon coupling constant λ is found to be of the order of unity which can lead to physical T_c values.

The order parameters Δ_1 and Δ_2 can also be written in the real space, i.e. by using the layer index rather than the band index. Since Δ_1 and Δ_2 are symmetric and antisymmetric combinations of the layer orbitals, the real space representation $\Delta_1 \pm \Delta_2$ give rise to pair wave functions localized either in layer 1 or 2. The generalization of the problem to infinite number of layers also gives the same result. In this case, there is band formation in the perpendicular direction and hence the order parameter is labeled by a wave number k_z instead of the discrete values 1 and 2. Since, Δ_{k_z} is more or less independent of k_z owing to the small dispersion in the z direction, the real space representation of Δ is given by

a Dirac delta-like function. Thus, electron pairs are localized in the layers. This is also what is observed in experiments on high- T_c materials.

Electron-phonon coupling in solids is a result of the modification of the lattice structure by phonons.⁴⁵ Depending upon the nature of the solid this interaction is dominated by a certain type of coupling (deformation, piezoelectric, polar etc.). In our model, the interaction is due to the change in the interlayer hopping matrix elements caused by the phonons existing in the medium. If the interlayer distance becomes smaller, it becomes easier for an electron to tunnel from one layer to the other. Now the pairing can be visualized in terms of this interpretation. Consider two electrons in the same layer. If one of them tunnels to the other layer owing to the shrinking interlayer separation caused by transversal phonons, then the other one will also choose this way. As in the conventional systems, the many body ground state is attained if electrons having opposite momenta couple to each other. Consequently, it is energetically more favorable for electrons to tunnel in pair.

At this point we should note that the interaction we mentioned has nothing to do with Josephson tunneling. In the latter there are two systems which are already in superconducting state and the phases of the order parameters at two sites are locked by means of the interaction between them. On the other hand in our model, superconductivity is induced by the interaction itself. Two conducting layers here, are in the normal state unless they are brought together to allow interlayer tunneling. Then, tunneling causes a kind of pairing interaction which results in superconductivity of whole system. Superconductivity of systems composed of layers coupled via Josephson interaction have been studied in detail earlier.⁷² It has been shown that Josephson tunneling does not contribute to the pairing.⁴¹

In order to explore the stability of the solution with respect to imperfections (defects, impurities), one has to investigate the behavior of the system in the presence of scattering centers. This is, however, very similar to the problem of two-band superconductivity with impurities studied earlier.^{73,74} The present problem corresponds to the strong intraband coupling limit of the two-band model

where the interband phonon coupling is neglected. The temperature dependence of the order parameters is given by two coupled equations whose general solution is quite complicated and thus is beyond the scope of the present study. An interesting observation is that if the order parameter of one band is much larger than that of the other, the interband impurity scattering enhances the lower critical temperature.^{73,74}

It is easy to modify the model for the continuum limit which is relevant especially for metals where the tight binding approximation is replaced by a more realistic nonlocal picture. For 2D noninteracting electron gas, DOS is independent of energy and therefore identity of the critical temperatures of the two energy bands is fully satisfied. The continuum model is analogous to jellium model^{31,45} of conventional systems. Phonons are now the quantized vibrations of the two membranes. The cut off frequency is related to the sharpest possible deformation on the membranes. In this respect, the assumption that the conducting layers are identical and have lattice sites on top of each other can be generalized to cover incommensurate layers.

In summary, a possible mechanism was proposed for the superconductivity of layered systems. The only interaction between the 2D Fermi liquid layers, is assumed to be tunneling. We show that transversal phonon modes with displacements perpendicular to these layers causes an attractive electron-electron interaction which can induce a superconducting transition. According to this model electrons and phonons can couple via tunneling and as a result a bare interlayer interaction can cause otherwise normal layers to go into superconducting state. In this respect, short periodicity semiconductor superlattices (consisting of consecutive quantum wells and barriers) can be interesting systems to explore.

Chapter 4

Fullerenes

4.1 Review

In 1985, Kroto *et al.*⁷⁵ have succeeded in isolating a special carbon molecule by laser vaporization of graphite. It was proposed that the molecule, composed of 60 carbon atoms, had the truncated-icosahedron structure and was named Buckminsterfullerene, after the engineer Buckminster Fuller who had pioneered the concept of geodesic domes. The name *fullerene* is now used for the cage-structure carbon clusters, C_m , with even number of atoms where each atom is connected to three nearest neighbors. Each polyhedral network consists of pentagons and hexagons. According to a relation due to the 18th-century Swiss mathematician Leonhard Euler, for any polyhedron the number of pentagons must always be 12 while the number of hexagons can be anything other than one, but including zero. Among the possible carbon clusters, C_{60} and C_{70} have been found to be relatively stable (figure 4.1). The extraordinary stability of the 60-atom species stems from the symmetry of the molecule. Having the icosahedron point group, C_{60} is the most symmetric molecule possible in three-dimensional Euclidean space. The C_{60} structure can be visualized as a single, two dimensional (2D) graphite layer consisting of pentagons and hexagons which is wrapped on a sphere of diameter 7.1 Å. The effective dimensionality of this sphere and properties in conjunction with it are of interest for studies on low dimensional

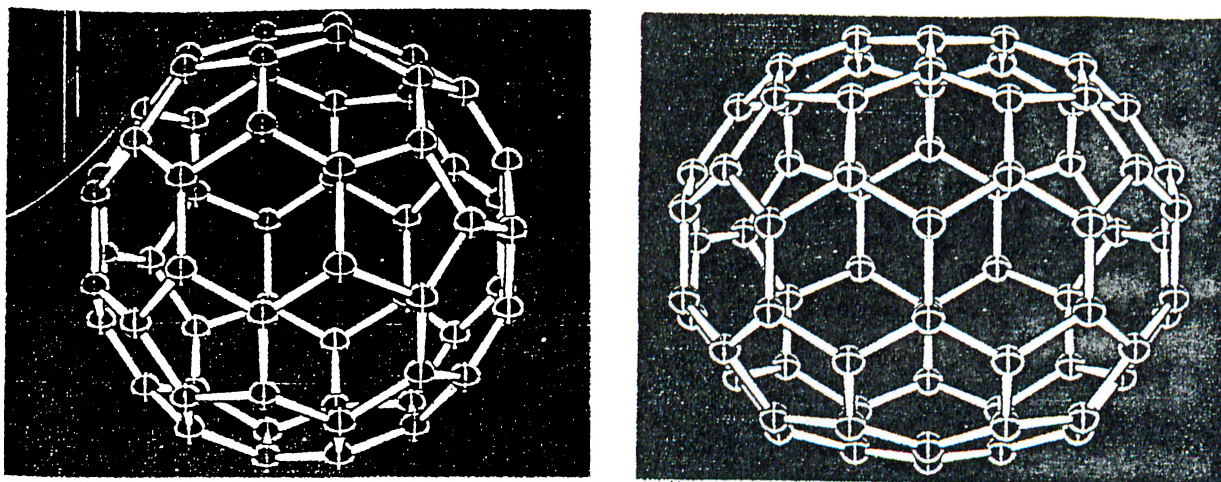


Figure 4.1: Fullerenes

The two stable molecules: C_{60} (left) and C_{70} (right). The number of pentagons is always 12. The soccer ball structure of C_{60} has 20 hexagons, while C_{70} has 25 producing a shape reminiscent of a rugby ball. From Reference 76.

electron systems. Five years after the discovery of buckminsterfullerene, or *buckyball* in short, Krätschmer and Fostiropoulos developed a method to produce macroscopic amounts of the third crystalline form of pure carbon after diamond and graphite.⁷⁷ According to single crystal x-ray diffraction measurements, at room temperature solid C_{60} (fullerite) form a face centered cubic (fcc) Bravais lattice with the cubic lattice parameter $a_0=14.2 \text{ \AA}$, and with a high degree of rotational disorder of the basis formed by C_{60} molecules at the lattice sites.⁷⁸ Synchrotron x-ray powder diffraction and differential scanning calorimetry measurements on solid C_{60} by Heiney *et al.*⁷⁹ show that at 249 K fcc structure changes to a low temperature simple cubic structure by a first order phase transition. The properties of solid C_{60} are summarized in table 4.1.

One of the most critical developments in the field was the synthesis of the conducting solid fullerenes C_{60} and C_{70} doped by alkali-metals.⁸⁰ Haddon *et al.* prepared films of those materials having conductivities at room temperature that are comparable to those attained by n-type doped polyacetylene. Thus, the possibility of intercalating small dopant ions into the fullerene crystal without

Structural Data		
Crystal structure	cubic	Fm $\bar{3}$ m (T > 260 K) Pa $\bar{3}$ (T < 260 K)
Cage diameter		7.1 Å
Bond lengths	r(C-C)	1.391 Å six-six ring fusions 1.455 Å five-six ring fusions
C ₆₀ -C ₆₀ nearest neighbor distance		3.1 Å
Bulk modulus		18 GPa
Density		1.65 g/cm ³
Electronic/Spectroscopic Data		
Electron affinity		2.6–2.8 eV
Ionization energy		7.6 eV
Band gap		1.9 eV
NMR chemical shift		142.68 ppm
Vibrational frequencies		
infrared		528, 577, 1183, 1429 1/cm
Raman		272, 429, 495, 711, 772, 1099, 1250, 1422, 1467, 1573 1/cm
librations		22 1/cm (5 K)
Refractive index		2.2 (630 nm)

Table 4.1: Properties of solid C₆₀
From Reference 76.

disrupting the network of contacts between the spheroids led to the production of the first 3D isotropic organic conductor. The most exciting news came from the same group again. Potassium-doped C₆₀ was found to be superconducting at 18 K.⁸¹ Further studies showed that only K₃C₆₀ exhibits the superconducting behavior. Zhou *et al.*⁸² found that K₃C₆₀, in which C₆₀'s form an fcc lattice at room temperature, undergoes a transition from fcc to bcc upon further doping (figure 4.2). They have demonstrated that K₆C₆₀, which is an insulator, form a bcc lattice.

The isotope experiment is one of the cleanest ways to understand the role of lattice vibrations in superconductivity. Measurements of Ramirez *et al.*⁸⁴ yield an exponent of $\alpha = 0.37 \pm 0.05$ for the relation $T_c \propto M^{-\alpha}$, where M is the ionic

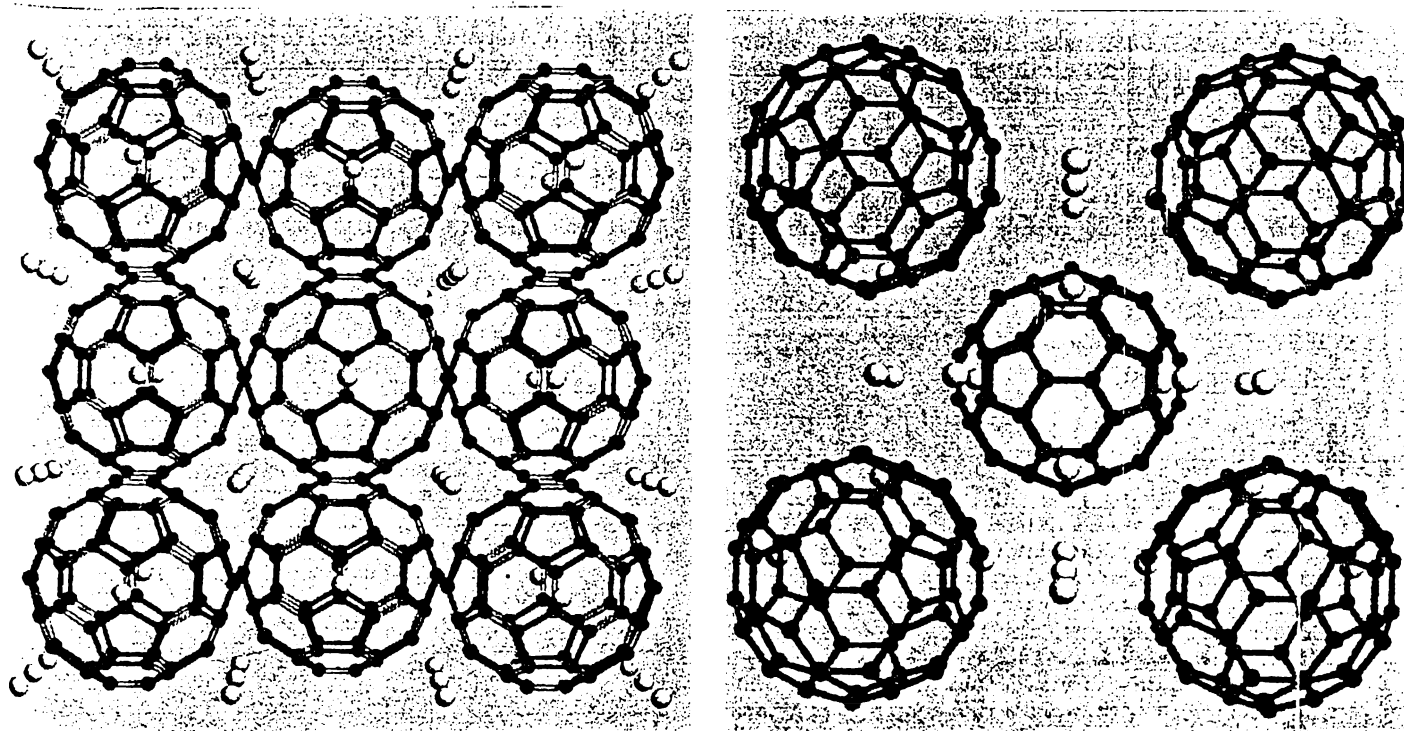


Figure 4.2: Doped fullerenes
 K_3C_{60} has an fcc structure (left)⁸³ while K_6C_{60} is bcc (right).⁸²

mass. This result can be interpreted as an evidence for phonon-mediated pairing.

Another interesting observation is that it is possible to obtain a ferromagnetic solid if C_{60} is reduced not by alkali-metal but by reaction with organic electron donors. (TDAE=tetrakis(dimethylamino)-ethylene) C_{60} has a Curie temperature of 16 K, which is higher than any other known molecular ferromagnet.⁸⁵

Properties of alkali-metal doped A_3C_{60} are summarized in table 4.2. Note that the superconducting critical temperatures are higher than any other known molecular superconductor and only the cuprate superconductors have higher T_c .

Shortly after the synthesis of C_{60} , Haddon *et al.*⁸⁷ calculated the energy levels of the molecule by using the Hückel method. The hexagons involve the sp^2 hybridization while the pentagons have the sp^3 hybridization. The bond angle 108° in the pentagon is very close to the angle $109^\circ 28'$ in the ideal sp^3

Crystal structure	cubic	Fm $\bar{3}$ m
Superconductivity		type II
Transition temperature T_c	K_3C_{60}	19 K
	Rb_3C_{60}	29 K
	Cs_2RbC_{60}	33 K
	$Rb_{2.7}Tl_{2.2}C_{60}$	42.5 K
Pressure dependence		$\delta T_c/\delta P = -0.63$ to -0.078 K/kbar
Effective mass of carriers		$1.3 m_e$
Lower critical field	$H_{c1}(0)$	0.013 T
Upper critical field	$H_{c2}(0)$	49 T
Coherence length	$\xi(0)$	26 Å
Penetration depth	$\lambda(0)$	2400 Å
NMR chemical shift		186 ppm

Table 4.2: Properties of alkali-metal doped A_3C_{60} fullerides
 m_e is the mass of free electron. From References 76 and 86.

hybridization. Since C_{60} is nearly spherical, it is very convenient to label the states according to their approximate transformations under the operations of the full rotation group as shown in figure 4.3. The electronic spectrum is similar to the spectrum of 60 noninteracting electrons on the surface of a sphere. The low-lying states correspond approximately to the angular momenta $l = 0, 1, 2, 3,$ and 4 states. The lowest-lying unoccupied orbitals consist of a pair of triply degenerate orbitals (t_{1u} and t_{1g}) and they constitute the $l=5$ states along with the 5-fold degenerate highest-lying occupied orbital (h_u).

C_{60} solid was found to be a direct band gap semiconductor in the solid phase.⁸⁸ Self-consistent field (SCF) calculations based on the local density approximation have predicted that the solid phase is stable in the fcc structure with a 1.6 eV (per basis, i.e. C_{60} cluster) cohesive energy and has a direct band gap of 1.5 eV (figure 4.4). The deeper levels of the cluster, forming very narrow bands in the solid, are considered to be bonding states due to the σ -bonds. The bands formed by the π -bond states (those between -6 and + 7 eV) are more dispersive due to their relatively larger intermolecular overlap. The antibonding states of

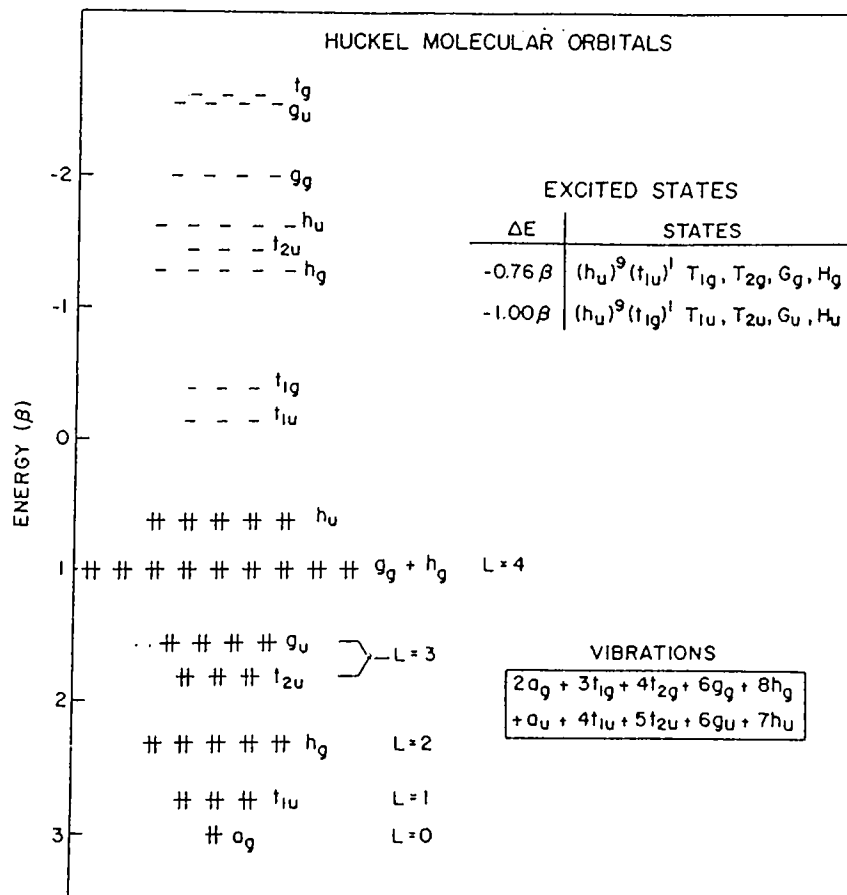


Figure 4.3: Electronic energy levels of C_{60}

The corresponding energy levels of the spherical harmonics are also indicated. β is the hopping integral for the carbon π -orbitals. From Reference 87.

σ bonds are above 7 eV. The calculated electronic structure of the solid C_{60} indicates that intermolecular interactions are weak owing to small overlap of molecular orbitals.^{88,89} Nearest neighbor interaction in the solid phase can be compared with the interlayer interaction in graphite. The latter is known to be weak. In fact, photoemission measurements⁹⁰ along with the results of those SCF calculations imply that the electronic states of solid phase can be described to some extent by the states of isolated C_{60} . Figure 4.5 shows the contour plot of the valence-electron density of the fcc C_{60} crystal on the (010) plane. As can be seen, the electron density between C_{60} clusters is much lower than the densities

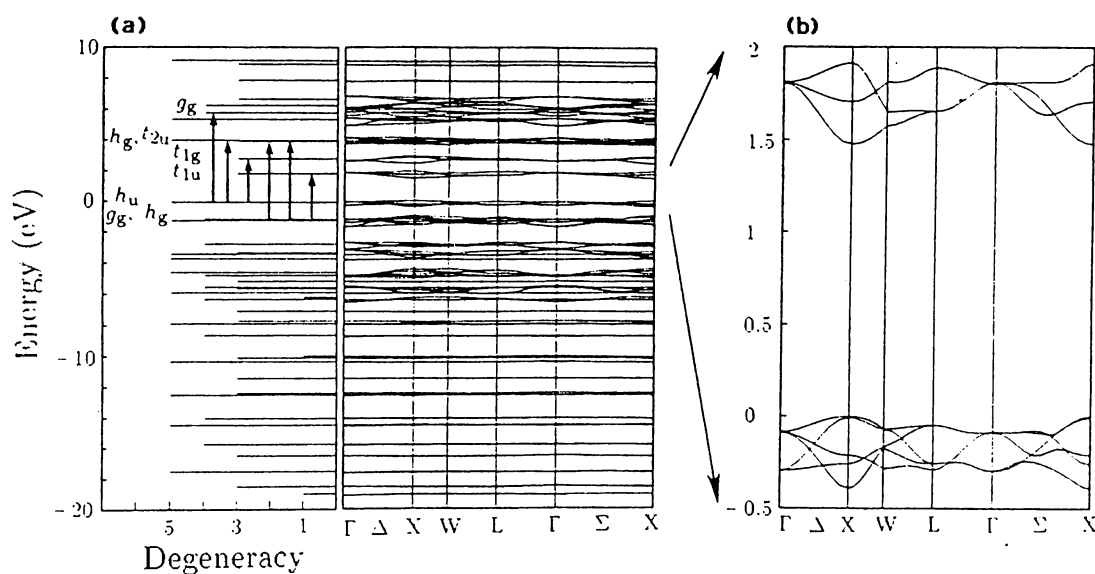


Figure 4.4: The band structure of the fcc C_{60} solid

(a) Electronic energy levels of isolated C_{60} molecule. The arrows denote the optically allowed transitions. (b) Band structure of the solid phase near the energy gap. The valence and the conduction bands are closest at the X point. From Reference 88.

at single (five-six ring fusion) and double (six-six ring fusion) bonds within a C_{60} cluster.

In the isolated C_{60} , the lowest unoccupied molecular orbital (LUMO) state is $\simeq 5$ eV below vacuum level and also is 1.9 eV above the highest occupied molecular orbital (HOMO) state.⁸⁸⁻⁹⁰ The valence electron of an alkali atom has low affinity, and thus can easily be donated to LUMO. A similar situation was already pointed out for K and Na adsorbed on Si surfaces.⁹¹⁻⁹³ According to the results of the SCF pseudopotential calculations based on the local density approximation, the alkali atoms are adsorbed at the centers of the hexagonal rings above the atomic plane. These are the low charge density locations on the surface. At low coverage, the adsorbed alkali atoms donate their valence electrons to the empty surface states which attributes a 2D metallic character to the semiconductor surface.

An important clue about the mechanism of superconductivity came from

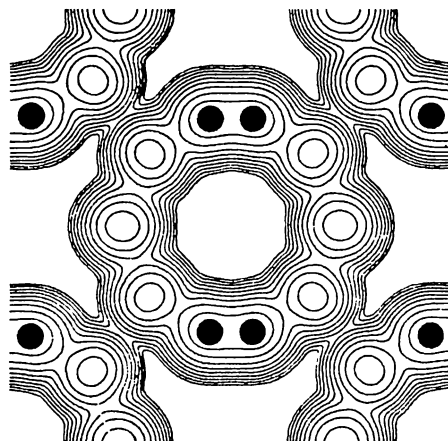


Figure 4.5: Contour plot of valence-electron density

The fcc structure is viewed in the (010) direction. Solid circles are carbon atoms. Each contour represents twice (or half) the density of neighboring contours. From Reference 88.

the measurements on the pressure dependence of the critical temperature T_c . Sparn *et al.*⁹⁴ have measured T_c of single-phase K_3C_{60} compound as a function of pressure (figure 4.6). Their powder sample showed a very large *decrease* of T_c with increasing pressure. A simple argument, piling of the density of states at the Fermi level, can explain this behavior. According to BCS theory, $T_c \propto \omega \exp(-1/\lambda)$, where ω is a characteristic phonon frequency and λ is the dimensionless electron-phonon coupling parameter which is proportional to density of states at the Fermi level $N(E_F)$ and inversely proportional to ω^2 . Pressure is expected to increase ω and broaden the conduction band and hence decreasing $N(E_F)$. Since the exponential factor is dominant, we expect a negative slope in T_c versus pressure curve. A similar argument, can also be used to understand the increase of T_c with larger alkali metal radius (table 4.2).

The development of the field have been so rapid that the applications of the fullerenes yet to be established. Interestingly, varying the doping concentration and temperature, C_{60} can be made to function as an insulator, a conductor, a semiconductor and a superconductor. Its direct band gap along with the

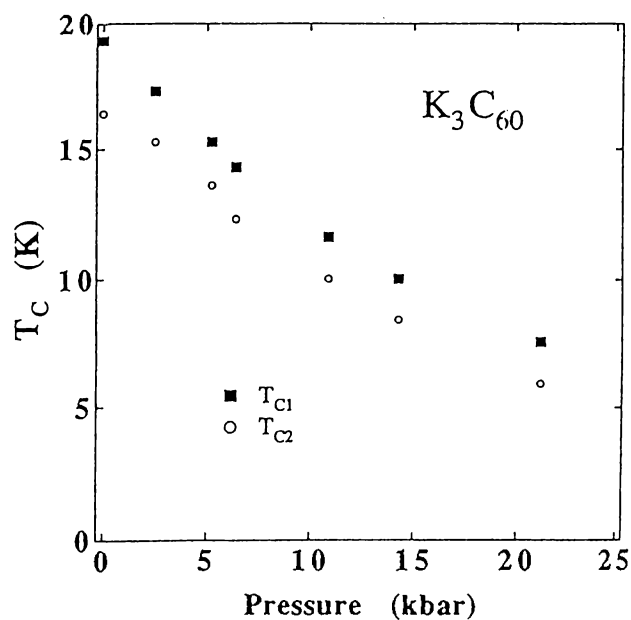


Figure 4.6: T_c versus pressure

The superconducting critical temperature T_c of K_3C_{60} decreases with increasing pressure. Since the experiment has been performed on a powder sample, there are two critical temperatures. T_{c2} is related to Josephson coupling of superconducting grains. From Reference 94.

peculiar rotational disorder of the C_{60} molecules in solid phase makes fullerenes a new kind of semiconductor. Highly ordered C_{60} films have been grown on crystalline substrates like gallium arsenide, which is a promising result for microelectronic applications. High transition temperatures for superconducting and ferromagnetic orderings may be very important for technological applications. Since alkali metal doped C_{60} is a 3D superconductor, it is a candidate for the production of practical superconducting wires. C_{60} molecules, due to their ability to accept and release of electrons, can be used as charge carriers (in batteries for example). There has also been developments in putting a dopant atom *in* the cage. The properties of these materials are yet to be found. Liquid solutions of fullerenes have shown interesting optical harmonic generation properties. It has been found that under pressure C_{60} solid can be converted to diamond. Finally,

fullerene tubules, tubular graphitic filaments, have been proposed to a new class of materials yet to be studied on.

The dependence of the critical temperature T_c only on the distance between the C_{60} molecules⁹⁴ has been interpreted as an evidence for an intramolecular superconductivity mechanism. However, whether this intramolecular mechanism originates from electron-phonon coupling; or whether purely repulsive electron correlations cause an effective attractive interaction between the electrons; or else whether both are operative is still an open question. Another point to be clarified is the coupling strength which determines the state of the system between the weak coupling BCS type superconductivity and the Bose-Einstein condensation of bosons formed by two electrons as a result of strong interaction. Several models using phonons⁹⁵⁻¹⁰⁰ or electron correlations^{101,102} have been proposed as the mechanism of superconductivity in the alkali metal doped C_{60} .

The models based on the electron-phonon interaction generally concentrate on the particular molecular and chemical nature of the compounds and they use the standard BCS-type coupling to molecular vibrations. Schlüter *et al.*⁹⁶ consider intramolecular Jahn-Teller type modes. As a result of the geometry of the system, the dimensionless BCS coupling parameter $\lambda = NV$ is factorized in real space. The coupling V is largely an isolated molecule property while the density of states N of conduction electrons is controlled by the intermolecular hopping. However, the point to be kept in mind is that since the average phonon energy and the electron kinetic energy are comparable, Migdal's approximation used in BCS theory is questionable.

It has been argued that the π -electrons on the surface of a single C_{60} molecule by themselves can provide an effective attractive interaction for the electrons, favoring even occupancy of the molecules, that is, electron pairing.¹⁰¹ For an on-site repulsive interaction U , Chakravarty and Kivelson¹⁰¹ claimed that the energy to add two electrons to a C_{60} molecule is less than the twice the energy to add one electron. Therefore, it is lower in energy for electrons to form pairs. However, this and similar models generally treat the problem by perturbation theory to the second order and it is an open question whether the same result

holds with the higher order corrections.

Finally, it is not clear whether the superconductor A_3C_{60} is an off-stoichiometric composition. Lof *et al.*¹⁰³ proposed that stoichiometric or ordered K_3C_{60} is a half-filled shell Mott-Hubbard insulator. They also claim that since the on-site molecular Coulomb repulsion is very large in comparison to the bandwidth, C_{60} should be considered as a strongly correlated system. The photoemission and the inverse photoemission measurements of Takahashi *et al.*¹⁰⁴ indicates that the change of the electronic structure by alkali metal doping is not a rigid and simple band filling but a transfer of the electronic states from the LUMO band to an additional band produced by the doping below the Fermi level. Furthermore, they identify a pseudo-gap opening at the Fermi level in K_3C_{60} .

In order to understand the electronic structure and possible electron-electron interactions of an isolated C_{60} molecule, we should start with a model which takes at least 60 electrons into account. However, it is still very helpful to study two electron problem which gives an idea about the pairing due to an attractive electron-electron interaction. In the next section, we solve the problem of two fermions on a truncated-icosahedron interacting via a short-range attractive interaction. This problem turns out to be very useful in determining the dimensional effects. In the last section, we propose a simple model to understand the physics of electron-phonon interaction in solid C_{60} .

4.2 Two-Fermion Problem on a Truncated-Icosahedron

In this section we study the dimensional effects emerging from the confinement of electrons on a surface.¹⁰⁵ For this purpose, we consider two electrons (or fermions in general) moving on a truncated-icosahedron. What we want to understand is whether this surface is reminiscent of a plane from the point of view of the interaction of fermions to form a bound state. As is well known, in

one and two-dimensional (1D and 2D) cases, when two particles interact via a short-range potential, a bound state is formed no matter how weak the attractive interaction is.³ In 3D, on the other hand, one requires a critical coupling strength to form a discrete level below the continuous energy spectrum.

In the next section we study the local attraction problem in 1D, 2D and 3D, and we verify the above statement on the formation of bound-states. Then we consider the fullerenes. Taking the discrete structure of the C_{60} molecule into account, we first solve the negative U Hubbard model, which is obtained from the tight binding Hamiltonian by adding a term lowering the energy when two fermions occupy the same site, for two fermions on a lattice of sixty sites formed by the vertices of a truncated-icosahedron. By exact diagonalization, we find that even a very small but negative U value is enough to form a pair, i.e. a wave function decaying with distance between the fermions. Going to a continuum version of the problem, we then show that an attractive interaction between two particles confined to the surface of a sphere gives rise to a bound state, no matter how weak the interaction is. We explore the similarity between a sphere and a plane as far as pairing properties are concerned.

4.2.1 Bound-State Formation in 1D, 2D and 3D

The simplest way to study the dimensional effects on the formation of bound-states is to consider a shallow potential well and solve the one particle problem. Due to translational invariance the two particle problem can be reduced to one and the well potential can model simple short range interactions. This problem can easily be handled by using the Green's function technique.³ We first find the free particle Green's function G_0 and then introduce the interaction V by means of a perturbation expansion to evaluate the exact Green's function G . Since the poles of G are simply the eigenvalues of the Hamiltonian $H = H_0 + V$, we investigate whether G has any pole below the ground state eigenvalue of the unperturbed Hamiltonian H_0 , which we will take to be zero.

$G_0(E) = (E - H_0)^{-1}$ can be expressed in terms of the eigenvalues E_n^0 and the

Dimension	$G_0(\vec{r}, \vec{r}'; E)$	$E \rightarrow 0^-$
3D	$-\frac{m}{2\pi\hbar^2} \frac{\exp(-k_0 \vec{r}-\vec{r}')}{ \vec{r}-\vec{r}' }$	finite
2D	$-\frac{m}{\pi\hbar^2} K_0(k_0 \vec{r}-\vec{r}')$	$\frac{m}{\pi\hbar^2} \ln(k_0 \vec{r}-\vec{r}') + \text{const.} + o(k_0 \vec{r}-\vec{r}')$
1D	$-\frac{m}{\hbar^2 k_0} \exp(-k_0 r-r')$	$-\sqrt{\frac{m}{2\hbar^2 E }}$

Table 4.3: Free particle Green's functions

$k_0 = \sqrt{2m|E|}/\hbar$, m : mass of the particle, K_0 : zeroth order modified Bessel function

complete set of orthonormal eigenfunctions $\psi_n^0(\vec{r})$ of H_0 by the equation

$$G_0(\vec{r}, \vec{r}'; E) = \int dn \frac{\psi_n^0(\vec{r})\psi_n^0(\vec{r}')}{E - E_n^0} \quad (4.1)$$

where $\int dn$ is an (multiple for 2D and 3D) integral over the continuous spectrum. Using the above expression or the differential equation satisfied by $G_0(\vec{r}, \vec{r}'; E)$, the free particle Green's functions for negative energies ($E < 0$) can easily be found (table 4.3).³ Note that because we are searching the poles of G below zero, we need G_0 for $E < 0$. Furthermore, since we are going to take V to be very small and negative, $E \rightarrow 0^-$.

Now, using $G(E) = [E - (H_0 + V)]^{-1}$, it is easy to obtain a power series expansion for G ,

$$G = G_0 + G_0 V G_0 + G_0 V G_0 V G_0 + \dots \quad (4.2)$$

We are interested in finding whether or not a discrete level appears and how it varies with V . For simplicity, we assume that

$$V(\vec{r}) = \begin{cases} -V_0 & \text{for } \vec{r} \text{ inside } R_0 \\ 0 & \text{otherwise} \end{cases} \quad (4.3)$$

where R_0 is a finite region in real space, e.g. a sphere, and V_0 is the depth of the attractive potential which we will take to be very small. Since V is defined in the real space, it is convenient to write equation 4.2 in this representation also. Therefore,

$$G(\vec{r}, \vec{r}'; E) = G_0(\vec{r}, \vec{r}'; E) - V_0 \int_{R_0} d\vec{r}_1 G_0(\vec{r}, \vec{r}_1; E) G_0(\vec{r}_1, \vec{r}'; E) \quad (4.4) \\ + V_0^2 \int_{R_0} d\vec{r}_1 \int_{R_0} d\vec{r}_2 G_0(\vec{r}, \vec{r}_1; E) G_0(\vec{r}_1, \vec{r}_2; E) G_0(\vec{r}_2, \vec{r}'; E) + \dots$$

For our purposes what is important is whether the above expansion is finite or not. This sum exhibits drastically different behaviors for different dimensions. Thus, we are going to study each case separately.

3D case

Since, G_0 is finite for $E \rightarrow 0^-$, given E , V_0 can be taken to be so small that the series in equation 4.4 converges, which means that $G(E)$ has no pole for $E \rightarrow 0^-$. Thus, to obtain a bound state, the small term $V_0 R_0$ in the expansion must be large enough (so that the series diverges). Here, R_0 is used both for the region and its volume.

2D case

Small argument expansion of $G_0(\vec{r}, \vec{r}'; E)$, with its logarithmic dependence on $|\vec{r} - \vec{r}'|$, suggests that we can approximate the Green's functions in the second and the higher order terms in equation 4.4 by their mean value. Then, the sum turns out to be a geometric series

$$G(\vec{r}, \vec{r}'; E) \simeq G_0(\vec{r}, \vec{r}'; E) \sum_{n=0}^{\infty} \left[-\frac{V_0 R_0 m}{\pi \hbar^2} \ln(k_0 S^{1/2}) \right]^n \quad (4.5)$$

which can easily be summed, provided that $V_0 R_0$ is small enough, to give

$$G(\vec{r}, \vec{r}'; E) \simeq \frac{G_0(\vec{r}, \vec{r}'; E)}{1 + \frac{V_0 R_0 m}{\pi \hbar^2} \ln(k_0 S^{1/2})} \quad (4.6)$$

where S is of the order of the area of the region R_0 . We see that the pole corresponding to bound state is given by

$$-\frac{\hbar^2}{2mS} \exp\left(-\frac{2\pi \hbar^2}{mV_0 R_0}\right) . \quad (4.7)$$

Note that the exact solution of the problem, i.e. calculation of the multiple integrals explicitly, would only change the effective value of S , and it would not alter the exponent. As a result, independent of the details of the potential, a local attractive interaction creates a bound state no matter how weak it is.

1D case

Approximating the multiple integrals by their averages as in the 2D case (this is a very good approximation since G_0 is independent of $|r - r'|$ as $E \rightarrow 0^-$),

$$G(\vec{r}, \vec{r}'; E) \simeq \frac{G_0(\vec{r}, \vec{r}'; E)}{1 - V_0 R_0 \sqrt{m/2\hbar^2} |E|} , \quad (4.8)$$

which gives a pole at

$$-\frac{mR_0^2V_0^2}{2\hbar^2} . \quad (4.9)$$

Thus, for the 1D case a discrete level is always formed.

In summary, for a particle to form a bound state around an attractive potential, in 3D case it is necessary for the potential to be stronger than a threshold value, while in 1D and 2D cases a bound state is always formed no matter how weak the attractive interaction is.

4.2.2 Hubbard Model on Truncated-Icosahedron

Before solving the Hubbard model¹⁰⁶ for two fermions on a truncated-icosahedron, we are going to solve it on the 1D chain having the lattice constant a . The energy eigenvalues and the eigenstates for the latter can be obtained analytically and therefore it is very helpful to gain an idea about the behavior of the two particle problem in higher dimensions. In fact, as we are going to show below, both in 1D chain and on truncated-icosahedron, the two electron ground state wave function for negative U decay in the same way, namely $\exp(-\kappa|\vec{r}_1 - \vec{r}_2|)$ where $\kappa \propto |U|/|t|$.

The Hubbard Hamiltonian is given by

$$H = t \sum_{\langle ij \rangle \sigma} c_{i\sigma}^\dagger c_{j\sigma} + U \sum_i n_{i\uparrow} n_{i\downarrow} , \quad (4.10)$$

where $c_{i\sigma}^\dagger$ is the creation operator for the state at site i with spin σ and $n_{i\uparrow} = c_{i\uparrow}^\dagger c_{i\uparrow}$ is the number operator. Here t is the nearest neighbor ($\langle ij \rangle$) hopping integral and U is the Coulomb repulsion energy. Although, the Hubbard model was originally proposed¹⁰⁶ for correlated electron systems and therefore U is always positive, in the context of electron and local excitation systems the same Hamiltonian but with negative U values has been derived.¹⁰⁷

It is very helpful to rewrite the Hamiltonian in the momentum space representation by defining the operators

$$c_{k\sigma} = \frac{1}{\sqrt{N}} \sum_j \exp(-ikja) c_{j\sigma} , \quad (4.11)$$

where a is the lattice constant and N is the number of sites which we eventually let to go to infinity. Defining the band energy $\epsilon_k = 2t \cos ka$, we can write the transformed Hamiltonian as

$$H = \sum_{k\sigma} \epsilon_k c_{k\sigma}^\dagger c_{k\sigma} + \frac{U}{N} \sum_{pp'q} c_{p+q}^\dagger c_{p'-q}^\dagger c_{p'} c_p . \quad (4.12)$$

Now, let us write the eigenkets $|\Psi\rangle$ in terms of the operators $c_{k\sigma}^\dagger$ which form a complete basis when applied on the vacuum $|0\rangle$ as

$$|\Psi\rangle = \sum_q L(q) c_{q1}^\dagger c_{Q-q1}^\dagger |0\rangle \quad (4.13)$$

Here, Q is the total momentum of the two fermion system and it is conserved due to the translational invariance of the lattice. By inserting $|\Psi\rangle$ into the Schrödinger equation $H|\Psi\rangle = E|\Psi\rangle$ we find that $L(q)$ satisfies the equation

$$(E - \epsilon_q - \epsilon_{Q-q})L(q) = \frac{U}{N} \sum_p L(p) . \quad (4.14)$$

The existence of a solution for $L(q)$ implies a self consistency condition which can be obtained by solving $L(q)$ from the left hand side and inserting into the right hand side. Let us write $L(q)$ as

$$L(q) = \frac{\frac{U}{N} \sum_p L(p)}{E - \epsilon_q - \epsilon_{Q-q}} , \quad (4.15)$$

and use this expression in the previous equation. Doing the necessary cancellations we end up with

$$1 = \frac{U}{N} \sum_q \frac{1}{E - \epsilon_q - \epsilon_{Q-q}} . \quad (4.16)$$

The above equation gives the eigenvalues E . Let us confine ourselves to the ground state for which $Q = 0$, and let us approximate the sum by an integral by means of the transformation

$$\frac{1}{N} \sum_q \rightarrow \frac{a}{2\pi} \int_{-\frac{\pi}{a}}^{\frac{\pi}{a}} dq . \quad (4.17)$$

Therefore, we can write the eigenvalue equation as

$$1 = \frac{U}{2\pi} \int_{-\pi}^{\pi} \frac{d\theta}{E - 4t \cos \theta} , \quad (4.18)$$

and upon integration we find the ground state energy eigenvalue to be

$$E = \text{sign}(U) \sqrt{U^2 + 16t^2} , \quad (4.19)$$

where $\text{sign}(U)$ stands for the sign of U . Since we are interested in the negative U case, $\text{sign}(U)$ will be -1. After finding E , we can calculate the wave function $L(x)$, which is defined by

$$L(x) = \frac{1}{\sqrt{2\pi}} \int_{-\pi}^{\pi} d\theta \exp(i\theta x) L(\theta) \quad (4.20)$$

where

$$L(\theta) = \frac{\frac{U}{N} \sum_p L(p)}{E - 4t \cos \theta} . \quad (4.21)$$

Since, we are interested in the shape of the wave function, we do not need the exact value of the normalization constant $\frac{U}{N} \sum_p L(p) = c$. Hence,

$$L(x) = \left(\frac{c}{\sqrt{2\pi}} \right) \int_{-\pi}^{\pi} d\theta \frac{\exp(i\theta x)}{E - 4t \cos \theta} . \quad (4.22)$$

The integration can easily be done by going to the complex plane and choosing the unit circle as the contour. Defining $z = E/4t$, we find that

$$L(x) = \left(\frac{c}{\sqrt{2\pi}} \right) \left(-\frac{1}{2it} \right) \oint_{|w|=1} dw \frac{w^{|x|}}{w^2 - 2zw + 1} . \quad (4.23)$$

Since $|z| > 1$, the only pole falling into the unit circle is $z - \sqrt{z^2 - 1}$ and therefore

$$L(x) = \left(\frac{c\sqrt{2\pi}}{4t} \right) \frac{(z - \sqrt{z^2 - 1})^{|x|}}{\sqrt{z^2 - 1}} . \quad (4.24)$$

Grouping all the constants in \tilde{c} , the probability density $|L(x)|^2$ is found to be of the form

$$|L(x)|^2 = \tilde{c} \exp(x/\lambda) , \quad (4.25)$$

where $\lambda = -2 \ln(z - \sqrt{z^2 - 1})$. For weak coupling, i.e. $|U| \ll |t|$, $\lambda \simeq -2|t|/|U|$. Therefore, the ground state wave function of the negative U Hubbard model with two fermions is given

$$L(x) = \text{constant} \times \exp(-x|U|/|t|) \quad (4.26)$$

where x is the distance between the fermions in units of the lattice constant. Since this expression is obtained for weak coupling, the wave function will extend over several unit cells.

Now, we return to the truncated-icosahedron problem. In order to study a local attraction mechanism, we are going to solve the negative U Hubbard model for two fermions moving on a C_{60} molecule. Therefore, we consider a lattice formed by the sixty vertices of a truncated-icosahedron and write down the Hubbard Hamiltonian:

$$H = t \sum_{\langle ij \rangle \sigma} c_{i\sigma}^\dagger c_{j\sigma} + U \sum_i n_{i\uparrow} n_{i\downarrow}. \quad (4.27)$$

Here, i and j label the sites on the C_{60} molecule and $\langle ij \rangle$ denotes two nearest neighbor sites. Although, the general solution of the model has not been found, the two-body problem can be treated analytically.¹⁰⁸ We are going to diagonalize H by writing the matrix elements in the $|\Psi \rangle = |ij \rangle \otimes \chi$ basis where $|ij \rangle$ stands for the space part and χ is the spinor. For singlet pairing $\chi = \chi_S$, $|ij \rangle$ must be symmetric in i and j due to the antisymmetry of $|\Psi \rangle$. In fact, it is enough to study in $|ij \rangle$ basis since there is no spin flip term in the Hamiltonian. Thus, for $i \neq j$, $|ij \rangle$ will be defined by

$$|ij \rangle = \frac{1}{\sqrt{2}} (c_{i\uparrow}^\dagger c_{j\downarrow}^\dagger - c_{i\downarrow}^\dagger c_{j\uparrow}^\dagger) |0 \rangle, \quad (4.28)$$

while for $i = j$, it is

$$|ii \rangle = c_{i\uparrow}^\dagger c_{i\downarrow}^\dagger |0 \rangle \quad (4.29)$$

where $|0 \rangle$ denotes the vacuum.

There will be three different kinds of matrix elements of H . These are the on-site to on-site

$$\langle ii | H | jj \rangle = U \delta_{ij}, \quad (4.30)$$

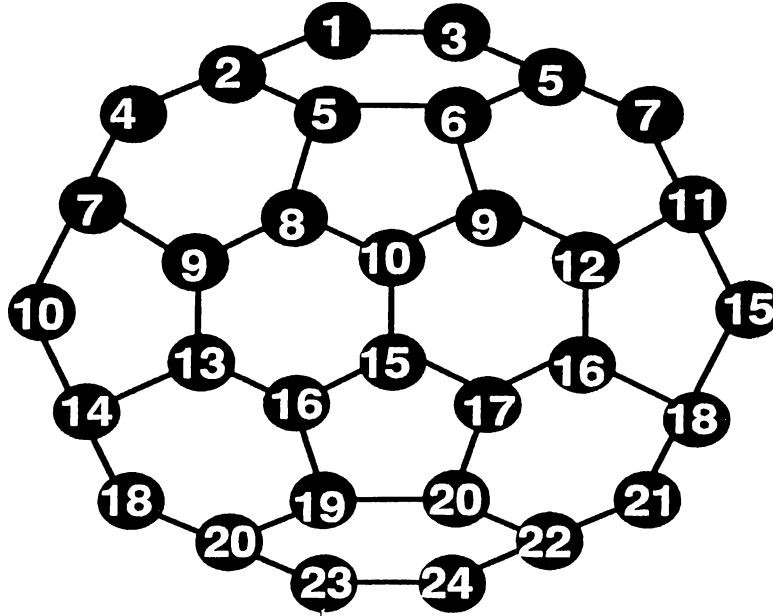


Figure 4.7: Labeling the sites on truncated-icosahedron
The figure shows all possible, *distinguishable* two by two combinations of the 60 sites.

the on-site to bond

$$\langle ij|H|kk \rangle = t\sqrt{2}(\delta_{ik}\delta_{<jk>} + \delta_{jk}\delta_{<ik>}), \quad (4.31)$$

and the bond to bond terms

$$\langle ij|H|kl \rangle = t(\delta_{jl}\delta_{<ik>} + \delta_{il}\delta_{<jk>} + \delta_{jk}\delta_{<il>} + \delta_{ik}\delta_{<jl>}). \quad (4.32)$$

The matrix representation of H will contain 1830×1830 elements. 1830 is the number of all possible two by two combinations of 60 elements (including the case in which an element is combined by itself). However, for the eigenstates having the symmetry of the truncated-icosahedron, i.e. all sites equivalent, the dimension is highly reduced and it becomes 24×24 . 24 is simply the number of possible line segments with ends at the vertices of the truncated-icosahedron (figure 4.7). Since, we are considering only singlet pairing, the real space wave function is symmetric and as a result of this it is enough to consider line segments without thinking of the ordering of the two ends. 24 different elements can be figured out by examining the surface of a truncated-icosahedron. We start with

an arbitrary vertex. Pairing it with itself is the first element. Then we go to nearest neighbors. Draw all the possible connections and check whether any two segments are equivalent by a symmetry transformation. After completing this process, we consider the next nearest neighbors etc.. In writing the indices we follow the increasing distance between the electrons. Therefore, we look for the eigenvalues and eigenfunctions of the following matrix:

$$\begin{bmatrix}
 U & 2\sqrt{2}t & \sqrt{2}t & 0 \\
 2\sqrt{2}t & 0 & 0 & 2t & 2t & 0 & 0 & 0 & 0 & 0 & 0 & 0 & 0 & 0 & 0 & 0 & 0 & 0 & 0 & 0 & 0 & 0 & 0 & 0 \\
 2\sqrt{2}t & 0 & 0 & 0 & 4t & 0 & 0 & 0 & 0 & 0 & 0 & 0 & 0 & 0 & 0 & 0 & 0 & 0 & 0 & 0 & 0 & 0 & 0 & 0 \\
 0 & 2t & 0 & 2t & 0 & 0 & 2t & 0 & 0 & 0 & 0 & 0 & 0 & 0 & 0 & 0 & 0 & 0 & 0 & 0 & 0 & 0 & 0 & 0 \\
 0 & t & t & 0 & 0 & 2t & t & t & 0 & 0 & 0 & 0 & 0 & 0 & 0 & 0 & 0 & 0 & 0 & 0 & 0 & 0 & 0 & 0 \\
 0 & 0 & 0 & 0 & 4t & 0 & 0 & 0 & 2t & 0 & 0 & 0 & 0 & 0 & 0 & 0 & 0 & 0 & 0 & 0 & 0 & 0 & 0 & 0 \\
 0 & 0 & 0 & t & t & 0 & t & 0 & t & t & t & 0 & 0 & 0 & 0 & 0 & 0 & 0 & 0 & 0 & 0 & 0 & 0 & 0 \\
 0 & 0 & 0 & 0 & 0 & 2t & 0 & 0 & 0 & 2t & 2t & 0 & 0 & 0 & 0 & 0 & 0 & 0 & 0 & 0 & 0 & 0 & 0 & 0 \\
 0 & 0 & 0 & 0 & 0 & t & t & t & 0 & t & 0 & t & t & 0 & 0 & 0 & 0 & 0 & 0 & 0 & 0 & 0 & 0 & 0 \\
 0 & 0 & 0 & 0 & 0 & 0 & t & t & t & t & 0 & 0 & 0 & t & t & 0 & 0 & 0 & 0 & 0 & 0 & 0 & 0 & 0 \\
 0 & 0 & 0 & 0 & 0 & 0 & 2t & 0 & 0 & 0 & t & 2t & 0 & 0 & t & 0 & 0 & 0 & 0 & 0 & 0 & 0 & 0 & 0 \\
 0 & 0 & 0 & 0 & 0 & 0 & 0 & 0 & -2t & 0 & 2t & 0 & 0 & 0 & 0 & 2t & 0 & 0 & 0 & 0 & 0 & 0 & 0 & 0 \\
 0 & 0 & 0 & 0 & 0 & 0 & 0 & 0 & 0 & 2t & 0 & 0 & 0 & 0 & 2t & 0 & 0 & 0 & 0 & 0 & 0 & 0 & 0 & 0 \\
 0 & 0 & 0 & 0 & 0 & 0 & 0 & 0 & 0 & 0 & 2t & 0 & 0 & 2t & 0 & 0 & 0 & 0 & 2t & 0 & 0 & 0 & 0 & 0 \\
 0 & 0 & 0 & 0 & 0 & 0 & 0 & 0 & 0 & t & t & 0 & 0 & 0 & t & t & t & t & 0 & 0 & 0 & 0 & 0 & 0 \\
 0 & 0 & 0 & 0 & 0 & 0 & 0 & 0 & 0 & 0 & 0 & t & t & 0 & t & 0 & t & t & t & 0 & 0 & 0 & 0 & 0 \\
 0 & 0 & 0 & 0 & 0 & 0 & 0 & 0 & 0 & 0 & 0 & 0 & 0 & 0 & 2t & 2t & 0 & 0 & 0 & 0 & 2t & 0 & 0 & 0 \\
 0 & 0 & 0 & 0 & 0 & 0 & 0 & 0 & 0 & 0 & 0 & 0 & 0 & 0 & 0 & t & 0 & t & 0 & t & 0 & t & 0 & 0 \\
 0 & 0 & 0 & 0 & 0 & 0 & 0 & 0 & 0 & 0 & 0 & 0 & 0 & 0 & 2t & 0 & 0 & 0 & 0 & 4t & 0 & 0 & 0 & 0 \\
 0 & 0 & 0 & 0 & 0 & 0 & 0 & 0 & 0 & 0 & 0 & 0 & 0 & 0 & 0 & t & t & 2t & 0 & 0 & t & t & 0 & 0 \\
 0 & 0 & 0 & 0 & 0 & 0 & 0 & 0 & 0 & 0 & 0 & 0 & 0 & 0 & 0 & 0 & 0 & 2t & 0 & 0 & 2t & 2t & 0 & 0 \\
 0 & 0 & 0 & 0 & 0 & 0 & 0 & 0 & 0 & 0 & 0 & 0 & 0 & 0 & 0 & 0 & 0 & 0 & 0 & 2t & 2t & 0 & 0 & 2t \\
 0 & 0 & 0 & 0 & 0 & 0 & 0 & 0 & 0 & 0 & 0 & 0 & 0 & 0 & 0 & 0 & 0 & 0 & 0 & 4t & 0 & 0 & 0 & 2t \\
 0 & 4t & 2t & 0
 \end{bmatrix}$$

(4.33)

The 24×24 matrix will give 24 eigenvalues for the states having the required symmetry. Among these, the lowest value corresponds to the ground state. Figure 4.8 shows a typical probability density distribution for the ground state corresponding to $t = -1$ and $U = -3$.

Our numerical analysis shows that the decay of the wave function with increasing electron-electron distance is exponential. Hence, it goes like $\exp(-\alpha|i-j|)$ with $\alpha \sim |U/t|$. From this result, we can conclude that the negative U Hubbard model for two fermions on a truncated icosahedron always gives a ground state wave function decaying with distance between the fermions. The extension of the wave function is determined by $|U/t|$. For $|U| > |t|$, two particles form a pair localized almost on a site.

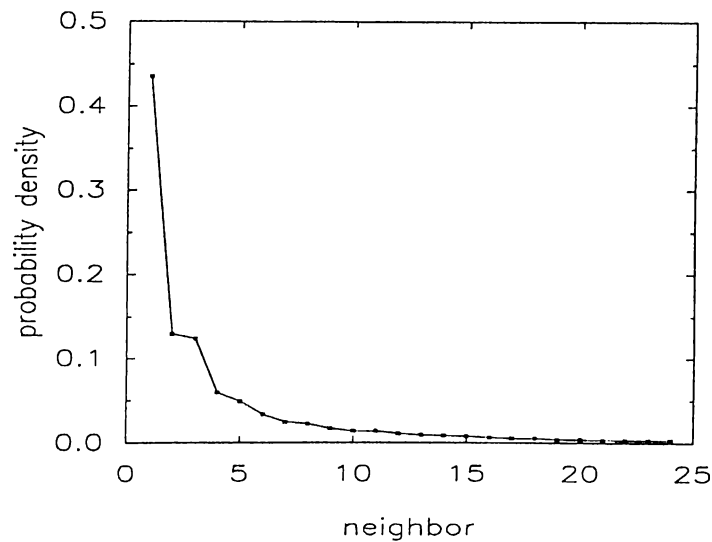


Figure 4.8: Two fermions on the truncated-icosahedron

Probability density for the ground state as a function of the distance between the fermions. On the horizontal axis 1 corresponds to the configuration where the two fermions sit on the same site. Here $t = -1$ and $U = -3$.

4.2.3 Bound-State Formation on a Sphere

In this section we are going to solve a continuum version of the above problem.¹⁰⁹ We first consider two particles moving on the surface of a sphere. The negative U is now replaced by an attractive interaction which depends upon the relative coordinates of the particles only. Rotational invariance of the system reduces the two-body problem to an effective one-body problem where the particle moves in the field of an attractive potential. We then apply the method that we have used for the bound state formation problem in 1D, 2D and 3D. We evaluate the Green's function G_0 for the free particle, and then treat the attractive interaction perturbatively. We sum the infinite perturbation series to find the new Green's function G and show that it has a pole at negative energies. We find that two particles on a sphere form a bound state no matter how weak the attractive interaction is.

In spite of the fact that the solid C_{60} is a 3D system, the surface of a C_{60}

molecule has a 2D character. Consequently, one expects a behavior reminiscent of the perfect 2D case, i.e. a bound state even for a very weak attractive interaction. To verify this conjecture, we first consider two particles moving on the surface of a sphere which are interacting with each other via a potential depending upon relative coordinates of the particles only. As a result of the invariance of the system under the displacement of the *center of mass* on the sphere, this problem can be reduced to an effective one body problem, or *central force problem* on the surface of a sphere. Thus, it is enough to study the motion of a particle in the field of an attractive potential. Now, we are going to investigate whether the above statement on the bound-state formation in reduced dimensional systems is also valid for sphere. Note that this is not in contradiction with the Cooper problem where two electrons are always bound. In the Cooper problem, two electrons above the Fermi surface of a many-electron system are assumed to be interacting via an attractive potential. In our system, however, there are only a few free electrons on a C_{60} sphere, so a Fermi surface cannot be defined. Therefore, it is not obvious whether an attractive interaction causes the electrons to form a pair.

To calculate the Green's function we first find the eigenvalues and the eigenfunctions for a particle moving on the surface of a sphere freely. This is nothing but 3D rotator problem. The Schrödinger equation

$$-\frac{\hbar^2}{2m} \left[\frac{1}{R^2 \sin \theta} \frac{\partial}{\partial \theta} (\sin \theta \frac{\partial}{\partial \theta}) + \frac{1}{R^2 \sin^2 \theta} \frac{\partial^2}{\partial \phi^2} \right] \Psi = E \Psi \quad (4.34)$$

is satisfied by the spherical harmonics and $\Psi(\theta, \phi) = R^2 Y_l^m(\theta, \phi)$. Therefore, the Green's function for a free particle of mass m constrained to move on the surface of a sphere of radius R is given by

$$G_0(\hat{n}, \hat{n}'; \epsilon) = \sum_{l=0}^{\infty} \sum_{m=-l}^{m=l} \frac{Y_l^m(\hat{n}) Y_l^{m*}(\hat{n}')}{E - E_l} \quad (4.35)$$

or by means of the addition theorem

$$P_l(\hat{n} \cdot \hat{n}') = \frac{4\pi}{2l+1} \sum_{m=-l}^{m=l} Y_l^m(\hat{n}) Y_l^{m*}(\hat{n}') \quad (4.36)$$

it takes the form

$$G_0(\hat{n}, \hat{n}'; \epsilon) = \frac{1}{4\pi E_R} \sum_{l=0}^{\infty} \frac{2l+1}{\epsilon - l(l+1)} P_l(\hat{n} \cdot \hat{n}'), \quad (4.37)$$

where \hat{n} and \hat{n}' are the position vectors on the unit sphere, P_l are Legendre polynomials and ϵ is the energy of the particle in units of $E_R = \hbar^2/2mR^2$.

We now assume that a weak attractive interaction V_0 is effective in a solid angle Ω_0 . Under these circumstances we examine the Green's function $G(\hat{n}, \hat{n}'; \epsilon)$ to find if it has a pole in the interval $[-V_0, 0]$. Since $V_0 \rightarrow 0^+$ for a weak interaction, we have to find $G(\hat{n}, \hat{n}'; \epsilon)$ as $\epsilon \rightarrow 0^-$. In this limit $G_0(\hat{n}, \hat{n}'; \epsilon)$ can be evaluated in a closed form. For this purpose, we approximate the summation in equation 4.37 by neglecting ϵ dependence of all the terms except $l = 0$. Noting that $(2l+1)/l(l+1) = 1/l + 1/(l+1)$, we obtain¹¹⁰

$$G_0(\hat{n}, \hat{n}'; \epsilon) \simeq \frac{1}{4\pi E_R} \left(\frac{1}{\epsilon} + \ln \frac{1 - \hat{n} \cdot \hat{n}'}{2} + 1 \right). \quad (4.38)$$

Here, the logarithm term indicates that the above model is similar to the 2D free particle problem. It is seen that G_0 exhibits a logarithmic singularity as the two point approach each other. This is consistent with the observation that a very small portion of the surface of a sphere can be approximated by a 2D plane. The singularity of G_0 as ϵ goes to zero in equation 4.38 is stronger than G_0 of the 2D plane which changes with logarithm of ϵ (table 4.3). Such a difference is expected since the energy spectra are quite different in two cases. In fact, $1/\epsilon$ behavior in equation 4.38 instead of $\ln \epsilon$ as in the perfect 2D case originates from discretization of the energy levels. If the difference between these discrete energy levels become very small, then the approximation made to obtain equation 4.38 is no longer valid. In this case, we cannot separate out $1/\epsilon$ and neglect the ϵ dependence of the other terms, but consider all the terms of the form $1/(\epsilon - x)$ where x is now a continuous variable instead of discrete $l(l+1)$. Adding those terms by integration over x , we end up with a logarithmic singularity. This is an expected result since the spacing of discrete energy levels is controlled by R , and the sphere approaches to a plane as R increases indefinitely. It is seen that Green's functions for a particle on the surface of a sphere and on the (2D) plane

are similar in the appropriate limits as far as the position (\hat{n}, \hat{n}') and energy (ϵ) dependences are concerned.

Knowing G_0 and V_0 , we can find G by means of the perturbation expansion

$$G(\hat{n}, \hat{n}'; \epsilon) = G_0(\hat{n}, \hat{n}'; \epsilon) - V_0 \int_{\Omega_0} d\hat{n}_1 G_0(\hat{n}, \hat{n}_1; \epsilon) G_0(\hat{n}_1, \hat{n}'; \epsilon) + \dots \quad (4.39)$$

Here, for the sake of simplicity we assume that V_0 is a constant interaction, i.e. independent of the relative positions of the electrons, and is effective only in solid angle Ω_0 . For $\hat{n} \cdot \hat{n}' \neq 1$ and $\epsilon \neq 0$, G_0 is finite. Thus, G can be calculated by summing the series. We approximate the product of Green's functions by factoring out G_0 and using the average values $\langle G_0 \rangle_{\Omega_0}$ for the rest. For our purposes it is enough to know the order of magnitude of $\langle G_0 \rangle_{\Omega_0}$. Therefore, we calculate $\langle G_0 \rangle_{\Omega_0}$, which is found to be $(1/\epsilon + 2\delta^2 \ln \delta - \delta^2 + 1)/4\pi E_R$ where $0 < \delta < 1$. Since $\epsilon \rightarrow 0^+$, $\langle G_0 \rangle_{\Omega_0}$ can be very well approximated by $1/4\pi E_R \epsilon$. At the end we obtain

$$G(\hat{n}, \hat{n}'; \epsilon) \simeq \frac{G_0(\hat{n}, \hat{n}'; \epsilon)}{1 + \frac{V_0 \Omega_0}{4\pi E_R \epsilon}} \quad (4.40)$$

It is seen that a negative energy level $E = \epsilon E_R = -V_0 \Omega_0 / 4\pi$ corresponding to a bound state is always formed, even for a very weak interaction. However, the extension of the wave function will depend upon the strength of the potential. Here, we assume that the net interaction between the electrons on the sphere is attractive. In principle, V_0 contains Coulomb repulsion and an attractive mechanism, perhaps due to the vibrational modes of fullerene. Note that the wave function of the two electron system has to be antisymmetrized. However, since the interaction we have considered is symmetric, the ground state energy remains unchanged after the antisymmetrization.

So far we have shown that two electron system on a sphere is unstable against pair formation. We next consider a solid phase formed by the spheres in the foregoing discussion. When these spheres are placed at lattice sites they begin to interact with each other weakly. The superconductivity has been observed for approximately three alkali atoms per C_{60} molecule. Two of these three electrons will fill the first conduction band while the third one creates a half-filled metallic band. Therefore, effectively we are left with one electron per C_{60} molecule and

these electrons are free to move from site to site. Thus, we can assume that two electrons can come together on a sphere to form a bound state as we discussed above. The increase in the Coulomb energy due to occupation of a sphere by a fourth electron is expected to be negligible. This is because these materials exhibit metallic behavior in the normal phase in contradiction to Mott-Hubbard insulator which is the expected ground state in the presence of strong Coulomb interactions.

Note that superconductivity is *not* achieved by Bose-Einstein condensation even though the electrons move in the form of tightly bound pairs. Otherwise, the measured critical temperature would require an on-site interaction of 30–40 eV since the value of transfer (hopping) integral inferred from band structure calculations is only ~ 0.1 eV. In view of this argument, we propose that superconductivity occurs as a result of formation of pairs in units (i.e., on C_{60} spheres), which are coupled by Josephson interaction. The situation is reminiscent of the superconductivity of layered systems where the 2D Fermi liquids in the layers are unstable against Cooper pairing and they interact via interlayer tunneling. In present case layers are replaced by spheres which can be occupied by only a few electrons and the origin of the pairing is not Cooper instability but a dimensionality effect. For layered materials it can be shown that the critical temperature T_c is not altered by the Josephson coupling.⁵¹ Therefore, in the present case it is expected that $k_B T_c \sim V_0 \Omega_0$, which leads to a reasonable value for the coupling constant V_0 . Since the infinite layers are replaced by finite spheres, charging effects due to the occupation of a sphere by an excess pair can be important. In fact, treating the C_{60} molecules as spherical capacitors we find that charging energy is in the range of a few eV. This implies that the C_{60} molecule can be occupied by only one pair (formed by the third and the fourth electrons donated by the alkali atoms) when the solid is in the superconductive phase. Nevertheless, for a correct description of the system, 3D net of Josephson junctions including charging effects should be considered in detail.

In conclusion, we have shown that two fermions moving on a truncated-icosahedron and interacting via a local attractive interaction form a pair whose

wave function decays exponentially with the distance between the fermions. Going to a continuum model we have also found that in analogy to 2D and 1D systems, an attractive interaction always yields a bound state for particles constrained to move on the surface of a sphere. Our results give clues about the wave functions of the Cooper pairs in the superconducting fullerenes. Moreover, they indicate that surface of C_{60} molecules causes to an instability for pair formation owing to the reduced dimensionality of the system. In the crystal composed of those spheres, a transition to the superconducting phase associated with the formation of pairs can be observed. Such a mechanism can be thought to be operational in the superconductivity of the alkali metal doped C_{60} solid.

4.3 Local Oscillator Model for Superconducting Fullerenes

In this section we study the coupling of electrons in alkali metal doped C_{60} by intramolecular vibrations.¹¹¹ The C_{60} molecules are treated as perfect spheres oscillating independently along their radial directions, and electron-phonon coupling is calculated by the adiabatic approximation. By the polaronic canonical transformation we show that this model is equivalent to the negative U Hubbard model where each C_{60} molecule is treated as a lattice site. For strong enough electron-phonon coupling this attractive interaction can overcome the Coulomb repulsion between two electrons sitting on the same site and the resulting interaction leads to superconductivity.

Since, the C_{60} molecules in fullerenes are free to rotate at their lattice points above the ordering temperature,⁸⁹ we treat the molecules as isolated oscillators. Recent Raman scattering studies have verified that the vibrational spectra of isolated C_{60} molecule and crystalline form are almost identical.¹¹² Therefore, we confine ourselves to high frequency intramolecular vibrations.⁹⁵ In view of the electronic structure calculations, we also assume that the low-lying states correspond approximately to the angular momenta $l=0, 1, 2, 3,$ and 4 states

of free electrons on the surface of a sphere.⁸⁷ The highest occupied molecular orbital (HOMO) is five fold degenerate and along with the two triply degenerate lowest unoccupied molecular orbitals (LUMO) they constitute the $l=5$ states. In this simple model, the electron-phonon coupling stems from the dependence of the electron energy eigenvalue $E_l = \hbar^2 l(l+1)/2m^*R^2$, on the radius R of the sphere. Here, m^* is the *effective mass* of the electron. We are going to consider a particular phonon mode, the one corresponding to the isotropic oscillation of the sphere in the radial direction. Writing R as $R_0 + \delta R$, where R_0 is the radius of the sphere at equilibrium, we expand E_l in small displacement δR and find that the change in energy is given by $[\hbar^2 l(l+1)/2m^*R_0^3]\delta R$. Now, we can express δR in terms of the phonon creation and annihilation operators as $\delta R = (\hbar/2M\omega)^{1/2}(b^\dagger + b)$ where M is the total mass of the shell and ω is the frequency of the phonons. Therefore, we propose the following Hamiltonian to describe the superconductivity of alkali metal doped C_{60} solid:

$$H = \epsilon \sum_{i\sigma} n_{i\sigma} + t \sum_{\langle ij \rangle \sigma} c_{i\sigma}^\dagger c_{j\sigma} + \lambda \sum_{i\sigma} (b_i^\dagger + b_i) n_{i\sigma} + \hbar\omega \sum_i (b_i^\dagger b_i + \frac{1}{2}). \quad (4.41)$$

Here, i labels the sites (spheres) and $\langle ij \rangle$ stands for the nearest neighbors. $n_{i\sigma} = c_{i\sigma}^\dagger c_{i\sigma}$ is the number operator for electrons at site i with spin σ . In this tight binding model, $\epsilon = \hbar^2 l(l+1)/2m^*R_0^2$ is the on-site energy of electrons and t is the nearest neighbor hopping integral. Since we will be dealing with conduction electrons, l will be the same for all of them and therefore we will not put any subscripts on ϵ . Finally, as we have shown above, the electron-phonon coupling parameter λ is given by

$$\lambda = \frac{l(l+1)}{mR_0^3} \left(\frac{\hbar^5}{8M\omega} \right)^{1/2}. \quad (4.42)$$

In writing the electron-phonon coupling term we have used the adiabatic approximation. The main adiabaticity criterion is the absence of electronic excitations with energies comparable to the frequencies of the ionic vibrations. This criterion is fully satisfied as can be seen from the electronic structure calculations⁸⁸ indicating that intramolecular excitations are of the order of a few eV. It should be noted that, here what we have to compare with vibrational

frequency is not the kinetic energy of electron due to intermolecular motion but its *rotational* energy on a sphere.

The most straightforward way to treat electron-phonon interaction is the polaronic canonical transformation⁴⁵ $H \rightarrow \tilde{H} = e^S H e^{-S}$ where the antihermitian operator S is given by

$$S = \frac{\lambda}{\hbar\omega} \sum_{i\sigma} (b_i^\dagger - b_i) n_{i\sigma}. \quad (4.43)$$

\tilde{H} is obtained by applying this transformation to each operator in equation 4.41. Using the operator transformation rule

$$\tilde{A} = e^S A e^{-S} = A + [S, A] + \frac{1}{2!} [S, [S, A]] + \dots \quad (4.44)$$

\tilde{H} is found to be

$$\tilde{H} = \left(\epsilon - \frac{\lambda^2}{\hbar\omega}\right) \sum_{i\sigma} n_{i\sigma} + t \sum_{\langle ij \rangle \sigma} e^S c_{i\sigma}^\dagger c_{j\sigma} e^{-S} - \frac{2\lambda^2}{\hbar\omega} \sum_i n_{i\uparrow} n_{i\downarrow} + \hbar\omega \sum_i (b_i^\dagger b_i + \frac{1}{2}). \quad (4.45)$$

An equivalent way to find equation 4.45 is to shift phonon operators as $b_i \rightarrow b_i - (\lambda/\hbar\omega) \sum_{i\sigma} n_{i\sigma}$. From the first term, we see that on-site energy levels are shifted down. The second term describes the hopping of electrons between nearest neighbors. Although we did not give the form of the transformed term explicitly, it is possible to show that the effect of phonons is to reduce t to $\tilde{t} = t e^{-\lambda^2/\hbar^2\omega^2}$.⁴⁵ The third term shows that electron-phonon coupling induces an attractive interaction between two electrons sitting on the same site. Therefore, we end up with the so called negative U model,¹¹³ where $U = -2\lambda^2/\hbar\omega$. For $\hbar\omega \simeq 500\text{cm}^{-1}$, which corresponds to the lowest A_g mode,⁹⁵ we find that $|U| \sim 10^{-2}$ eV. In principle, there is a positive contribution U_C to U due to the Coulomb repulsion. Thus, the correlation effects can easily be taken into account by reducing the magnitude of the attractive interaction properly. If $U_C > U$, our approach needs modifications to take into account the retardation effects. In this case, the electron can not attract each other if they sit on the same site simultaneously. However, there is still a chance for attraction if they occupy the same sphere at different times. One electron creates a deformation on a sphere and lives. The deformation, which is nothing but the radial modes we

have mentioned, is *retarded* so that a second electron can come and interact with it before it dies out.

As is well known, the renormalized parameters in \tilde{H} are effective as long as electron states live long enough relative to the phonon time. For \tilde{t} , this condition requires that $\hbar\omega/t \gg e^{-\lambda^2/\hbar^2\omega^2}$. The ratio has been estimated to be of the order of 10^{14} and therefore the polaronic band narrowing is observable. $U = -2\lambda^2/\hbar\omega$ is already effective since in the absence of Coulomb interaction, two electrons can occupy the same site for a long enough time ($\hbar\omega/t \gg 1$). For nonvanishing Coulomb repulsion U_C , we compare the life time \hbar/U_C of the double occupation configuration with the phonon time $1/\omega$. Thus, for U_C to be replaced by $U_C - 2\lambda^2/\hbar\omega$, we need $U_C \ll \hbar\omega$ which holds as long as the correlation effects are not very strong.

The idea of negative U interaction due to electron-phonon coupling has already been proposed. Mazin *et al.*⁹⁸ make a quantitative analysis of the coupling and find out that the tangential rather than the radial modes (among which we use a particular one) are more effective. In our simple model only the latter is considered. It is possible to take into account the tangential modes by means of a jellium but this is an unnecessary complication for our purposes. Our aim is to demonstrate that the spherical shell approximation for C_{60} molecules is good enough to understand the physics of superconductivity observed in these materials. Furthermore, we show rigorously that our electron-phonon model is equivalent to negative U Hubbard model, which is not possible to do for a complicated numerical calculation of phonon spectrum.

The negative U Hubbard model has been widely used to describe the physics of systems with an effective short range attraction of electrons or holes.¹⁰⁷ There are various microscopic mechanisms leading to a local attractive interaction other than strong electron-lattice coupling. Electrons can couple to quasibosonic excitations of electronic origin such as excitons or plasmons, or purely electronic excitations that cannot be reduced to quasiboson coupling like polarizability of anions or some internal coordinate.

The behavior of the half-filled (one electron per site) negative U Hubbard

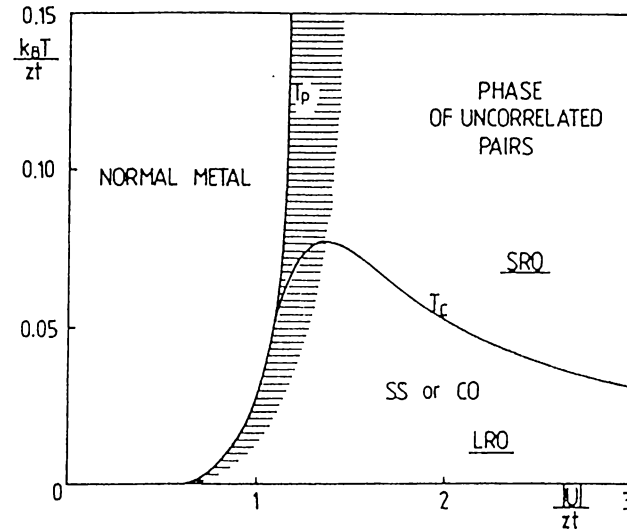


Figure 4.9: Phase diagram for negative U Hubbard model $2zt$:bandwidth, SRO: short range order, LRO: long range order, SS: singlet superconductor, CO: charge order. From Reference 107.

model is determined by the ratio $|U/t|$. Figure 4.9 shows the phase diagram for a simple cubic lattice at half-filling. T_c and T_p are the critical temperatures for the onset of long range ordering (LRO) and for the breaking of the electron pairs, respectively. SS denotes the singlet superconducting state whose two electron excitations are gapless. CO is the charge (or charge density wave—CDW) ordering state. In our case (at half-filling and in the absence of intersite interactions), the CDW and SS states are strictly degenerate. For small $|U/t|$, which corresponds to the BCS regime, the critical temperature T_c increases with $|U/t|$. At the strong attraction limit, the pairs exist above T_c which decreases as $t^2/|U|$ and they undergo Bose-Einstein condensation below T_c .

In conclusion, we have shown that a local oscillator model, where C_{60} molecules are treated as perfect spheres oscillating independently along their radial directions can be a potential candidate which induces attractive interaction and hence explain the superconductivity observed in alkali metal doped fullerenes. By means of the polaronic canonical transformation, we observe that the model is

equivalent to the negative U Hubbard model where each C_{60} molecule is treated as a lattice site. If the negative U interaction between the electrons can overcome the Coulomb repulsion to give a net attractive interaction, this model can explain superconductivity. For strong Coulomb repulsion, on the other hand, it should be modified to take into account the retardation effects.

Chapter 5

Conclusions

Recent developments in the field of superconducting systems of low dimensionality have attracted great interest not only for high critical temperatures but also for their exotic behaviors due to reduced dimensionality. Copper oxide and fullerene superconductors have higher T_c 's than all other known materials. In this thesis, we studied the effects of reduced dimensionality and possible mechanisms of superconductivity in these compounds and in coupled quantum well systems.

1. We analyzed the sudden reduction of the photoluminescence linewidth observed at low temperatures in coupled quantum wells, in view of possible 2D phase transitions occurring at different density limits. The linewidth calculated within a BCS-like transition is found to be proportional to the energy gap below the critical temperature.
2. We extended the theory of layered superconductors to describe superlattices in which layers of superconducting material consisting of M unit cells are separated by insulating layers that are N unit cells thick. We identified an intercell pairing interaction which controls the variation of T_c with M and N , and raises T_c from low to high temperatures. Then we explored the Ginzburg-Landau version of the model. We showed that the order parameter coupling turns out to be Heisenberg type, analogous to layered magnets. The mean field result for $T_c(M, N)$ is found to be in good

agreement with experiments for ultrathin NbSe₂ crystals and Sn-SiO, Al-AlO₂, YBCO/PrBCO superlattices. The fact that $T_c(M, N)$ increases with increasing M is traced back to a finite size effect, corresponding to crossover from nearly two to three dimensional superconductivity. This change from low to high temperature superconductivity is found to be independent of the sign of the interlayer interaction. An electrostatic model for interaction in YBCO/PrBCO superlattices is in reasonable agreement with experiment. The orbital upper critical field H_{c2}^{\parallel} turns out to be unlimited while H_{c2}^{\perp} is proportional to $T_c(M, N)$. We also investigated electron-phonon interactions in systems consisting of conducting layers separated by insulating media. The conducting layers are treated as 2D Fermi liquids, and the interaction between them is assumed to be tunneling. Phonon modes modifying the interlayer distances are found to lead to an attractive electron-electron interaction which can induce a superconducting transition.

3. We solved the negative U Hubbard model for two fermions on a lattice of sixty sites formed by the vertices of a truncated-icosahedron to understand the electron-electron interactions in C₆₀ molecule. By exact diagonalization, we find that nonvanishing U implies formation of a pair. We then show that an attractive interaction between two particles confined to the surface of a sphere gives rise to a bound state, no matter how weak the attractive interaction is and this result demonstrate that formation of the pair is a dimensional effect. Finally, we studied the coupling of electrons in alkali metal doped C₆₀ by intramolecular vibrations. Treating the C₆₀ molecules as perfect spheres oscillating independently along their radial directions, we obtain a negative U Hubbard model. For strong enough electron-phonon coupling, this attractive interaction can overcome Coulomb repulsion between two electrons sitting on the same sphere and the resulting interaction leads to superconductivity. However, even if the electron-phonon coupling is not strong enough, a retarded interaction can mediate pairing.

In summary, we investigated some effects of low dimensional structures of new superconductors having narrow conduction bands. The weak interatomic interaction leads not only to reduction of dimensionality but also to enhancement of correlation effects due to weak screening of the Coulomb repulsion. As a result, low dimensionality and strong correlations are the two important phenomena to be implemented into the theory of superconductivity.

Bibliography

- [1] Xiao-Gang Wen and Rui Kan, Charged boson condensation in high- T_c superconductors, *Physical Review B*, **37**:595, (1988).
- [2] L. D. Landau and E. M. Lifshitz, *Quantum Mechanics*, Pergamon Press, Oxford, (1977).
- [3] E. N. Economou, *Green's Functions in Quantum Physics*, Springer-Verlag, Berlin, (1979).
- [4] Shao-Jing Dong and Chen Ning Yang, Bound states between two particles in a two- or three-dimensional infinite lattice with attractive Kronecker δ -function interaction, *Reviews in Mathematical Physics*, **1**:139, (1989).
- [5] Leon van Hove, The occurrence of singularities in the elastic frequency distribution of a crystals, *Physical Review*, **89**:1189, (1953).
- [6] James C. Phillips, Critical points and lattice vibration spectra, *Physical Review*, **104**:1263, (1956).
- [7] Marston Morse, What is analysis in the large?, *American Mathematical Monthly*, **49**:358, (1942).
- [8] J. M. Kosterlitz and D. J. Thouless, Ordering, metastability and phase transitions in 2-dimensional systems, *Journal of Physics C: Solid State Physics*, **6**:1181, (1973).
- [9] R. E. Peierls, *Helvetica Physica Acta*, **7**:Supplement II 81, (1934).

- [10] N. D. Mermin, Crystalline order in two dimensions, *Physical Review*, **176**:250, (1968).
- [11] N. D. Mermin and H. Wagner, *Physical Review Letters*, **17**:1133, (1966).
- [12] P. C. Hohenberg, Existence of long-range order in one and two dimensions, *Physical Review*, **158**:383, (1967).
- [13] B. I. Halperin and David R. Nelson, Theory of two dimensional melting, *Physical Review Letters*, **41**:121, (1978).
- [14] Petter Minnhagen, The two dimensional Coulomb gas, vortex unbinding, and superfluid-superconducting films, *Reviews of Modern Physics*, **59**:1001, (1987).
- [15] B. I. Halperin and David R. Nelson, Resistive transition in superconducting films, *Journal of Low Temperature Physics*, **36**:599, (1979).
- [16] P. W. Anderson, An approximate quantum theory of the antiferromagnetic ground state, *Physical Review*, **86**:694, (1952).
- [17] R. Kubo, *Physical Review*, **87**:568, (1952).
- [18] H. Bethe, Zur theorie der metalle: I. Eigenwerte und eigenfunktionen der linearen atomkette, *Zeitschrift für Physik*, **71**:205, (1931).
- [19] T. Kennedy, E. H. Lieb, and B. S. Shastry, Existence of Neel order in some spin-1/2 Heisenberg antiferromagnets, *Journal of Statistical Physics*, **53**:1019, (1988).
- [20] P. W. Anderson, The resonating valence bond state in La_2CuO_4 and superconductivity, *Science*, **235**:1196, (1987).
- [21] T. Fukuzawa, E. E. Mendez, and J. M. Hong, Phase transition of an exciton system in GaAs coupled quantum wells, *Physical Review Letters*, **64**:3066, (1990).

- [22] L. V. Keldish and Y. V. Kopaev, *Soviet Physics-Solid State*, **6**:2219, (1964).
- [23] L. V. Keldish and A. N. Kozlov, Collective properties of excitons in semiconductors, *Soviet Physics-JETP*, **27**:521, (1968).
- [24] E. Hanamura and H. Haug, Condensation effects of excitons, *Physics Reports*, **33**:209, (1977).
- [25] Y. E. Lozovik and V. I. Yudson, A new mechanism for superconductivity: Pairing between spatially separated electrons and holes, *Soviet Physics-JETP*, **44**:389, (1976).
- [26] S. I. Shevchenko, *Soviet Journal of Low Temperature Physics*, **2**:251, (1976).
- [27] T. Fukuzawa, S. S. Kano, T. K. Guftafson, and T. Ogawa, Possibility of coherent light emission from Bose condensed states of SEHPs, *Surface Science*, **228**:482, (1990).
- [28] Z. Gedik and S. Ciraci, The field-induced phase transition of an electron-hole system in weakly coupled double quantum wells, *Journal of Physics: Condensed Matter*, **2**:8985, (1990).
- [29] R. K. Kalia and P. Vashishta, Interfacial colloidal crystals and melting transition, *Journal of Physics C: Solid State Physics*, **14**:L643, (1981).
- [30] J. A. Kash, M. Zachau, E. E. Mendez, J. M. Hong, and T. Fukuzawa, Fermi-Dirac distribution of excitons in coupled quantum wells, *Physical Review Letters*, **66**:2247, (1991).
- [31] V.L. Ginzburg and D. A. Kirzhnits, editors, *High-Temperature Superconductivity*, Consultants Bureau, New York, (1982).
- [32] J. G. Bednorz and K. A. Müller, Possible high T_c superconductivity in the Ba-La-Cu-O system, *Zeitschrift für Physik B-Condensed Matter*, **64**:189, (1986).

- [33] J.-M. Triscone, M. G. Karkut, L. Antognazza, O. Brunner, and Ø. Fischer, Y-Ba-Cu-O/Dy-Ba-Cu-O superlattices: A first step towards the artificial construction of high- T_c superconductors, *Physical Review Letters*, **63**:1016, (1989).
- [34] J.-M. Triscone, Ø. Fischer, O. Brunner, L. Antognazza, A. D. Kent, and M. G. Karkut, YBa₂Cu₃O₇/PrBa₂Cu₃O₇ superlattices: Properties of ultrathin superconducting layers separated by insulating layers, *Physical Review Letters*, **64**:804, (1990).
- [35] Ø. Fischer, J.-M. Triscone, L. Antognazza, O. Brunner, A. D. Kent, L. Mieville, and M. G. Karkut, Artificially prepared YBa₂Cu₃O₇/PrBa₂Cu₃O₇ superlattices: Growth and superconducting properties, *Journal of Less-Common Metals*, **164**:257, (1990).
- [36] Q. Li, X. X. Xi, X. D. Wu, A. Inam, S. Vadlamannati, W. L. McLean, T. Venkatesan, R. Ramesh, D. M. Hwang, J. A. Martinez, and L. Nazar, Interlayer coupling effect in high- T_c superconductors probed by YBa₂Cu₃O_{7-x}/PrBa₂Cu₃O_{7-x} superlattices, *Physical Review Letters*, **64**:3086, (1990).
- [37] Douglas H. Lowndes, David P. Norton, and J. D. Budai, Superconductivity in nonsymmetric epitaxial YBa₂Cu₃O_{7-x}/PrBa₂Cu₃O_{7-x} superlattices: The superconducting behavior of Cu-O bilayers, *Physical Review Letters*, **65**:1160, (1990).
- [38] A. W. Sleight, Chemistry of high-temperature superconductors, *Science*, **242**:1519, (1988).
- [39] S. S. P. Parkin, V. Y. Lee, E. M. Engler, A. I. Nazzari, T. C. Huang, and G. Gorman, Bulk superconductivity at 125 K in Tl₂Ca₂Ba₂Cu₃O_x, *Physical Review Letters*, **60**:2539, (1988).
- [40] R. F. Frindt, Superconductivity in ultrathin NbSe₂ layers, *Physical Review Letters*, **28**:299, (1972).

- [41] T. Schneider, Z. Gedik, and S. Ciraci, Transition temperature of superconductor-insulator superlattices, *Europhysics Letters*, **14**:261, (1991).
- [42] R. A. Klemm, A. Luther, and M. R. Beasley, Theory of the upper critical field in layered superconductors, *Physical Review B*, **12**:877, (1975).
- [43] T. Schneider, H. De Raedt, and M. Frick, On the theory of layered high-temperature superconductors, *Zeitschrift für Physik B-Condensed Matter*, **76**:3, (1989).
- [44] L. N. Bulaevskii and M. V. Zyskin, Energy gap in layered superconductors, *Physical Review B*, **42**:10230, (1990).
- [45] G. D. Mahan, *Many-Particle Physics*, Plenum Press, New York, (1981).
- [46] A. A. Abrikosov, L. P. Gorkov, and I. E. Dzyaloshinski, *Methods of Quantum Field Theory in Statistical Physics*, Prentice-Hall, New Jersey, (1963).
- [47] W. Harrison, Superconductivity on a $\text{YBa}_2\text{Cu}_3\text{O}_7$ lattice, *Physical Review B*, **38**:270, (1988).
- [48] M. Rona, Image-charge-mediated pairing in oxide superconductors, *Physical Review B*, **42**:4183, (1990).
- [49] A. J. Arko, R. S. List, R. J. Bartlett, S. W. Cheong, Z. Fisk, J. D. Thompson, C. G. Olson, A. B. Yang, R. Liu, C. Gu, B. W. Veal, J. Z. Liu, A. P. Paulikas, K. Vandervoort, H. Claus, J. C. Campuzano, J. E. Schirber, and N. D. Shinn, Large, dispersive photoelectron Fermi edge and the electronic structure of $\text{YBa}_2\text{Cu}_3\text{O}_{6.9}$ single crystals measured at 20 K, *Physical Review B*, **40**:2268, (1989).
- [50] W. E. Pickett, Electronic structure of the high-temperature oxide superconductors, *Reviews of Modern Physics*, **61**:433, (1989).

- [51] T. Schneider, Z. Gedik, and S. Ciraci, From low to high-temperature superconductivity: A dimensional crossover phenomenon? A finite size effect?, *Zeitschrift für Physik B-Condensed Matter*, **83**:313, (1991).
- [52] G. A. T. Allan, Critical temperatures of Ising lattice films, *Physical Review B*, **1**:352, (1970).
- [53] T. Weston Capehart and Michael E. Fischer, Susceptibility scaling functions for ferromagnetic Ising films, *Physical Review B*, **13**:5021, (1976).
- [54] D. S. Ritchie and M. E. Fischer, Finite size and surface effects in Heisenberg films, *Physical Review B*, **7**:480, (1973).
- [55] N. Parga and J. E. van Himbergen, Renormalization group studies of phase-diagrams of Ising and XY-model films of variable thickness, *Annals of Physics (New York)*, **134**:286, (1981).
- [56] L. J. De Jongh, Some applications of the quantum-lattice-gas model to high- T_c superconductivity, *Physica C*, **161**:631, (1989).
- [57] W. E. Lawrence and S. Doniach, Theory of layer structure superconductors, in *Proceedings of the 12th International Conference on Low Temperature Physics*, E. Kanda, editor, page 361, Academic Press of Japan, (1971).
- [58] Anthony J. Legget, A theoretical description of the new phases of liquid ^3He , *Reviews of Modern Physics*, **47**:331, (1975).
- [59] M. Strongin, O. F. Kammerer, D. H. Douglass, and Morrel H. Cohen, Effect of dielectric and high-resistivity barriers on the superconducting transition temperature of thin films, *Physical Review Letters*, **19**:121, (1967).
- [60] L. Genzel, A. Wittlin, M. Bauer, M. Cardona, E. Schönher, and A. Simon, Phonon anomalies and the range of superconducting energy gaps from infrared studies of $\text{YBa}_2\text{Cu}_3\text{O}_{7-\delta}$, *Physical Review B*, **40**:2170, (1989).

- [61] T. Schneider and M. P. Sorensen, Correlation between the Hall coefficient, penetration depth, transition temperature, gap anisotropy and hole concentration in layered high-temperature superconductors, *Zeitschrift für Physik B-Condensed Matter*, **81**:3, (1990).
- [62] O. Brunner, J.-M. Triscone, L. Antognazza, M. G. Karkut, and Ø. Fischer, Critical field anisotropy of artificial $\text{YBa}_2\text{Cu}_3\text{O}_7/\text{PrBa}_2\text{Cu}_3\text{O}_7$ superlattices, *Physica B*, **165&166**:469, (1990).
- [63] Z. Gedik and S. Ciraci, Tunneling induced superconductivity in layered systems, *Physical Review B*, page to be published, (1992).
- [64] T. Terashima, K. Shimura, Y. Bando, Y. Matsuda, A. Fujiyama, and S. Komiyama, Superconductivity of one-unit-cell thick $\text{YBa}_2\text{Cu}_3\text{O}_7$ thin film, *Physical Review Letters*, **67**:1362, (1991).
- [65] H. Fröhlich, *Proceedings of the Royal Society, A* **215**:291, (1952).
- [66] J. Bardeen, L.N. Cooper, and J. R. Schrieffer, Theory of superconductivity, *Physical Review*, **108**:1175, (1957).
- [67] H. Suhl, B. T. Matthias, and L. R. Walker, Bardeen-Cooper-Schrieffer theory of superconductivity in the case of overlapping bands, *Physical Review Letters*, **3**:552, (1959).
- [68] V. A. Moskalenko, Superconductivity of metals taking into account overlapping of the energy bands, *FMM-Fizika Metallov I Metallovedenie*, **8**:503, (1959).
- [69] J. Ashkenazi, M. Dacorogna, and M. Peter, On the equivalence of the Fröhlich and the Bloch approaches to the electron-phonon coupling, *Solid State Communications*, **29**:181, (1979).
- [70] F. Bloch, *Zeitschrift für Physik*, **52**:555, (1928).

- [71] Werner Weber, Electron-phonon interaction in the new superconductors $\text{La}_{2-x}(\text{Ba,Sr})_x\text{CuO}_4$, *Physical Review Letters*, **58**:1371, (1987).
- [72] R. A. Klemm and S. H. Liu, Intralayer-versus-interlayer pairing in the copper oxide superconductors, *Physical Review B*, **44**:7526, (1991).
- [73] V. A. Moskalenko, Thermodynamics of two-zone superconductors with a non-magnetic impurity, *FMM-Fizika Metallov I Metallovedenie*, **23**:585, (1967).
- [74] W. S. Chow, Theory of superconductors with overlapping bands in the presence of nonmagnetic impurities, *Physical Review*, **172**:467, (1968).
- [75] H. W. Kroto, J. R. Heath, S. C. O'Brien, R. F. Curl, and R. E. Smalley, Buckminsterfullerene, *Nature (London)*, **318**:162, (1985).
- [76] Kosmas Prassides and Harold Kroto, Fullerene physics, *Physics World*, **5** (April):44, (1992).
- [77] W. Krätschmer, Lowell D. Lamb, K. Fostiropoulos, and Donald R. Huffman, Solid C_{60} : A new form of carbon, *Nature (London)*, **347**:354, (1990).
- [78] R. M. Fleming, T. Siegrist, P. Marsh, B. Hessen, A. R. Kortan, D. W. Murphy, R. C. Haddon, R. Tycko, G. Dabbagh, A. M. Mujsce, M. L. Kaplan, and S. M. Zahurak, MRS Symposia Proceedings No. 206, in *Clusters and Cluster-Assembled Materials*, R. S. Averback, D. L. Nelson, and J. Bernholc, editors, Materials Research Society, Pittsburgh, (1991).
- [79] Paul A. Heiney, John E. Fischer, Andrew R. McGhie William J. Romanow, Arnold M. Denenstien, John P. McCauley Jr., Amos B. Smith III, and David E. Cox, Orientational Ordering Transition in Solid C_{60} , *Physical Review Letters*, **66**:2911, (1991).
- [80] R. C. Haddon, A. F. Hebard, M. J. Rosseinsky, D. W. Murphy, S. J. Duclos, K. B. Lyons, B. Miller, J. M. Rosamilia, R. M. Fleming, A. R. Kortan, S. H.

- Glarum, A. V. Makhija, A. J. Muller, R. H. Eick, S. M. Zahurak, R. Tycko, G. Dabbagh, and F. A. Thiel, Conducting films of C_{60} and C_{70} by alkali-metal doping, *Nature (London)*, **350**:320, (1991).
- [81] A. F. Hebard, M. J. Rosseinsky, R. C. Haddon, D. W. Murphy, S. H. Glarum, T. T. M. Palstra, A. P. Ramirez, and A. R. Kortan, Superconductivity at 18 K in potassium-doped C_{60} , *Nature (London)*, **350**:600, (1991).
- [82] O. Zhou, J. E. Fischer, N. Coustel, S. Kycia, Q. Zhu, A. R. McGhie, W. J. Romanow, J. P. McCauley Jr, A. B. Smith, and D. E. Cox, Structure and bonding in alkali-metal-doped C_{60} , *Nature (London)*, **351**:462, (1991).
- [83] P. W. Stephens, L. Mihaly, P. L. Lee, R. L. Whetten, S. M. Huang, R. Kaner, F. Deiderich, and K. Holczer, Structure of single-phase superconducting K_3C_{60} , *Nature*, **351**:632, (1991).
- [84] A. P. Ramirez, A. R. Kortan, M. J. Rosseinsky, S. J. Duclos, A. M. Mujsce, R. C. Haddon, D. W. Murphy, A. V. Makhija, S. M. Zahurak, and K. B. Lyons, Isotope effect in superconducting Rb_3C_{60} , *Physical Review Letters*, **68**:1058, (1992).
- [85] P. M. Allemand, K. C. Khemani, A. Koch, F. Wudi, K. Holczer, S. Donovan, G. Grüner, and J. D. Thompson, Organic molecular soft ferromagnetism in a fullerene C_{60} , *Science*, **253**:301, (1991).
- [86] Donald R. Huffman, Solid C_{60} , *Physics Today*, **44**:22, (1991).
- [87] R. C. Haddon, L. E. Brus, and Krishnan Raghavachari, Electronic structure and bonding in icosahedral C_{60} , *Chemical Physics Letters*, **125**:459, (1986).
- [88] Susumu Saito and Atsushi Oshiyama, Cohesive mechanism and energy bands of solid C_{60} , *Physical Review Letters*, **66**:2637, (1991).
- [89] Q. M. Zhang, Jae-Yel Yi, and J. Bernholc, Structure and dynamics of solid C_{60} , *Physical Review Letters*, **66**:2633, (1991).

- [90] J. H. Weaver, Jose Luis Martins, T. Komeda, Y. Chen, T. R. Ohno, G. H. Kroll, N. Troullier, R. E. Haufler, and R. E. Smalley, Electronic structure of solid C_{60} : Experiment and theory, *66*, **66**:1741, (1991).
- [91] S. Ciraci and I. P. Batra, Novel electronic properties of a potassium overlayer on $Si(001)-(2\times 1)$, *Physical Review Letters*, **56**:877, (1986).
- [92] S. Ciraci and I. P. Batra, Surface metallization of silicon by potassium absorption on $Si(001)-(2\times 1)$, *Physical Review B*, **37**:2955, (1988).
- [93] Inder P. Batra, Atomic and electronic structure of the $Na/Si(001)-(2\times 1)$ surface, *Physical Review B*, **39**:3919, (1989).
- [94] G. Sparr, J. D. Thompson, S. M. Huang, R. B. Kaner, F. Diederich, R. L. Whetten, G. Grüner, and K. Holczer, Pressure dependence of superconductivity in single-phase K_3C_{60} , *Science*, **252**:1829, (1991).
- [95] C. M. Varma, J. Zaanen, and K. Raghavachari, Superconductivity in fullerenes, *Science*, **254**:989, (1991).
- [96] M. Schluter, M. Lanoo, M. Needels, G. A. Baraff, and D. Tománek, Electron-phonon coupling and superconductivity in alkali-intercalated C_{60} solid, *Physical Review Letters*, **68**:526, (1992).
- [97] F. C. Zhang, Masao Ogato, and T. M. Rice, Attractive interaction and superconductivity for K_3C_{60} , *Physical Review Letters*, **67**:3452, (1991).
- [98] I. I. Mazin, S. N. Rashkeev, V. P. Antropov, O. Jepsen, A. I. Liechtenstein, and O. K. Andersen, Quantitative theory of superconductivity in doped C_{60} , *Physical Review B*, **45**:5114, (1992).
- [99] Gernot Stollhoff, Anomalous electron-lattice coupling in C_{60} , *Physical Review B*, **44**:10998, (1991).
- [100] L. Pietronero, Superconductivity mechanisms in doped C_{60} , *Europhysics Letters*, **17**:365, (1992).

- [101] S. Chakravarty and S. Kivelson, Superconductivity of doped fullerenes, *Europhysics Letters*, **16**:751, (1991).
- [102] G. Baskaran and E. Tosatti, A theory of the normal and superconducting states of doped solid C_{60} , *Current Science*, **61**:33, (1991).
- [103] R. W. Lof, M. A. van Veenendal, B. Koopmans, U. T. Jonkman, and G. A. Sawatzky, Band gap, excitons, and Coulomb interaction in solid C_{60} , *Physical Review Letters*, **68**:3924, (1992).
- [104] T. Takahashi, S. Suzuki, T. Morikawa, H. Katayama-Yoshida, S. Hasegawa, H. Inokuchi, K. Seki, K. Kikuchi, S. Suzuki, K. Ikemoto, and Y. Achiba, Pseudo-gap at the Fermi level in K_3C_{60} observed by photoemission and inverse photoemission, *Physical Review Letters*, **68**:1232, (1992).
- [105] Z. Gedik and S. Ciraci, Two-fermion problem on a truncated-icosahedron, in *Adriatico Research Conference on Clusters and Fullerenes, Trieste, Italy*, V. Kumar, T. P. Martin, and E. Tosatti, editors, International Centre for Theoretical Physics, World Scientific, July 1992.
- [106] J. Hubbard, Electron correlations in narrow energy bands, *Proceedings of the Royal Society, A* **276**:238, (1963).
- [107] R. Micnas, J. Ranninger, and S. Robaszkiewicz, Superconductivity in narrow-band systems with local nonretarded attractive interactions, *Reviews of Modern Physics*, **62**:113, (1990).
- [108] Daniel C. Mattis, The few-body problem on a lattice, *Reviews of Modern Physics*, **58**:361, (1986).
- [109] Z. Gedik and S. Ciraci, Bound-state formation on a spherical shell: A model for alkali-metal-doped C_{60} , *Physical Review B*, **45**:8213, (1992).
- [110] I. S. Gradshteyn and I. M. Ryzhik, *Table of Integrals, Series and Products*, Academic Press, San Diego, (1980).

- [111] Z. Gedik and S. Ciraci, Local oscillator model for superconducting fullerenes, in *NATO Advanced Study Institute on Chemical Physics of Intercalation II, Chateau de Bonas, France*, Plenum, July 1992.
- [112] Ran Liu and M. V. Klein, Raman studies of vibrational properties in solid C_{60} , *Physical Review B*, **45**:11437, (1992).
- [113] P. W. Anderson, Model for the electronic structure of amorphous semiconductors, *Physical Review Letters*, **34**:953, (1975).
- [114] K. Holczer, O. Klein, G. Grüner, J. D. Thompson, F. Diederich, and R. L. Whetten, Critical magnetic fields in the superconducting state of K_3C_{60} , *Physical Review Letters*, **67**:271, (1990).

Vita

Mehmet Zafer Gedik was born in Ankara, on 1 December 1966. He was top-ranking in the entrance examinations of Ankara Fen Lisesi and he graduated from that high school as the first top. In 1984, he entered Middle East Technical University with the highest score of the University in the entrance examination. He received his B.S. degree in Physics in three years ranking the first of the University with grade 4.00 out of 4.00. In 1987, he started his graduate study under the supervision of Prof. Salim Çıracı, in the Department of Physics of Bilkent University as a Research Assistant. He got his M.S. degree in 1989 with the thesis titled "High T_c Superconductivity". He worked as a Visiting Researcher at IBM Zurich Research Laboratory for a three months period in 1990. In 1991, he became an Instructor at the Department of Physics of Bilkent University. During his Ph.D. study with Prof. Çıracı he worked on the theory of high temperature superconductivity and the superconductivity of C_{60} , theory of metallization on semiconductor surfaces, exciton condensation in coupled quantum wells and ballistic electron emission microscopy. He published articles in Journal of Physics: Condensed Matter, Europhysics Letters, Zeitschrift für Physik B-Condensed Matter and Physical Review B. Presently, he is employed as an Assistant Professor at Department of Physics, Bilkent University.